AD-A041 900 COLD REGIONS RESEARCH AND ENGINEERING LAB HANOVER N H F/G 13/2
CONTRIBUTION TO THE STUDY OF FREEZING WET SOILS--INTERSTITIAL P--ETC(U)
FEB 77 M CHALHOUB

UNCLASSIFIED CRREL-TL-588 NL

1 OF 1
ADA041900

END
DATE FILMED
8-77

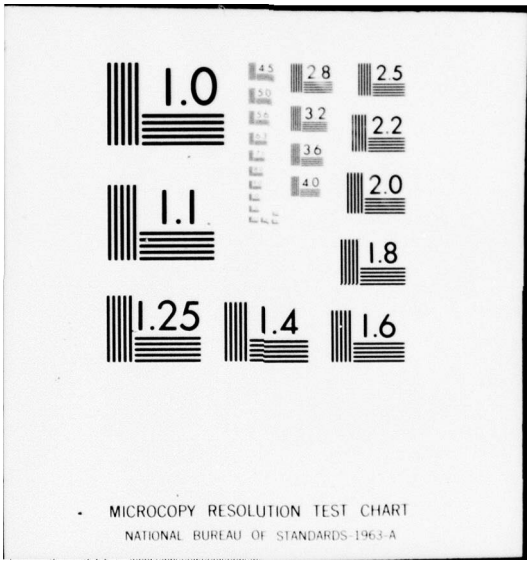
1.0
1.1
1.25
1.4
1.6
1.8
2.0
2.2
2.5
2.8
3.2
3.6
4.0
4.5
5.0
MICROCOPY RESOLUTION TEST CHART
NATIONAL BUREAU OF STANDARDS-1963-A

Draft Translation 588
February 1977

CONTRIBUTION TO THE STUDY OF FREEZING WET SOILS — INTERSTITIAL PRESSURE NEAR THE FREEZING POINT

M. Chalhoub

CORPS OF ENGINEERS, U.S. ARMY
COLD REGIONS RESEARCH AND ENGINEERING LABORATORY
HANOVER, NEW HAMPSHIRE

Unclassified

SECURITY CLASSIFICATION OF THIS PAGE (When Data Entered)

REPORT DOCUMENTATION PAGE		READ INSTRUCTIONS BEFORE COMPLETING FORM
1. REPORT NUMBER Draft Translation 588	2. GOVT ACCESSION NO.	3. RECIPIENT'S CATALOG NUMBER
4. TITLE (and Subtitle) CONTRIBUTION TO THE STUDY OF FREEZING WET SOILS --INTERSTITIAL PRESSURE NEAR THE FREEZING FRONT		5. TYPE OF REPORT & PERIOD COVERED 6. PERFORMING ORG. REPORT NUMBER
7. AUTHOR(s) M. Chalhoub		8. CONTRACT OR GRANT NUMBER(s)
9. PERFORMING ORGANIZATION NAME AND ADDRESS U.S. Army Cold Regions Research and Engineering Laboratory Hanover, New Hampshire		10. PROGRAM ELEMENT, PROJECT, TASK AREA & WORK UNIT NUMBERS
11. CONTROLLING OFFICE NAME AND ADDRESS		12. REPORT DATE February 1977 13. NUMBER OF PAGES
14. MONITORING AGENCY NAME & ADDRESS(if different from Controlling Office)		15. SECURITY CLASS. (of this report) 15a. DECLASSIFICATION/DOWNGRADING SCHEDULE

16. DISTRIBUTION STATEMENT (of this Report)

Approved for public release; distribution unlimited.

17. DISTRIBUTION STATEMENT (of the abstract entered in Block 20, if different from Report)

18. SUPPLEMENTARY NOTES

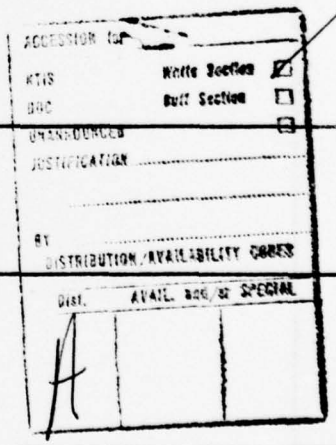

19. KEY WORDS (Continue on reverse side if necessary and identify by block number)

SOIL MOISTURE FROZEN SOIL

20. ABSTRACT (Continue on reverse side if necessary and identify by block number)

This study deals with certain aspects of ice segregation which takes place when a fine soil is subjected to freezing. On the basis of experimental observations, there was proposed a physical mechanism of secondary phenomena accompanying the displacement of a frost front in a fine moist soil.

DD FORM 1 JAN 73 1473 EDITION OF 1 NOV 65 IS OBSOLETE

Unclassified

SECURITY CLASSIFICATION OF THIS PAGE (When Data Entered)

(14) CRREL-TL-588

DRAFT TRANSLATION 588

(6)

ENGLISH TITLE: CONTRIBUTION TO THE STUDY OF FREEZING WET SOILS--INTERSTITIAL PRESSURE NEAR THE FREEZING FRONT

FOREIGN TITLE: (CONTRIBUTION A L'ETUDE DE LA CONGELATION DES SOLS HUMIDES. PRESSION INTERSTITIELLE AU VOISINAGE DU FRONT DE CONGELATION),

(10) Michel

AUTHOR: M. Chalhoub

(11) Feb 77

(12) 74 p.

SOURCE: Paris, University of Paris, 1971, 49p.

Translated by Office of the Assistant Chief of Staff for Intelligence for U.S. Army Cold Regions Research and Engineering Laboratory, 1977,

037100

4/6

Sequential No.:

K-6859

THESIS

Submitted to the

Department of Sciences, Paris University

to qualify
for the

Title of Doctor in Engineering

by

Michel CHALHOUB

Subject of Thesis: Contribution to the Study of Freezing Wet Soils--
Interstitial Pressure Near the Freezing Front

Defended on 1 March 1971 before the Examination Board

Mr. Ed. BRUN, Chairman
Mr. J. J. BERNARD
Mr. R. SIESTRUNCK
Examiners
Mr. J. AGUIRRE-PUENTE, Invited Board Member

Paris 1971

I must express to Professor BRUN, member of the Academy of Sciences, my profound appreciation for having received me in his laboratory and having always aided and encouraged me during this effort.

I want to express my profound gratitude to Professor BERNARD, the new director of the Aerothermal Laboratory of the CNRS [National Scientific Research Council], for having permitted me to pursue this effort and for having agreed to be a member of the examining board.

I want to thank Professor SIESTRUNCK for having likewise been kind enough to be a member of the board.

I want to thank Mr AGUIRRE-PUENTE, in charge of freezing studies at the Aerothermal Laboratory, who very closely followed the development of this work and whose help was very useful to me.

Finally I want to express my gratitude to all of the laboratory personnel and in particular Mr CREFF for their friendly assistance.

[Translator's note. Symbols are rendered in the translation to the extent that they were reliably identifiable, reproducible, or present in the photostatic copy.]

SYMBOLS

σ interfacial tension (erg/cm^2)

L fusion heat (J/kg)

ΔT cryoscopic decline (degrees Celsius)

p_i interstitial pressure (mb)

V_Q filtration speed (mm/sec)

P_a atmospheric pressure (mb)

X abscissa of a point with respect to the initial cold face (m)

X^1 abscissa of a point with respect to the mobile cold face (m)

L sample height (m)

γ_d dry density (kg/m^3)

W_e water content

ε porosity

γ_s density of grains (kg/m^3)

ρ density of porous medium (kg/m^3)

Φ heat flow (W)

T temperature (degrees Celsius)

k permeability (cm^2)

I freezing index (degrees)

X_G swelling (m)

S_r saturation degree

e vacuum index

Indices

$( )_e$ pertaining to water

$( )_f$ pertaining to the freezing front

$( )_g$ pertaining to ice

$( )_i$ initial

$( )_o$ pertaining to the cold face

INTRODUCTION

The study we are presenting here is a part of the research being done on frost [freezing] at the Aerothermal Laboratory of the CNRS; it deals with certain aspects of ice segregation which takes place when a fine soil is subjected to freezing (1).

On the basis of experimental observations, which we conducted (2, 3) as well as studies on frost undertaken in other laboratories, there was proposed a physical mechanism of secondary phenomena accompanying the displacement of a frost front in a fine moist soil (1). Certain hypotheses adopted are now being studied but certain effects of these secondary phenomena could already be examined and tied in with conditions that determine the rate of heat transfer in the environment [medium].

Thus we earlier in particular studied the swelling of soils due to frost which made it possible to evidence the variation in this swelling with a rather large parameter: the frost index (4, 5, 6); this swelling, which takes place during the freezing of fine soils and which is due to the accumulation of water in the form of ice in the frozen part of the samples, can be explained only by the existence of aspiration on the level of the frost front.

This aspiration, which originates in the displacement of the thermodynamic equilibrium during the change in the state of the water in the pores of the medium, is not yet perfectly known and we devoted ourselves to a study of it from the experimental viewpoint.

We set ourselves the goal of determining the interstitial pressure of water in the porous medium when a freezing front moves. We used two methods:

The first is an indirect method; it consists in estimating, by means of the Darcy Law, the depression necessary to establish the flow of water through the porous medium which must feed the ice that is being formed. Darcy's Law is applied here, taking into account the flow rate of water aspirated and measured during our freezing experiments as well as the characteristics of the medium through which the flow runs;

The second is a direct method; it consists in measuring the interstitial pressure of the water with the help of tensiometers and a pressure detector.

A knowledge of the permeability of soils studied being necessary here, we had to perfect a permeameter [permeation meter] adapted to the soil types and samples studied in the freezing cell which are made up of very fine, nonconsolidated porous media.

Moreover we had to work out a system for measuring the interstitial pressure which we adapted consequently to a freezing cell.

After having briefly reviewed the research already done on the problem and after having discussed the validity of Darcy's Law in our case, we will describe in this study the experimental installations which we set up and used.

We will then present the experiments which, on the basis of Darcy's Law, were used in studying the interstitial pressure in the vicinity of the freezing front and we discuss the measurements of the permeability of porous media study. We present the experiments which served for the direct measurement of interstitial pressures in the porous media.

Finally we show how certain parameters of capital importance intervene in the phenomenon and how new correlations are obtained.

2. BRIEF REVIEW OF EARLIER WORKS

2.1. Theoretical Schemes

2.1.1. Scheme Based on Gibbs-Thomson Law

The research conducted in various countries enabled certain authors (7, 8) to formulate hypotheses concerning the physical mechanism involved in ice segregation.

The theoretical scheme currently adopted regarding the secondary phenomena accompanying the freezing of fine soils is based on cryoscopic decline of water at the interface between water and ice in a capillary. The Gibbs-Thomson Law (8)

$$\Delta T = \frac{2 \cdot \sigma \cdot T_E}{L \cdot R_c}$$

where σ is the water-ice interface tension,

T_E is the equilibrium temperature at a flat (plane)

and L is the fusion heat,

gives us this cryoscopic decline ΔT as a function of the radius of the capillary R_c.

When the forced cooling causes the water temperature in the medium's pores in the vicinity of an ice front to be such that the cryoscopic decline, given by the Gibbs-Thomson Law, is not attained, then the ice does not enter into the pores and the freezing front stops. However, the formation of ice may continue, provided that there is water support which traverses the porous medium up to the ice, said water being capable of being furnished by the nonfrozen medium or by a water table.

In the case where the water of the pores exceeds the cryoscopic decline corresponding to the equilibrium, the ice penetrates into the pores and the freezing front advances in [into] the medium.

In the first case, we have the formation of ice lenses and, consequently, the soil swells up. This water transport is due to the appearance of a drop in interstitial pressure in the water in the vicinity of the freezing front

resulting from the displacement of the thermodynamic equilibrium. This pressure drop increases as the cryoscopic decline grows (9).

The expression of the interstitial pressure in the two water-ice phases in the vicinity of an interface was obtained either on the basis of thermodynamic laws (10, 7) or by analogy with the phenomenon of capillarity (11). It is written as follows (14):

$$(p_i)_g - (p_i)_e = \frac{2\sigma}{R}$$

where P_g, P_e are, respectively, the pressure in the ice and in the water, where σ is the water-ice interface tension, and R is the pore radius.

This physical scheme helps in gaining an overall understanding of the mechanism involved in the freezing of moist soils; it does not however explain the various secondary phenomena which accompany it, particularly regarding the differences in the cryogenic aspect which appear in the frozen zone of a sample submitted to freezing; as a matter of fact, the microscopic examination of this zone reveals the existence, on the one hand, of particles congealed "on the spot" in the ice, and, on the other hand, absolutely pure glass lenses which have no soil particles at all.

2.1.2. Theory of K. A. Jackson, D. R. Uhlmann, and B. Chalmers

For the purpose of making a more in-depth approach to the problem, K. A. Jackson, D. R. Uhlmann, and B. Chalmers (12) studied the influence of a soil particle on a liquid-solid (water-ice) interface in motion. The microscopic observation of the interface and the particle showed the existence of a "critical speed" of the solidification front for each type of particle and liquid used. When the speed of advance of the interface (or the rate of ice formation) is greater than or equal to this critical speed, the particle is incorporated into the ice; when it is smaller, the particle is pushed by the interface, in front of it.

The critical speed depends on the viscosity of the liquid used; for given thermal conditions and for a given liquid, it is a function of the shape of the particle and it is independent of electrostatic interactions; this made it possible to think that the mechanism of particle incorporation or movement is a phenomenon of free surface energy.

The fact that the particle is not "taken into" the ice shows:

the existence of a repulsion between the particle and the interface which prevents the incorporation of the particle;

the possibility of feeding the film of water when the inteface is very close to the particle.

This theory sets up the hypothesis:

- of a series of repulsions between the particle and the interface;

these repulsions take place only if the particle-ice interface tension σ_{sp} is greater than the sum of particle-water interface tension σ_{Lp} and the water-ice interface tension σ_{SL}

$$(\Delta\sigma = \sigma_{Sp}-(\sigma_{Lp}+\sigma_{LS}) > 0);$$

of a sufficiently rapid flow to feed the interface.

If the above two conditions are not met, the particle is incorporated into the ice.

On a microscopic scale, the interactions between the particle and the solidification front cause the chemical potential and the free surface energy to vary with the distance of the solidification front from the particle surface. Taking these variations into account, the study of water diffusion in the zone situated between the particle and the front shows that there is a pull of water in this zone.

In the case of an assembly of particles constituting a soil, this water pull [tension] brings about a flow coming either from the subjacent zone of the soil which is becoming consolidated or from a water table [underground water level] placed at a certain distance from the freezing front.

The theoretical study of the problem conducted first of all for a single particle gives us the evolution, for each type of particle, of the interface advance speed (or the rate of accumulation of ice behind the particle with regard to [opposite] the interface] as a function of the distance between the particle and the interface; for a given particle curvature radius, the speed goes through a maximum corresponding to an unstable equilibrium which is the critical speed for the type of particle considered. This study, conducted for the case of a single particle, was then extended to the problem of freezing wet soils. A soil sample, subjected to freezing, is the site of a heat transfer, a transfer of mass within the nonfrozen zone, and of interface phenonena on the level of the freezing front.

The elaboration of a theory concerning the ready congealability of soils must thus envisage three aspects of the problem. The mass transfer consists in a flow of water into the nonfrozen zone; this water can come either from the freezing front through the drying of the subjacent zone, or from a water table. The theory of K. A. Jackson, D. R. Uhlmann, and B. Chalmers considers that this flow obeys the diffusion equation. We note that the solution of this equation, in the case of a unidimensional transfer and in a saturated soil, shows that the flow, in a permanent regimen, follows a linear pressure gradient (Darcy's Law).

The study of heat transfer into the sample is reduced, in this theory, to the establishment of a thermal balance near the freezing front in the two water-ice phases. The problem as a matter of fact is quite complex;

regarding the thermal aspect, we referred in our study to already known theories (13, 14). The theory of K.A. Jackson, D.R. Uhlmann, and B. Chalmers in particular concerns the interface phenomena in the problem of soil freezing; it ties the soil swelling speed to other parameters involved in the course of freezing; it provides the following in particular:

- that the freezing speed [illegible symbol] is maximal when the front advance speed is maximal (in the area where it is less than the critical speed),

- that, in the case of a soil made up of grains having the same diameter, the speed v_g is inversely proportional to the interstitial pressure at the freezing front; it is furthermore inversely proportional to the diameter of the grains in the case of a soil with a fine grain size and to the square of that diameter in the case of a soil with coarse grain sizes.

2.2. Experimental Work

We used two methods to measure the interstitial pressure in the unfrozen zone of a sample subjected to unidimensional freezing.

2.2.1. Indirect Method

Certain materials are susceptible to becoming consolidated while losing their moisture. In this type of soils, when they are submitted to frost, the aspiration of the water toward the zone where the ice is forming brings about a consolidation of the unfrozen zone and consequently a variation in the dry density in this zone.

The principle of the method rests on the determination--by a separate operation for the soil considered--of the curve of interstitial pressure variation in this soil as a function of the water content and the dry density. At the end of the freezing experiment, the water content as well as the dry density are determined in the unfrozen zone. The relation $p_1(W_e, \gamma_d)$ gives the value of the interstitial pressure corresponding to the consolidation characteristics.

Two researchers used this method with considerably different experimental devices.

2.2.1.1. Experimental Setup of E. Penner (7)

The experimental setup of E. Penner is similar, in terms of its operating principle, to our setup. The curve $p_i(W_c, \gamma_d)$ is determined by means of the membrane suction apparatus of L. A. Richards (15). At the end of the freezing experiment, the unfrozen zone is cut up into sections whose water content and dry density are to be determined.

2.2.1.2. Experimental Setup of P. J. Willians (16)

The experimental setup of Willians is made up of three rings with a diameter of 2.2 cm and a height of 0.4 cm. These rings are filled

with compacted materials. The central ring is separated from the two lateral rings by water-permeable membranes of the type used in the membrane suction apparatus of L. A. Richards (15). The entire assembly is placed into a thermostat-controlled enclosure [container] at a selected temperature between 0° C and -3° C. The cessation of superfusion [supercooling] in the lateral rings is caused by contact with ice crystals; the freezing does not take place in the soil contained in the central ring because the passage of ice through the very small pores of the membranes takes place only at very low temperatures.

At the end of the experiment, which takes 2 or 3 days, we find that the water content in the soil of the central ring has declined considerably and that this soil has become consolidated. The relationship between the consolidation pressures or the effective pressures, the water content W_e in the soil and the dry density γ_d were obtained through separate tests conducted with the oedometer (odometer). This relationship is unique if the soil is saturated. The effective pressure is equal to the confinement pressure minus the interstitial water pressure; in equilibrium, the interstitial pressure is equal to the atmospheric pressure; it is thus zero with respect to the latter and the effective pressure becomes equal to the confinement pressure.

2.2.2. Direct Method

It consists in measuring the interstitial pressure with the help of a liquid-column pressure gauge placed at the base of the soil samples subjected to unidimensional freezing (17, 18). More recently, P. J. Williams (19) used this method again but the sample was soaked in a container where a pressure on the order of 3 bars was established. This artifice enabled P. J. Willians to confirm the existence of pressure drops [depressions] on the order of 2 bars in very fine media such as certain clays.

2.2.3. Critique of These Methods

2.2.3.1. Indirect Method

This method applies only to cases involving materials susceptible of becoming consolidated.

It necessitates a knowledge of interstitial pressures as a function of the water content and the dry density through a separate operation (this relation is unique [1:1 ratio] and is reduced to $p_i(\gamma_d)$ if the material remains saturated). The interstititial pressures, determined at different levels, correspond to the final consolidation characteristics and the evolution of these pressures thus remains unknown.

2.2.3.2. Direct Method

This method tells us something about the evolution of interstitial pressures; it is superior to the preceding one; however the measurement instruments used so far are not at all satisfactory and only give us approximate values; as a matter of fact:

The measurements are made at the base of the soil sample and a knowledge of the interstitial pressure at the freezing front is not obtained; moreover, for soil samples with very poor permeability, the measurement of the interstitial pressure even a few millimeters from the freezing front does not tell us anything about the real value of the interstitial pressure on the level of the latter;

The instrument almost always used here, that is, the mercury pressure gauge, induces major errors in the interstitial pressure values by reason of the volumetric coefficient of the pressure gauge (the volumetric coefficient is equal to the volume of water which must come out of the pressure gauge [illegible words in photostat] so that the latter will indicate a determined pressure variation). This causes us to make two remarks here:

the first is that the pressure gauge response time is long and that it increases as the medium becomes less permeable;

the second is that the transfer of a volume of water from the soil studied to the pressure gauge entails the risk of disturbing the flow in the porous medium and, consequently, the phenomenon of freezing especially in the vicinity of the pressure detection point.

The measurement of the pressure gauge is limited to 1 atmosphere (as a matter of fact, up to the water vapor tension which is on the order of 850 mb) and it is therefore impossible to make a continuous registration of the measurement by means of this instrument.

In the following paragraph we will describe the indirect method which we adopted for the determination of the interstitial pressure in the vicinity of the freezing front.

Regarding the direct method, we tried to perfect a measurement system that would give us more precise values for the interstitial pressure; we consequently put together a study cell derived from the thermal study cell but equipped with this measurement system.

3. INDIRECT METHOD ADOPTED FOR DETERMINATION OF INTERSTITIAL PRESSURE

3.1. Principle of Method

It consists in applying, to the flow in the unfrozen zone, Darcy's Law

$$V_Q = \frac{k}{\mu} \frac{\Delta p}{\ell}$$

where V_Q is the water flow rate which goes through this zone per unit of surface or the filtration speed, k is the permeability, μ is the viscosity of the water, Δp is the difference in the pressure at the ends of the sample having a length ℓ.

The determination of Δ_p requires a knowledge of other magnitudes which figure in this law.

The base of the sample in connection with the water table is, roughly at the level of this underground table, at atmospheric pressure P_a and the pressure difference Δ_p is equal to $P_a - p_i$; μ is the viscosity of the water going through the unfrozen zone (the temperature of this zone in our experiments varied from 0.5° C at the base of the sample to 0° C at the freezing front and we therefore took, for the value of the viscosity, the figure for the water at 0° C). The value V_Q of the water flow rate going through the sample is known with precision at any instant during the freezing experiment due to the system of measurement of the aspirated water volume which we describe in our experimental setup.

The length L of the unfrozen portion is obtained from the adscissa χ_F of the freezing front, referenced with respect to the initial position of the cold face of the sample having initial length L_i; it is equal to $L_i - \chi_F$. In our installation, we use a system which enables us with precision to keep track of the displacement of the freezing front. The permeability value is measured with the help of a permeameter.

We will distinguish two cases in the application of this law: the case of nonconsolidable soils and the case of consolidable soils. The latter type of soil is susceptible--due to the effect of a diminution in the interstitial pressure--to becoming compressed while losing water, which brings about an increase in the medium's dry density.

3.1.1. Case of Nonconsolidable Soils

When a freezing front moves in a nonconsolidable saturated soil, the characteristics of the unfrozen zone, that is to say, the water content W_e, the dry density γ_d, and the permeability k are not modified.

The permeability value to be used in Darcy's Law is the one measured by the permeameter which corresponds to a dry density equal to that of the sample experimented upon during the freezing.

3.1.2. Case of Consolidable Soils

In these soils, the characteristics γ_d, ρ, and W_e are modified in the unfrozen zone by virtue of the consolidation due to the freezing. To figure out the distribution of interstitial pressure in the unfrozen zone at any point in this zone and at the freezing front, we worked out the following method.

It consists, in the first stage, of determining the permeability of a given soil at a function of its consolidation characteristics. The manufactured samples are saturated, as shown in the operating procedure which we described in connection with our experimental setup. Moreover,

they are manufactured for different dry densities; this is done by modifying either the compacting water content or the compacting energy or both of them simultaneously. We thus determine the specific curve of the soil considered $k(\gamma_d)$ In a similar spirit, the dimensions of the body of the permeameter and the arrangement of the pistons of the permeameter with exactitude reproduce the dimensions and the shape of the unfrozen zone.

At the end of the freezing experiment, the soil considered is cut up into sections with different levels x whose water content and dry density we determine. We thus know the curve $\gamma_d(x)$.

Referring now to the first curve [illegible], we deduce from that the curve $k(x)$ for the soil considered. The method worked out here thus boils down to gradually applying Darcy's Law to a soil sample one of whose ends is under atmospheric pressure and consists of a succession of sections [slices] with different permeabilities, arranged in series with respect to the flow. It thus enables us to find out what the interstitial pressure is in each slice. This method however presents the inconveniences inherent in the application of Darcy's Law in our case and those of the indirect methods which are based on the principle of soil consolidation.

3.2. Discussion on Validity of Darcy's Law

3.2.1. Theoretical Considerations

In case of a permanent flow (21), Darcy's Law is valid when [blank space in photostat] does not depend on the time, the space, the direction, and the pressure, that is to say that:

The porous medium is homogeneous and isotropic; in other words, the average geometry [geometric size] is the same at any point and in all directions; it is stable from the geometric, physical, and chemical viewpoints; its pores communicate between each other and are filled with liquid, without any free gases; there is no biological activity;

The liquid is isotropic, homogeneous, incompressible, with constant temperature, density, and viscosity, and it is physically and chemically inactive;

The flow is very slow and its Reynolds number is between 1 and 10.

$$R_c = \frac{V_Q \cdot d}{\mu} < 1 \text{ to } 10$$

where V_Q is the filtration speed, μd is the average grain diameter, and μ is the viscosity.

3.2.2. Establishment of Permanent Rate Experimentally for Certain Samples

In the course of experiments dealing with measuring the permeability, we noted the time after which the movement of the air bubble, for the

measurement of the flow rate in the capillary, as described in paragraph 3.2.1.3., becomes uniform. We proceeded in the following manner: when the sample put in place in the permeameter is saturated, we subject its ends first of all to atmospheric pressure and then to a constant pressure difference. In figures 1 and 2 we illustrated the successive times it takes an air bubble to travel 1 cm in the measurement capillary having a diameter of 3 mm (see description of permeameter) as of the moment a different pressure is applied to the ends of the sample.

We considered soil No. 3 whose permeability is the lowest of all of the soils studied.

3.2.3. Conclusion

We experimented with clean artificial soils with a fine grain size. The flow during the freezing is slow; the samples are saturated before the freezing process and the fluid used is distilled water [handwritten marginal note: degassed?]. The conditions for the validity of Darcy's Law, at steady flow, are thus practically met.

As the sample freezes, a freezing front advances in the latter and the unfrozen zone of the sample is thus subjected to atmospheric pressure at its fixed end and to variable pressure at its mobile end, delimited by the moving freezing front.

We thus submit our sample--whose length is variable--to a variable pressure difference. Darcy's Law is valid only in steady flow conditions and its validity in our case can be conditioned by two factors--the nature of the medium regarding the time needed for the establishment of the permanent state, the speed of advance of the freezing front. The freezing experiments conducted show that the speed of the freezing front is relatively slow; moreover, figures 1 and 2, which illustrate the establishment of the permanent state or the least permeable soil, show that the permanent state is attained after a very short time; moreover, this time is shorter as the pressure difference goes up and as the soil becomes more permeable.

4. DESCRIPTION OF EXPERIMENTAL INSTALLATIONS

For our study we used experimental installations of different types:

A study installation for the thermal problem,

A permeability measurement installation,

An installation equipped with an interstitial pressure measurement system.

The first type of installation (2, 5) was perfected at the Aerothermal Laboratory to study certain aspects of the soil freezing problem; we will hereafter give a summary description of this installation. The second type was developed for our study.

Regarding the third type of installation, it consists of an installation derived from the first and adapted to the system for the measurement of interstitial pressures which we worked out.

4.1. Installation for Study of Thermal Problem

This experimental installation (2, 5) involves the following elements:

a thermal studies cell,

a temperature control system,

a temperature measurement and registration system,

a sample swelling registration system,

a freezing front observation system,

a system for water supply and for measuring the water volume aspirated by the sample.

4.1.1. Thermal Studies Cell (Figure 8)

It consists of two transparent concentric cylinders (1 and 2, Figure 8) made of plexiglass, in one piece, with two ring-shaped bases (3, 4, Figure 8); between the two cylinders, there is a tight chamber where we establish the vacuum to minimize lateral heat exchanges. The inside cylinder is tronconic; it is intended to house the soil sample. The diameter of this sample varies between 4.2 cm and 4.9 cm and its height is about 20 cm.

To increase the unidimensionality of the phenomenon, these cylinders are surrounded by two thermostat-controlled envelopes in the shape of shells traversed by a fluid (alcohol) at a temperature slightly higher than 0° C (Figure 9).

Two pistons, traversed by alcohol circulation and arranged at the two ends of the soil sample, give the latter the desired temperature. The upper piston (5, Figure 8) is at the lowest temperature corresponding to the thermal state imposed and the lower piston (6, Figure 8) as well as the thermostat-controlled envelope are at the same temperature selected for our experiments (about 0.5° C).

4.1.2. Temperature Control System

The temperatures of the two pistons and the thermostat-controlled envelope are controlled. This control is performed by two assemblies made up of a cryostat and a thermostat (Figure 9). The process imposed upon the sample involves two phases:

the sample soaking phase during which the temperature of the two pistons and the thermostated envelope is controlled at a value close to 0°;

the sample freezing phase, where the temperature of the cold face, imposed by the upper piston, is lowered abruptly to the value corresponding to the selected thermal state, while the temperature of the lower piston and the thermostat-controlled envelope have remained unchanged.

4.1.3. Temperature Measurement and Registration System (Figure 9)

Along the wall of the tronconic cylinder there are arranged, at well-defined levels, thermocouples which indicate the evolution of the soil sample temperature. The lower and upper pistons are provided with thermocouples. A flowmeter is arranged in the upper piston.

4.1.4. The Sample Swelling Registration System

The upper piston is free to move due to the action of the possible soil swelling. A displacement detector (7, Figure 8), attached to this piston, furnishes a signal which is recorded. The swelling is thus known in a continuous and precise fashion during the freezing test.

4.1.5. Freezing Front Observation System

The temperature at the freezing front is presumed to be equal to 0° C; when a thermocouple indicates this temperature, the freezing front is on the level of the welding of that thermocouple; the positions of the various weldings are known and the evolution of the temperatures as a function of the time is being registered; now the level of the freezing front is therefore known with precision several moments after the experiment. To visualize and keep track of the evolution of the freezing front with the cathetometer, we were able, for certain soils, to use water colored with fluorescein; the latter have the property of changing color when passing from the liquid state to the solid state and the fluorescein concentration of 0.5 g per liter of water practically does not change the freezing temperatures. For the case of soils where the preceding visualization could not be made, we perfected a special detector for the purpose of this thesis; it was furthermore used in various experiments at the Aerothermal Laboratory and we will take the liberty of describing it once again.

The freezing depth detector is a tube with a diameter of 2 mm; it is flexible and is made of nylon to prevent its rupture during soil swelling; it is attached to the lower piston and passes along the sample between the latter and the inside wall of the cell. It contains a solution of methylene blue in water in a proportion of 0.5 g per liter.

During freezing, the methylene blue is driven from the frozen portion, which becomes colorless, toward the nonfrozen portion whose blue coloration it accentuates.

This tube is in perfect contact with the soil sample and thus has the same temperature and the color change in the tube indicates the position of the freezing front.

Since the methylene blue solution has a very low supercooling temperature (-14° C), we also added to that solution some metaldehyde powder which acts as a nucleating agent.

4.1.6. System of Water Supply and of Measurement of Water Volume Aspirated by Sample (Figure 9)

The height of the water table [underground water level] must remain constant during the freezing test for reasons of experiment reproducibility; the water volume aspirated by the sample must also be known with precision for the application of Darcy's Law.

The system consists of two burettes, one of which is equipped with a wide-diameter funnel; they are linked by a three-way faucet [valve]. The first is filled with water and connected to the lower piston to feed the soil samples; above the water in the burette, we put oil for a height of 10 cm so that the free surface of the oil would be in the enlarged zone corresponding to the funnel. The displacement of the oil-water meniscus in the course of time gives us the volume of water aspirated by the sample.

The second burette is entirely filled with water; it serves periodically to supply the first in order to maintain the meniscus in the burette within a relatively short space; the level of the free oil surface is likewise kept constant during the experiment.

4.1.7. Operating Procedure

A freezing experiment involves the following stages:

choice of initial characteristics of soil sample,

placement of soil in experimental cell,

soaking and establishment of initial temperature,

freezing process,

study of final sample characteristics at end of freezing.

4.1.7.1. Choice of Sample Characteristics

To standardize our tests, we adapted, to the dimensions of our cell, the operating procedure of the standard Proctor test being used by the Department of Bridges and Highways (23). For each soil and for a given energy, the dry density γ_d of this soil (that is to say, the ratio between the weight of the dry matter and the total volume) is a function of the initial water content. This curve reveals a maximum for a water content value called "optimum water content." We made our examples with this water content.

4.1.7.2. Placement of Soil in Experimental Cell

The material is compacted directly in the tronconic housing of the freezing cell according to the operations described below. In order not

to interfere with the possible swelling of the soil, it is necessary to reduce the friction between the sample and the cell walls to a maximum. For that purpose, the tronconic housing is coated with a layer of fat; this layer of fat [grease] is covered by thin circular strips of transparent paper greased on both sides; these horizontally arranged strips are several millimeters high. The cell is then put in place, the lower piston is filled with water coming from the water table, and the porous pastille, arranged on the latter, is saturated beforehand. The water table is closed and the material is then compacted by layers of 2 cm for the number of impacts of the compacting rammer calculated according to the desired compacting. Once the soil is compact, we determine precisely the compacting characteristics which figure in the tables preceding the description of the results.

4.1.7.3. Sample Soaking and Establishment of Initial Temperature

The oil level in the water table is arranged at the height of the top of the sample. The water table [underground water level] is opened at the same time as the establishment of the temperature (around 0.5° C). When the oil-water meniscus no longer moves in the burette, the sample is presumed to be saturated.

4.1.7.4. Freezing Process

The temperature is lowered abruptly to the value desired in the upper piston. Freezing begins.

4.1.7.5. Study of Final Sample Characteristics

At the end of the freezing experiment, the sample is taken out of its housing; the structure of the sample is then observed directly. The sample is then cut up into slices whose water content W_e and whose dry density γ_d we determined.

4.2. The Permeameter

The determination of the interstitial pressure in the vicinity of the freezing front, on the basis of Darcy's Law, implies a knowledge of the permeability of the soil we are experimenting with. In our freezing experiments, we used pulverulent artificial soils. The measurement of the permeability of such soils by means of conventional permeameters cannot be accomplished here and so we had to perfect a special permeameter for unconsolidated media.

The permeameter perfected for this study is so designed that we can measure the permeability of materials in two different cases:

the materials are compacted directly in the sample carrier of the permeameter,

the materials are compacted in the freezing cell and are subjected to a freezing process.

The unfrozen portion of the sample is then taken out and put on the permeameter's sample carrier.

4.2.1. Description of Permeameter

4.2.1.1. Sample Carrier

This is a tronconic cylinder (1, Figure 10) made of plexiglass, with a conicity equal to one degree, 20 cm long, with the smaller diameter being 4 cm. To the ends of the cylinder we attach two flanges on which we adjust two lids (2 and 3, Figure 10) made up of two plexiglass discs, with toric joints assuring tightness; these discs are pierced in the center so as to permit the passage of sliding fixation rods for the pistons (4 and 5, Figure 10). Two pistons (6 and 7, Figure 10), provided with porous pastilles, to permit the water flow, serve to hold the sample. These pistons attached to the end of the sliding rods have different diameters so that they can adapt to the two levels of the cell which determine the height of the sample. The rods are attached to the lids by means of staples (8 and 9, Figure 10) and screws.

4.2.1.2. Supply and Flowback Tanks (Figure 11)

Two receptacles (burettes) (1 and 2, Figure 11), containing distilled and deaerated water, are connected by pipes to the two ends of the cell. The water level is kept constant and equal in the two receptacles. The first receptacle communicates with a graduated burette by means of an overflow tube.

In the second receptacle, the level is kept constant manually by opening a valve which establishes communication between this receptacle and a tank (3, Figure 11) containing deaerated and distilled water and where the same depression prevails as in the receptacle. The depressions [reduced pressures] p_1 and p_2 which prevail in each of the two receptacles are different and remain constant throughout the test.

4.2.1.3. System for Measuring the Water Flow Rate Going Through the Sample (Figure 11)

The flow rate is measured in two different ways: a first, rough measurement by means of the graduated burette of the overflow tube. A second, precise measurement using the displacement of the air bubble in a calibrated tube (Figure 11) with a diameter of 3 mm and a length of 80 cm.

4.2.1.4. Pressure Measurement

Three pressure gauges (5, 6, 7, Figure 11) indicate the upstream and downstream pressure and their difference which is applied to the two ends of the sample. A set of three-way valves makes it possible--by inverting the direction of flow in the sample--to switch from the saturation process to measurement as such, that is, the measurement of the permeability.

A mercury flask and two valves (V_1 and V_2) make it possible with precision to control the pressure declines imposed upon the system and obtained with the help of a vacuum pump. The air is dried prior to its entry into the circuit through its passage into a flask containing grains of silica gel.

4.2.1.5. Pressure Regulators

While putting the installation together, we ran into one particular difficulty: it consisted in eliminating the "preferential paths" taken by the fluid; as a matter of fact, not only could the latter flow between the sample and the walls, but the flow could also involve only a portion of the sample's cross-section. For experiments conducted at overpressure with respect to atmospheric pressure, the coloration of the fluid revealed that fact.

To remedy this situation, we had to make measurements "at reduced pressure," with pressures lower than atmospheric pressure and pressures of different values being applied on either side of the sample; thus the grains have a tendency to stick to the cell wall.

Another difficulty consisted in maintaining a constant pressure decline difference, down to almost 1/10 mm mercury. For that purpose we designed and built a regulating system.

A glass tube T_i (Figure 11)--a certain length of which is dipped into the mercury contained in a flask--is connected at atmospheric pressure with the help of a micrometric valve V_i, the submerged length of this tube is calculated in accordance with the pressure difference which we want to impose upon the sample. A second glass tube T_2, placed above the mercury, is connected to a micrometric valve V_2 which is linked to the vacuum pump.

Above the mercury we have pressure p2 created by the vacuum pump and regulated by valve V_2. In tube T_i we have pressure p_1 which is greater then p_2. At any moment we have:

$$p_1 = p_2 + \Delta_p$$

p_2 which is created by the vacuum pump and valve V_2 has a tendency to diminish and p_1 which is the pressure in the container linked to the atmosphere by means of valve V_1 has a tendency to go up. If P_2 diminishes, an air bubble escapes from tube T_1, goes up the mercury, and equilibrium is restored.

4.2.2. Operating Procedure

The soil sample is put in place and we establish the flow in direction AB up to the complete saturation of the sample. Once the sample is saturated, we reverse the direction of flow in the sample; the reversal is accomplished by means of three-way faucets which enable us to maintain

the initial flow direction in the rest of the circuit. To make the measurement, we wait for the establishment of the permanent state.

4.2.3. Apparatus Test

We repeated the same experiment under the same pressure and ambient temperature conditions (the measurement room is airconditioned) and we obtained similar permeability values.

In the course of one experiment, we modified the pressure difference at the sample terminals (5, 10, 15 cm of mercury) and we found a very small difference between these measurements.

4.3. Study Installation for Interstitial Pressure Measurement

The installation comprises the following:

a study cell derived from the thermal study cell which we had modified for our study,

some of the measurement systems already described in our first installation,

a system for the measurement of interstitial pressures.

To find the value of the interstitial pressure in the soil samples with greater precision than by means of the instruments already used--and which we described in paragraph 2.2.2.--we adapted, to the freezing problem, the improvements made in the measurements of the interstitial pressures in porous media. The work of L. A. Richards (21) was the first to demonstrate the usefulness of employing a porous element (tensiometer) with a measurement instrument to find the interstitial pressures in the soils; since then, researchers have kept improving this system (22). We were thus persuaded to perfect a system involving a tensiometer and a pressure translator appropriate for our soils and our measurements.

The shape of the tensiometer is determined by the place where we must put it with respect to the soil in order to make the measurement.

If the permeability of the soils is low, the interstitial pressure value, measured even at a small distance from the freezing front, is different from its real value on the latter's level; we thus try to introduce the porous element into the interior of the soil sample so that the freezing front would traverse that element in the course of its displacement. This made us use tensiometers in the shape of porous needles and slightly to modify the freezing cell which we had used for the study of the heat problem.

4.3.1. Study Cell

We will now describe the changes made in the heat study cell.

4.3.1.1. Choice of Tensiometer Emplacement

There are three possibilities for introducing the tensiometer into the soil sample:

through the upper piston: the upper piston is mobile to permit the swelling of the soil; moreover it is traversed by a liquid (alcohol) at a temperature on the order of -10° C. The tensiometer and the connecting tubulature would be subjected to a high thermal gradient (the temperature is 0° at the freezing front); moreover, the mobility of the piston would create problems in terms of tightness. We therefore rejected this possibility.

Through the lower piston: since the sample is supplied through the lower piston, the passage, into this piston, of a tensiometer would lead to a reduction in the latter's dimensions which in turn would contribute to increasing the response time of the apparatus.

Through the lateral walls: this solution persuaded us to modify the freezing cell.

4.3.1.2. Description of Cell (Figure 12)

This cell is identical from the viewpoint of dimensions to the cell already described in connection with the heat problem study. It comprises three concentric cylinders. The first inside cylinder is tronconic, the [air, water] tight chamber is between the latter and the second; the third outside cylinder, with the latter, constitutes the thermostat-controlled envelope (1, Figure 12). This envelope in this case is thus an integral part of the cell. It helps increase the unidimensionality of the phenomenon but it also helps thermostat-control the connecting circuit of the measurement system which to a great extent is housed in the latter. Three telescopic tubes, made of plexiglass, with an inside diameter of 18 mm (2, 3, Figure 12) are glued upon these cylinders in three places at different heights, with the axes of these tubes forming [an angle] of 120° between them in the horizontal planes. The respected position of these tubes with regard to the top of the cell is 10, 16, and 20 cm. The position of the cold face with respect to these tubes can be variable (between 2 and 8 cm with respect to the place of the highest tube); by repeating the freezing test under the same conditions but by modifying the height of the soil sample, this enables us to measure the interstitial pressure at several different heights in the sample.

The cell comprises a device which makes it possible to establish the response of the tensiometer "on the spot" in the soil. This device is similar to the one described in paragraph 4.2.1.1. and comprises a lid (2, Figure 10) consisting of a disc which is pierced in the center, permitting the passage of a sliding rod to whose end there is attached a piston. The latter--provided with a porous pastille so as to permit waterflow--serves to hold the sample. The rod is attached to the lid by means of a staple and screws. While measuring the response of the

tensiometer "on the spot," the piston is attached above the soil sample and the top of the cell above the sample is filled with water in which we establish constant pressure.

4.3.1.3. Measurement Systems

The cell is equipped with all measurement systems already described for the heat problem study cell, with the exception of thermocouples glued to the lateral wall. It furthermore comprises a measurement system for the interstitial pressures.

Principle of tensiometer

The study of water movements (23) in a moist porous medium is conditioned by a knowledge of the free energy potential gradients causing them [the movements]. To find out what these potentials are, we must use a measurement instrument that can be locally placed into an equilibrium [which can locally be balanced] with the water that surrounds it and which would materially express its free energy level.

The water tensiometer consists of a small water tank, limited with relation to the medium by a porous wall and whose pressure state is measured by a measurement apparatus (pressure gauge or electrical pressure detector, etc.) to which it is linked by a connecting circuit L.

The water has two functions:

It assumes a pressure equilibrium with the average phase of the water of the soil in its vicinity. This establishment of equilibrium is accomplished through transfer across [through] the porous wall P which permits the water locally to filter into the soil without air entering the tank when the pressure decline increases;

It hydrostatically transmits the pressure to be measured at the measurement apparatus.

The establishment of the equilibrium between the measurement instrument and the medium requires a transfer of water through the porous capsule. The quality of the tensiometric measurement will depend on the speed and volume of this transfer.

Considerations on the functioning of tensiometers

Response of tensiometer in free water

The analysis of the tensiometer's response in free water shows that the system, which enables us more accurately to figure out the variations in tension or pressure in the medium surrounding the capsule, is the one which offers the smallest response time constant

$$\tau = 1/K's$$

where $1/\tau$ is the slope at the origin of the curve representing the equation

$$\Psi_T = \Delta\Psi \cdot (1-e^{-t/\tau})$$

$\psi_T^{(t)}$ being the pressure inside the porous capsule and Δ_{ψ_0} being a pressure echelon. [blank space in photostat] thus appears as the product of two characteristics, K' being the conductance [anode] of the porous capsule and S being the sensitivity of the pressure translator (as a matter of fact, the influence of the connecting circuit upon the response dynamics is far from negligible).

The search for a reduced τ thus persuades us to use the porous capsule with the greatest possible conductivity; but there is one limitation and that is the air entry pressure. This pressure, called critical pressure, is the pressure decline beyond which the water can enter the pores of the capsule. The study of the circuit's influence shows that the circuit tends to reduce the translator's sensitivity; it leads to the use of connecting circuits with great rigidity.

The sensitivity of the translator (or of the measurement apparatus in general) is, by definition, the ratio between the pressure variation indicated by the translator Δ_ψ and the water volume necessary ΔV for this translator so that the indicated pressure would vary by [illegible symbol]. A translator becomes more satisfactory in a mounting if the coefficient S is greater; there are two reasons for that:

the response speed $\tau = 1/K'S$;

the displacement of the smallest possible water volume so as not to modify the measurement conditions (in the case where the porous needle is implanted in the soil).

tensiometer response in porous medium.

The theoretical study of the tensiometer's response in a porous medium shows that the latter is influenced by the characteristics of the soil, that is to say, the volume content of water, the capillary conductivity, and the diffusiveness.

The study recommends the experimental determination of the tensiometer response "on the spot."

Description of measurement system chosen (figures 13, 14)

The porous capsule. We used hollow aluminum "cartridge" tubes closed off at one end (1, Figure 13). These cartridges are 32 mm long and their outside diameter is 7 mm.

The device for mounting the pressure translator (Figure 14) involves a cylinder (1, Figure 14) made of inoxidable steel with a diameter of 26 mm and a height of 21 mm. This cylinder is threaded on the inside over a height of 6 mm. The translator is screwed into this cylinder and tightness is assured by a toric joint. The water volume contained in this cylinder is about 2 cm^3.

The cylinder is perforated by two holes which are diametrically opposed and which have a diameter of 3 mm. Two metal tubes with a length of 15 mm are welded to the cylinder around these holes.

On these tubes are attached the branches of valves R_1 and R_2.

Connecting tubulature (Figure 13). We used the most rigid and the shortest possible connecting circuit. We made two different mountings, the first one permitting the simultaneous measurement of the interstitial pressure in the vicinity of the freezing front, the second one permitting the latter's measurement at two different points with a single pressure translator.

The porous "cartridges" are glued for 2 or 3 mm (Figure 13) with an epoxy glue on plexiglass tubes. These tubes (2, Figure 13) have the same diameter as the "cartridge" over several millimeters of length. This small-diameter length, covered with a cement [mastic] on a base of silicons (silastene) penetrates with the porous element into the soil sample; this is done to permit better tightness between the latter and the tensiometer. The plexiglass tube diameter then increases to 10 mm over a total length of 70 mm. This shoulder makes it possible to apply silastene to the outside wall of the tronconic cylinder where we have the soil sample. The inside diameter of the plexiglass tube is 3 mm. The assembly consisting of cartridge and plexiglass tube may be dismantled [taken down] with a view to saturating the porous element in a vacuum.

Measurement of interstitial pressure at two different points on sample

The tube T_1 (figure 13) is then connected to a three-way valve made of glass and Teflon with a passage diameter of 2.5 mm. Connection is proviced by means of a rigid tube. A second tube T_2 identical to the first one is connected by a rigid tube to the second branch of valve (illegible); the third branch is glued on the cylinder (1, Figure 13) which carries the translator.

With valve [illegible] we establish connection between the translator and circuit I (Figure 13) because, when the freezing front arrives on the level of the cartridge of the first circuit, connection is established with circuit II (Figure 13).

Measurement of interstitial pressure at a given point

For this measurement, we eliminate valve R_2 and the tensiometer is connected directly to the translator.

Experimental characteristics of measurement system

The diameter of the cartridge pores is on the order of 2-4 [illegible symbol; mu?], and the value measured for the conductance of the cartridge is on the order of 6.10^{-4} cm^3/s m bar. The critical air entry pressure measured is on the order of 400-500 m bar. The tensiometer response time in free water is several seconds.

Figure 15 shows the response of the tensiometer in place. The translator is of the membrane type; the latter's diameter is 10 mm, the

measurement range is between 0 and 1 bar absolute. The sensitivity coefficient corresponds to a volume variation of 1/3 mm^3 for a pressure of 1 bar.

4.3.2. Operating Procedure

System assembly. The porous cartridges are saturated in a vacuum. The connecting tubulature, the valves, and the pressure translator are then assembled in previously distilled and deaerated water.

Water circulation is then induced in the direction of the porous cartridge toward the outlet valve R_1. When there are no more air bubbles visible in the circuit, valve R_1 is closed.

Tensiometer mounting. The translator is then connected to the measurement tension adaptor and the system is equilibrated. The pressure indicated is atmospheric pressure. When the soil sample is saturated (when the water-oil meniscus no longer moves in the burette of the water table), a forehole with a diameter 6.5 mm smaller than the cartridge diameter is perforated on the levels where we desire to measure the interstitial pressure. The plexiglass tube is then covered with silastene and the tensiometer is introduced into the soil sample. The free space left between the measurement system and the freezing cell is filled with silastene.

Once equilibrium has been attained (the recorder then indicates the atmospheric pressure value), we start freezing the sample as indicated earlier.

5. EXPERIMENTS CONDUCTED

In the following we will present:

the experimental conditions and the characteristics of all artificial soil samples in the course of freezing tests conducted;

the evolution of all parameters which come up in the course of a soil freezing test;

the interstitial pressure measurement results in the course of freezing tests conducted on two soils;

the results obtained during freezing tests performed with three different soils.

5.1. Experimental Conditions and Soil Characteristics

5.1.1. Experiments To Study Heat Problem and Indirect Determination of Interstitial Pressure

We conducted five experiments with three different soils. Experiments I and II were conducted with artificial soil No. 1 which consists of a

mixture of 10% mineral talc and 90% pure silica powder. We gave that soil, for experiments I and II, compacting characteristics close to those shown in Table A (I, II); we gave the cold face a temperature of -3° C during experiment I and -8° C during experiment II.

Experiment III was performed with artificial soil No. 2 which consists of a mixture of 30% mineral talc and 70% pure silica powder.

Experiments IV and V were performed with soil No. 3 which is made up of a mixture of 50% mineral talc and 50% pure silica powder.

The soil samples for exeriments I, II, III, and IV were prepared according to the operating procedure described in paragraph 3.1.7. and for "optimum" water content.

For experiment V, we made up the soil sample with arbitrary water content and compacting energy so as to modify the dry density of the sample quite noticeably.

The grain size curves of the soils studied are given in figures 3 and 4.

Figure 16 shows the evolution of the dry density γ_d as a function of the water content [illegible symbol] for soil No. 3 and for the energy corresponding to the operating procedure described in paragraph 3.1.7.

The characteristics of the samples before and after soaking are given in the following tables:

A (I, II) and B (I, II), respectively, before and after soaking for soil No. 1;

C (III) and D (III), respectively, before and after soaking for soil No. 2.;

E (I, V) and F (IV, V), respectively, before and after soaking for soil No. 3.

TABLE A (I, II)

characteristics of samples

soil No. 1; mixture of 10% mineral talc powder + 90% pure silica powder

		Expérience I	Expérience II
2	hauteur	$2,18 \times 10^{-1}$ m	$2,12 \times 10^{-1}$ m
3	diamètre de la face froide	$4,97 \times 10^{-2}$ m	$4,96 \times 10^{-2}$ m
4	diamètre de la face chaude	$4,21 \times 10^{-2}$ m	$4,21 \times 10^{-2}$ m
	volume	345×10^{-6} m^3	335×10^{-6} m^3
5	masse volumique P_L	$1,818 \times 10^{3}$ kg/m^3	$1,780 \times 10^{3}$ kg/m^3
6	masse volumique des grains du mélange γ_s	$2,655 \times 10^{3}$ kg/m^3	$2,655 \times 10^{3}$ kg/m^3
7	teneur en eau W_e	0,20	0,20
8	indice de vide e	0,7617	0,7844
9	degré de saturation S_r	0,7006	0,6770
10	densité sèche γ_d	1,51 kg/m^3	150 kg/m^3
11	perméabilité mesurée k	$10,4 \times 10^{-11}$ cm^2	$10,4 \times 10^{-11}$ cm^2

Legend: 1--experiment; 2--height; 3--cold face diameter; 4--hot face diameter; 5--weight per volume; 6--weight per volume of grains of mixture; 7--water content; 8--vacuum index; 9--saturation degree; 10--dry density; 11--permeability measured.

TABLE B (I, II)

characteristics of samples after period of soaking

Soil No. 1; mixture of 10% mineral talc powder + 90% pure silica powder

		Expérience I	Expérience II
2	hauteur initiale L_i	$2,185 \times 10^{-1}$ m	$2,124 \times 10^{-1}$ m
3	masse volumique initiale P_{Li}	1,90 kg/m^3	1,87 kg/m^3
4	teneur en eau initiale W_{ei}	0,260	0,256
5	degré de saturation S_{ri}	0,9097	0,8665
6	porosité ε	0,4323	0,4402

Legend: 1--experiment; 2--initial height; 3--initial weight per volume; 4--initial water content; 5--degree of saturation; 6--porosity.

TABLE C (III)

sample characteristics	Soil No. 2; mixture of 30% mineral talc powder + 70% pure silica powder
0 hauteur	2.100×10^{-1} m
2 diamètre de la face froide	4.96×10^{-2} m
3 diamètre de la face chaude	4.21×10^{-2} m
volume	331×10^{-6} m^3
4 masse volumique P_L	1.798×10^3 kg/m^3
5 masse volumique des grains du mélange γ_s	2.665×10^3 kg/m^3
6 teneur en eau W_e	0.17
7 degré de saturation S_r	0.5916
8 densité sèche γ_d	1.53 kg/m^3
9 perméabilité mesurée	5.9×10^{-11} cm^2

Legend: 1--height; 2--cold face diameter; 3--hot face diameter; 4--weight per volume; 5--weight per volume of grains of mixture; 6--water content; 7--saturation degree; 8--dry density; 9--permeability measured.

TABLE D (III)

characteristics of sample after period of soaking	Soil No. 2
1 hauteur initiale L_i	2.115×10^{-1} m
2 masse volumique initiale P_{Li}	1.970×10^3 kg/m^3
3 teneur en eau initiale W_{ei}	0.332
4 degré de saturation S_{ri}	1
5 porosité ε	0.47

Legend: 1--initial height; 2--initial weight per volume; 3--initial water content; 4--degree of saturation; 5--porosity.

TABLE E (IV, V)

characteristics of samples — Soil No. 3; mixture of 50% mineral talc powder + 50% pure silica powder

		① Expérience V	② Expérience IV
2	hauteur	$2{,}162 \times 10^{-1}$ m	$2{,}20 \times 10^{-1}$ m
3	diamètre de la face froide	$4{,}97 \times 10^{-2}$ m	$4{,}97 \times 10^{-2}$ m
4	diamètre de la face chaude	$4{,}21 \times 10^{-2}$ m	$4{,}21 \times 10^{-2}$ m
	volume	340×10^{-6} m^3	341×10^{-6} m^3
5	masse volumique P_L	$1{,}747 \times 10^3$ kg/m^3	$1{,}797 \times 10^3$ kg/m^3
6	masse volumique des grains du mélange γ_s	$2{,}675 \times 10^3$ kg/m^3	$2{,}675 \times 10^3$ kg/m^3
7	teneur en eau W_e	0,18	0,15
8	indice de vide e	0,8087	0,7089
9	degré de saturation S_r	0,5954	0,5660
10	densité sèche γ_d	1,48 kg/m^3	1,57 kg/m^3
11	perméabilité mesurée $\frac{D}{R}$	$4{,}1 \times 10^{-11}$ cm^2	2×10^{-11} cm^2

Legend: 1--experiment; 2--height; 3--cold face diameter; 4--hot face diameter; 5--weight per volume; 6--weight per volume of grains of mixture; 7--water content; 8--vacuum index; 9--saturation degree; 10--dry density; 11--permeability measured.

TABLE F (IV, V)

characteristics of samples after period of soaking — soils studied

		① Expérience V	② Expérience Iv
2	hauteur initiale L_i	$2{,}178 \times 10^{-1}$ m	$2{,}22 \times 10^{-1}$ m
3	masse volumique initiale P_{Li}	1,880 kg/m^3	1,976 kg/m^3
4	teneur en eau initiale W_{ei}	0,27	0,265
5	degré de saturation S_{ri}	0,8931	0,9980
6	porosité ε	0,447	0,4131

Legend: 1--experiment; 2--initial height; 3--initial weight per volume; 4--initial water content; 5--saturation degree; 6--porosity.

5.1.2. Experiments for Direct Measurement of Interstitial Pressure

Earlier we showed--in observing, on the cathetometer, the evolution of tracers arranged at different levels in the sample--that the artificial soils, which we use, are not susceptible to becoming consolidated under our experimental conditions; moreover, the permeability of these soils is within an average spread of values as compared to natural soils which are very little permeable and susceptible to consolidation, such as clays; these two considerations, combined with the fact that the indication of the pressure decline state of the medium by the measurement system, demands a water transfer from the tensiometer's tank across the porous element of the latter, did not enable us to measure the interstitial pressures in the vicinity of the freezing front in an open system (where the sample is supplied through the water table [underground water level]). We know furthermore that the soils, with which we experimented, do not begin to swell up until after a given period of time and for a given value of the abscissa x_f of the freezing front; this happens because of the critical speed corresponding to the imposed heat state.

To be able to compare the order of magnitude of the values measured and the values calculated for the interstitial pressure at the freezing front, based on Darcy's Law, we positioned our tensiometer at a distance from the cold face near the value x_f known, for each soil experimented with and corresponding to a well determined heat condition [rate]; thus, when the freezing front reaches the level of the tensiometer, the distribution of the water content in the unfrozen zone is practically not disturbed and this happens for the following reasons:

the swelling of the soil at the moment the freezing front touches the tensiometer is still very minor;

because of the relatively average value of the permeability, the disturbance of the medium's saturation, caused by the water volume transferred in correspondence to that swelling, involves the entire unfrozen zone;

the unfrozen zone has a volume equal to several times that of the frozen zone.

We performed two experiments VI and VII with soils No. 2 and No. 3. Tables G (VI, VII), as well as H (VI, VII) show the compacting characteristics of soils No. 2 and No. 3, respectively, before and after soaking.

They furthermore show--for the heat state which imposes a temperature of -8° C at the cold face--the value x_f of the abscissa of the front with respect to the initial level of the cold face at which each soil begins to swell up, as well as the distance chosen for each soil from the position of the measurement tensiometer with respect to the cold face.

Since the measurements are made in a closed system, the operating procedure is strictly identical to the earlier experiments (I, II, III, IV, V), except that, at the end of the sample saturation period and the tensiometer equilibrium establishment period, the underground water level is closed (closed system).

TABLE G (VI, VII)

① caractéristiques des échantillons	2 sol n° 2 3 Expérience VI	2 sol n° 3 3 Expérience VII
4 hauteur	$2,313 \times 10^{-1}$ m	$2,285 \times 10^{-1}$ m
5 diamètre de la face froide	$5,02 \times 10^{-2}$ m	$5,02 \times 10^{-2}$ m
6 diamètre de la face chaude	$4,21 \times 10^{-2}$ m	$4,21 \times 10^{-2}$ m
7 distance de la face froide au 1er tensiomètre	$5,085 \times 10^{-2}$ m	$4,838 \times 10^{-2}$ m
8 cote χ_f à laquelle le sol commence à gonfler	40×10^{-3} m	38×10^{-3} m
volume	369×10^{-6} m^3	$365,45 \times 10^{-6}$ m^3
9 masse volumique P_L	illegible	$1,721 \times 10^3$ kg/m^3
10 masse volumique des grains du mélange γ_s	$2,655 \times 10^3$ kg/m^3	$2,675 \times 10^3$ kg/m^3
11 teneur en eau W_e	0,17	0,18
12 indice de vide ε	0,7083	0,8322
13 densité sèche γ_d	1,56 kg/m^3	1,46 kg/m^3
14 degré de saturation S_r	0,6396	0,5783

Legend: 1--characteristics of samples; 2--soil; 3--experiment; 4--height; 5--cold face diameter; 6--hot face diameter; 7--distance between cold face and first tensiometer; 8--level χ_f at which soil begins to swell up; 9--weight per volume; 10--weight per volume of grains of mixture; 11--water content; 12--vacuum index; 13--dry density; 14--saturation degree.

TABLE H (VI, VII)

① caractéristiques des échantillons après la période d'imbibition	② sol n° 2 Expérience VI ③	② sol n°3 Expérience VII ③
④ hauteur initiale L_i	$2{,}329 \times 10^{-1}$ m	$2{,}304 \times 10^{-1}$ m
⑤ masse volumique initiale ρ_{Li}	$1{,}985 \times 10^{3}$ kg/m^3	$1{,}857 \times 10^{3}$ kg/m^3
⑥ teneur en eau initiale W_{ei}	0,28	0,27
⑦ degré de saturation S_{ri}	1,065	0,8740
⑧ porosité ε	0,4230	0,4542

Legend: 1--characteristics of samples after period of soaking; 2--soil; 3--experiment; 4--initial height; 5--initial weight per volume; 6--initial water content; 7--saturation degree; 8--porosity.

5.2. Presentation of Different Parameters Involved During a Freezing Test

We will now present the evolution of all of the parameters which we followed in the course of a complete soil freezing test. We selected experiment V involving soil No. 3.

Figure 17 represents the abscissa $x^I_F (x^1_F = x_F + x_G)$ of the freezing front referenced with respect to the mobile cold face in terms of time as well as the abscissa x_F of the freezing front referenced with respect to the initial fixed position of the cold front prior to freezing.

Figure 18 shows the volume of water aspirated during the freezing and the volume is measured in the supply burettes of the water table.

Figure 19 shows the swelling [heave] x_G of the sample in terms of time.

The behavior of the tracers during the test is represented in Figure 20. The distribution of the water content in the various slices of the sample, as well as the distribution of the dry density in the different slices of the unfrozen zone at the end of the experiment, are illustrated in Figure 21. Figure 22 shows the variation as a function of the time in the heat flow going through the old face and measured with the help of the flowmeter of the piston.

The evolutions of the sample temperatures during the experiment are illustrated in Figure 23. The abscissas x corresponding to the measurement points are referenced with respect to the initial position of the cold face. For a given instant, the abscissa x' of any point, counting as of the cold face, will be $x^1 = x + x_G$ taking into account the swelling x_G.

5.3. Interstitial Pressure Measurement

Tables G (VI, VII) and H (VI, VII) show the characteristics of soils No. 2 and No. 3 experimented with during experiments VI and VII, respectively. These tables indicate the position of the measurement tensiometer with respect to the initial level of the cold face; moreover, they indicate the level [illegible symbol] at which each of these soils begins to swell up in the case of the established heat condition [state] and which corresponds to a cold face temperature of -8° C.

The examination of tables G (VI, VII), H (VI, VII), C (III), D (III), and E (V), F (V) shows that, during experiments III and IV, soil No. 2 reveals closely related characteristics; the same is true of soil No. 3 during experiments V and VII.

Figure 24 illustrates the evolution of the interstitial pressure at the mobile freezing front, indicated by the pressure translator connected to the measurement tensiometer.

It shows the interstitial pressure values when the freezing front reaches the tensiometer level and the values calculated in the earlier experiments and corresponding to the same level in the soil sample. We find that these values are on the same order of magnitude.

5.4. Interpretation of Results

The observation of the behavior of the tracers (Figure 20) during the freezing tests which we conducted reveals, on the one hand, that these tracers retain their initial level when they are not reached by the freezing front and that, on the other hand, throughout the entire duration of the experiment, the level of these tracers is not modified in the sample's unfrozen zone.

The combined observation (Figure 21) of the distribution of the dry density at the end of the experiment in the different slices of the sample's unfrozen zone shows that the latter remains practically constant.

These two facts caused us to consider that the soils, which we subjected to freezing under previously described experimental conditions, are not of the consolidable type. Consequently, to determine the evolution of the interstitial pressure at the freezing front, we applied the exploitation of Darcy's Law to the case of nonconsolidable soils as described in paragraph 3.1.1.

5.4.1. Influence of Heat State

Tables A (I, II) and B (I, II) show the compacting characteristics of soil No. 1 for the two experiments I and II; we note that these characteristics are closely related. Figure 25 shows the evolution, as a function of the abscissa x_F, of the freezing front, of the interstitial pressure p_i in the vicinity of the latter, referenced with relation to the atmospheric pressure Pa. At a given level of the sample and consequently for the same height of the unfrozen zone, we can see that the pressure difference at the ends of this zone is constantly greater for experiment II. We must thus expect--in view of the fact that the permeability of the soil is the same in experiments I and II--that the soil would be more freezable in the course of experiment II.

Figure 26 shows the evolution in terms of time for the swelling speed $v_G = dx_G/dt$ for these two experiments; we can see that this speed, contrary to what we anticipated, is at any moment less for experiment II. This apparently contradictory fact is explained if we consider the speeds of the freezing front advance $v_F = dx_F/dt$ in the course of these experiments; as a matter of fact, Figure 27 shows the evolution in terms of time of the abscissa x_F of the freezing front and of the swelling x_G for experiments I and II; at a given level of the sample, the slopes of curves I and II represent the freezing front speeds v_F ; we note that v_F is at any point greater in the course of this latter experiment and we therefore get a greater swelling. A leeway [interplay] now develops between the pressure gradient created by the heat state imposed on the sample and the freezing point advance speed; we can now easily realize that, under certain conditions, their ...[bottom of photostat page missing].

The theory (12, 14, 6, 5) provides that the swelling x_G is linear with respect to the square root of the freezing index $\sqrt{I}$. Figure 28 shows the duration during which which this linearity remains valid in the course of experiments I and II; we note that, for experiment I, in the course of which the soil has a more freezable character, the slope

$\Delta x_G / \Delta \sqrt{I}$ is higher.

5.4.2. Influence of Grain Size

Figure 29 shows the evolution in terms of time of the swelling speed v_G for experiment II involving soil No. 1 and for experiment III involving soil No. 3; these experiments were performed under the same thermal conditions (the cold base temperature is equal to $-8^{\circ}C$ sic); we note that v_G is at any moment higher for soil No. 3 which contains a higher proportion of fines (talc) (30%).

Figure 30 shows, for the two soils, the evolution, in terms of time, of the interstitial pressure p_i at the freezing front, referenced with respect to the atmospheric pressure; we can see that the interstitial pressure is at any moment less in terms of absolute value for soil No. 3 which has the finer grain size.

Figure 31, which, for the two earlier soils, shows the swelling x_g as a function of the square root of the freezing index, again reveals the more accentuated freezable character of soil No. 3.

5.4.3. Influence of Dry Density

Tables E (IV, V) and F (IV, V) show the compacting characteristics of soil No. 3 for the two experiments IV and V; the examination of these tables indicates that soil No. 3, made up of 50% mineral talc and 50% pure silica powder, has a much smaller dry density and a higher permeability in experiment V. The two experiments were performed under the same thermal state (the cold face temperature is -8° C).

The examination of figures 20 and 32, illustrating the evolution of the abscissa x_f of the freezing front in terms of time, shows that the freezing front advance speed v_F is close in experiments IV and V.

Figure 33 illustrates the evolution in terms of time of the interstitial pressure p_i, referenced with respect to the atmospheric pressure Pa, in the vicinity of the freezing front, for experiments IV and V; we note that the interstitial pressure, in terms of absolute value, is at any moment smaller during experiment IV, where soil No. 3 has a higher dry density.

The increase in the dry density in a soil with a given grain size contributes to the diminution in the diameter of the pores in this soil. Figure 33 shows that its influence is expressed--as in the case of the increase in the percentage of fines (talc) (see paragraph 5.4.2.)--in a diminution of the absolute interstitial pressure value.

The freezing front advance speeds are closely related in experiments IV and V; at a given height [level] L of the sample, Figure 33 shows that the pressure difference $P_a - p_i(L)$ between this level and the sample is greater for experiment IV. Figure 34 shows the evolution in terms of time of the swelling speed in experiments IV and V; this speed is always greater for experiment V.

This apparently contradictory result is explained by the fact that the permeability is much weaker in the zone traversed by the flow during experiment IV; the supply of the thin sheets of ice on the freezing front level is therefore rendered more difficult. A leeway [interplay] now develops between the freezable character imposed by the dimensions of the pores and the permeability of the medium; for a range of variation in the dry density it thus happens that the tendencies are reversed.

Figure 35 shows the range for each experiment where the linearity between the swelling and the square root of the freezing index provided for by theory (12, 14) remains valid.

5.4.4. Influence of Specific Surface and Percentage of Fines

Figure 36 illustrates the evolution of the swelling x_g as a function of the percentage of fines and the specific surface at different instants

in the course of the experiments. These experiments are performed with samples put in place with the same compacting energy and for "the optimum water content" involved in the operating procedure of the standard Proctor [test] (23) [deleted by hand entry on photostat], as described in paragraph 4.1.7. We note that the freezability increases with the percentage of fines but tends to decrease as a result of the diminution in the soil's permeability (24) [hand-entered deletion].

The specific surfaces of the soils are calculated on the basis of the Kozeny-Carman formula, where the permeability value is the value measured for each soil by means of the permeameter. Figure 37 shows the evolution of the slopes $\Delta\chi_G/\Delta\sqrt{I}$ as a function of the percentage of fines and the specific surface.

5.4.5. General Relations

Figures 38 and 39 illustrate the evolution of the swelling speed [illegible; v_g], as a function of the absolute interstitial pressure in the vicinity of the freezing front for soil No. 2 and for experiment V involving soil No. 3. The heat state in the two experiments is the same and corresponds to a temperature of -8° C imposed upon the cold face. The theory of K. A. Jackson, D. R. Uhlmann, and B. Chalmers calls for a soil made up of grains having the same diameter, where the speed [blank space in photostat] is inversely proportional to the pressure [blank space in photostat].

Finally, Figure 40, which illustrates the variation in the linear pressure $\Delta(P_a - p_i)/\Delta(L - \chi_F)$ as a function of the variation $\Delta\sqrt{I}/\Delta\tau$ in the course of time in the square root of the freezing index [blank space in photostat] for one of the soils studied, [shows] that these magnitudes vary in a linear manner in the course of a relatively long period of time in the freezing experiment.

6. CONCLUSION

In this thesis we assumed the existence of a pressure drop which would appear on the level of the freezing front in a fine soil sample subjected to unidimensional freezing.

We worked out a calculation method based on Darcy's Law which enables us to determine the interstitial pressure in the unfrozen zone of soils of the consolidable and nonconsolidable type.

To apply this law we had to perfect a special permeameter for nonconsolidated pulverulent media. The experiments performed enable us to verify certain theoretical results obtained by K. A. Jackson, D. R. Uhlmann, and B. Chalmers in 1966. During these experiments we determined the evolution of the interstitial pressure in the vicinity of the freezing front in artificial soil types [typical artificial soils] and we studied the influence of the various parameters which are involved during the freezing upon the interstitial pressure and the swelling speed of these soils.

Finally we perfected a system for the measurement of the interstitial pressure which enabled us to show the existence of pressure drops on the level of the freezing front and to compare, under the same thermal conditions, the interstitial pressure values measured and those calculated by the above method.

ANNEX

1. Considerations on the Formula of Kozeny-Carman and on the Permeability of Pulverulent Porous Media

The use of the method for the determination of the interstitial pressure as a function of the dry density, explained earlier, as well as the precise knowledge of the permeability of soils experimented with in the freezing tests, persuaded us beforehand, for each soil, to determine the curves giving the permeability as a function of the dry density, said soils being saturated.

These curves can be determined by means of direct measurements on the permeameter. We wanted to figure them out on the basis of the Kozeny-Carman formula for the purpose of comparison; to do that, we developed a calculation method which we will now describe.

1.1. Principle of Method

The Kozeny-Carman formula is written as follows:

$$k = \varepsilon^3/2t^2(Ssp)^2$$

where ε is the porosity, t is the tortuousness, and Ssp is the specific surface. To calculate the permeability, we had to know these three characteristics of the soil considered.

1.1.1. Determination of Porosity

By definition [we have] $\varepsilon = V_T - V_s / V_T$ where V_T is the total volume, while V_s is the solid matter volume. For a soil sample, we can measure its total volume and determine its weight m. If we furthermore know the weight per volume of the solid material γ_s we can derive from it its solid volume V_s:

$$M = V_s X \gamma_s$$

If V_s is not known, we can obtain ε by means of one of the different customary experimental methods.

1.1.2. Tortuousness

The tortuousness value is assumed to be equal to $\sqrt{5/2} = 1.58$;

This is the average of the experimental results obtained from various porous media with little dispersion.

1.1.3. Determination of Specific Surface

There are two direct ways which enable us to get as precise as possible a figure on the specific surface of a given artificial soil;

through direct measurement, based on the gas adsorption phenomenon, currently performed in specialized laboratories;

on the basis of the grain size distribution of the soil used, in the manner described below: with the help of the soil grain size diagram (figures 3 and 4), which gives us the weight of smaller grains at each diameter, related to the total weight of the sample, one can, point by point, trace the variation of the inverse of the diameter as a function of the following percentage:

$$\%W = \frac{\text{weight of grains smaller than}}{\text{total weight of sample}} \times 100$$

Figures 5 and 6 show this variation for pure silica powder and for talc, respectively.

These figures were obtained with the help of the grain size curves in figures 3 and 4.

Let us figure on a total soil weight equal to its weight by volume of solid matter γ_s. Let us consider a weight [mass] element dm where we consider that all grains have the same diameter δ.

The integral:

$$\int_0^{\gamma_s} \frac{dm}{\delta} = A \qquad \text{(hachured area in figures 5 and 6)}$$

becomes, if dvs is the solid volume element occupied per dm,

$$\int_0^{\gamma_s} \frac{dm}{c} = \gamma_s \int_0^1 \frac{dv_s}{c} = A$$

in effect $dm = \gamma_s \cdot dv_s$ $\qquad \gamma_s = \gamma_s \cdot v_s$ and $v_s = 1$

when $m = \gamma_s$

If we assimilate these grains to spheres with diameter δ, then $dv_s \Big/ \frac{4}{3}\pi\left(\frac{\delta}{2}\right)^3$ will represent the number of spheres with diameter contained in the volume element dvs. $\left[\frac{4}{3}\pi\left(\frac{\delta}{2}\right)^3\right]$ is the volume of a sphere with diameter δ. The surface of these spheres therefore will be:

$$\frac{dv_s}{\frac{4}{3}\pi\left(\frac{\delta}{2}\right)^3} \cdot 4\pi\left(\frac{\delta}{2}\right)^2 = 6\frac{dv_s}{\delta}$$

The surface of the spheres with any diameter contained in one cubic centimeter of solid volume will therefore be:

$$I = 6\int_0^1 \frac{dv_s}{\delta}$$

and, comparing with the above integral, we find:

$$I = 6\frac{A}{\gamma_s}$$

In a solid volume Vs, the surface S of the solid phase thus is:

$$S = V_s \cdot I = V_s \cdot 6\frac{A}{\gamma_s}$$

If we know the total volume V_T of the soil sample prepared, whose solid volume is V_s $\left(V_s = \frac{M}{\gamma_s}\right)$, then we derive from that the specific surface of this soil which, by definition, is the surface of the solid phase out of the total volume of the sample

$$S_{sp} = \frac{S}{V_T} = \frac{V_s}{V_T} \cdot 6\frac{A}{\gamma_s} \qquad \frac{V_s}{V_T} = 1-\varepsilon$$

Now

$$S_{sp} = (1-\varepsilon) \times 6\frac{A}{\gamma_s}$$

The relation with which we wind up shows therefore that the specific surface of a given soil is a function of the porosity ε of the area A and the weight by volume of solid matter γ_s relative to this soil. The magnitudes A and γ_s are connected to the solid matter and consequently are fixed characteristic magnitudes, independent of the manner of preparation (compacting energy and water content of sample).

It follows from this that:

$$S_{sp} = F(1-\varepsilon)$$

for a given soil, in other words

$$1-\varepsilon = \frac{V_s}{V_T} = \frac{V_s\gamma_s}{\gamma_s V_T} = \frac{M}{V_T} \cdot \frac{1}{\gamma_s} = \frac{\gamma_d}{\gamma_s}$$

where γ_d is the dry density. Hence

$$S_{sp} = G(\gamma_d)$$

for a given soil and the Kozeny-Carman formula relative to a given soil now becomes:

$$P_k = \frac{F(\varepsilon)}{g(\gamma_d)} = f(\gamma_d) \qquad (1)$$

2. Employment of Method

The examination of the grain size diagram for talc (Figure 6) shows that this diagram is not entirely known. We thus tried to determine the area A by some other means. We envisaged comparing the permeability values obtained, on the basis of the formula and by the permeameter measurements for the case of soil No. 3, consisting of a mixture of 50% talc and 50% pure silica. We proceeded in the following manner: we measured the permeability of this soil for a 15% water content and for a dry density of 1.567. From that value of k and through application of the previously explained method, we determined the specific surface Ssp and the area A for talc (the area for silica being prefectly known and obtained on the bais of the grain size diagram). We then made different samples characterized by a given water content and dry density whose permeability we had measured with the help of the permeameter. These different values are illustrated in Figure 7.

For each of these soils, whose dry density we know, we calculated the value of the permeability by the method explained and for the known values of the dry density of that soil and the area A. These different values are illustrated in Figure 7.

3. Conclusion

The examination of the curves in Figure 7 shows a big gap between the permeability values measured and those calculated. The gap grows considerably when the dry density diminishes; moreover, its variation between two given values of γ_d is not constant.

The use of the Kozeny-Carman formula necessitates the knowledge of the precise value of the specific surface of soils; to use the method, which we explained, we must have a knowledge of the value of area A and for talc (Figure 6) this area can only be estimated.

For a comparison of permeability values obtained through calculation on the basis of the Kozeny-Carman formula and those measured with the permeameter, the preceding data are indispensable.

The gap which we found (Figure 7) could come from the particular way in which we tried to use the method we presented. [Hand entry on margin: at what level?]

BIBLIOGRAPHY

/1/ J. AGUIRRE-PUENTE et A. PHILIPPE - Quelques recherches effectuées en France sur le problème de la congélation des sols. R.G.T., 8, n° 96, p. 1123-1142, decembre (1969)

/2/ J. AGUIRRE-PUENTE, B. LE FUR et I. SZANTO - Congélation unidimensionnelle d'un echantillon de sable saturé d'eau. C.R. Colloque Int. du C.N.R.S. n° 160 "Phenomènes de transport avec changement de phase dans les milieux poreux ou colloïdaux" pp 149-164, Paris avril (1966)

/3/ J. AGUIRRE-PUENTE et B. LE FUR - Gelivite des sols VII : Etude expérimentale de la congélation unidimensionnelle de différents échantillons de sol. Rapport 67-9 du laboratoire d'Aérothermique du C.N.R.S.

/4/ B. KHASTOU et J. AGUIRRE-PUENTE - Gonflement des sols par le gel. C.R. Acad. Sc. Paris, t. 271, p. 526-529 (1970)

/5/ B. KHASTOU - Etude du gonflement des sols par le gel. Thèse de Docteur-Ingenieur, Paris (1970)

/6/ M. CHALHOUB - Contribution à l'etude de la congélation des sols. Rapport de stage de D.E.A. Laboratoire d'Aérothermique du C.N.R.S. juillet (1969)

/7/ E. PENNER - Les pressions qui se manifestent dans un système granulaire poreux par suite du phénomène de ségrégation de la glace. Special report 40 Highway research board Washington D.C. juil. (1959)

/8/ K.A. JACKSON, D.R. UHLMANN et B. CHALMERS - Frost heave in soils. J. of Appl. Phys. vol. 37, n° 2, fév. 1966

/9/ P.J. WILLIAMS - Unfrozen water content of frozen soils and soil moisture suction. Norges Geoteknishe institutt, n° 72, Ottawa (1968)

/10/ E. HESSTVEDT - The interfacial energy ice/water. Norwegian Geotechnical Institute, n° 56, p. 7-10 (1964)

/11/ R. PELTIER - Contribution à l'élaboration d'une théorie capillaire du gel des sols routiers. 3ème Congrès int. de mécanique des sols et des travaux de fondations. Zurich (1953)

/12/ D.R. UHLMANN et B. CHALMERS - Interaction between particles and a solid-liquid interface. J. of Appl. Phys. vol. 35, n° 10 oct. (1964)

/13/ I.G. PORTNOV - Solution de certains problèmes avec changement de phase par la méthode de calcul operationnel. 1st All Union Conf. on Heat and Mass Transfer. t. 5, pp 106-117 Minsk.

/14/ G.M. FEL'DMAN - Calcul de la migration d'humidite et determination de la texture du sol pendant la congelation. In. fiz. Zur. n° 6 (1967)

/15/ L.A. RICHARDS - Pressure membrane apparatus ; construction and use. Agricultural Engineering vol. 28 (1947)

/16/ P.J. WILLIAMS - Suction and its effect in unfrozen water of frozen soils. Norges Geotekniske institutt, n° 72 Ottawa (1968)

/17/E. PENNER - The mechanism of frost heave in soils. Highw. Res. bull. n° 225, pp 1-22 Ottawa, déc. (1959)

/18/ G. BESKOW -Soil freezing and frost heaving with special application to roads and railroads, traduit par J.O. OSTERBERG, Tech. Inst. Northwestern Univ. (1947)

/19/ P.J. WILLIAMS - Pore pressures at a penetrating frost line and their prediction. Norwegian Geotechnical Inst. n° 72, Ottawa (1968)
/20/ S. IRMAY - Solutions générales des écoulements incompressibles. Potentiels du type laplacien et du type de Poisson. C.R. Acad. Sc. Paris t. 259, juil. (1964)
/21/ L.A. RICHARDS - Methods of measuring soil moisture tension. Soil Sc. 68, 95-112 année.
/22/ L. SORMAIL et G. VACHAUD - Mesure des potentiels d'humidite dans les sols non saturés au moyen de tensiomètres classiques et osmotiques. Communication presentée au Comité Technique de la Société Hydrotechnique de France le 12 juin 1969
/23/ ESSAI PROCTOR - Modes opératoires du Laboratoire Central des Ponts et Chaussées. Modes opératoires S.C-1 Dunod, Paris (1966)
/24/ K.A. JACKSON et B. CHALMERS- Freezing of liquids in porous media with special reference to frost heave in soils. J. of Appl. Phys. 29, n° 8 août (1958)

[Translation of Bibliography items]

Legend: et = and; t. = vol.

1. "Some Research Conducted in France on the Problem of Soil Freezing."

2. "Unidimensional Freezing of a Water-Saturated Sand Sample," Minutes of the International Conference of the CNRS, No. 160, "Phenomena of Transport With Change in Phase in Porous or Colloidal Media," pp 149-164, Paris, April 1966.

3. "Freezability of Soils VII: Experimental Study of Unidimensional Freezing of Different Soil Samples," Report No. 67-9 of the Aeorthermal Laboratory of the CNRS.

4. "Soil Swelling Due to Freezing," Reports of the Academy of Sciences.

5. "Study of Soil Swelling Due to Freezing," Doctor-Engineer Dissertation.

6. "Contribution to the Study of Soil Freezing," Training Course Report, DEA [Abbreviation Unknown], Aerothermal Laboratory, CNRS, July 1969.

7. "Pressures Manifest in a Porous Granular System Due to the Phenomenon of Ice Segregation."--July 1959.

11. "Contribution to the Preparation of a Capillary Theory of Highway Soil Freezing," Third International Congress on Soil Mechanics and Foundation Structures.

13. "Solution of Certain Problems With a Change in Phase by the Operational Calculation Method."

14. "Calculation of Moisture Migration and Determination of Soil Texture During Freezing."

20. "General Solutions of Incompressible Flows--Potentials of the Laplace Type and the Poisson Type," Reports of the Academy of Sciences, Paris, Vol. 259, July 1964.

22. "Measurement of Moisture Potentials in Unsaturated Soils by Means of Conventional and Osmotic Tensiometers," Communication Presented to the Technical Committee of the Hydrotechnology Society of France on 12 June 1969.

23. "Operating Procedures of the Central Laboratory of the Department of Bridges and Highways," Operating Procedures....

24. ...August...

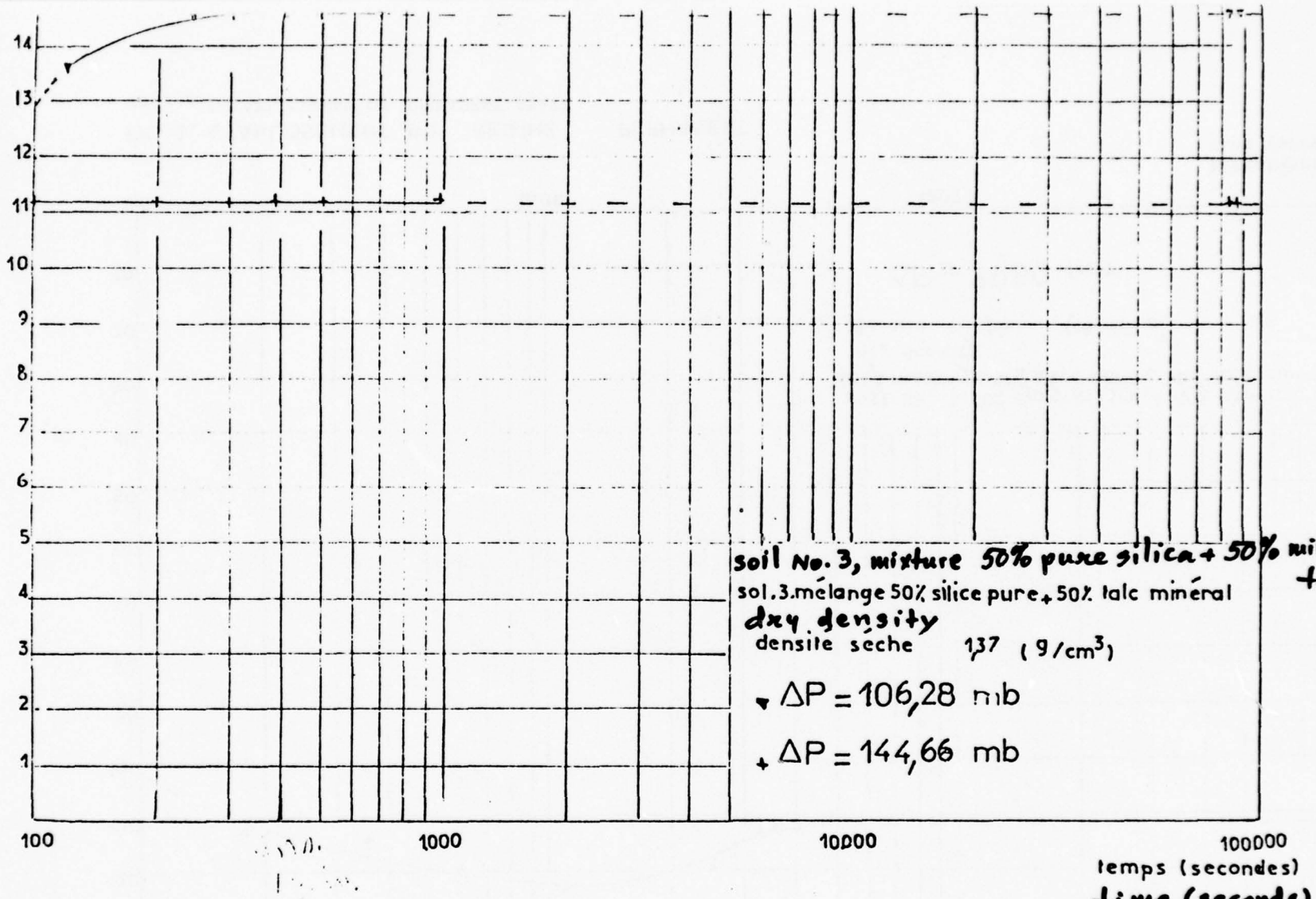

FIG. 1. ETABLISSEMENT DU REGIME PERMANENT

FIG 1. ESTABLISHMENT OF PERMANENT STATE.

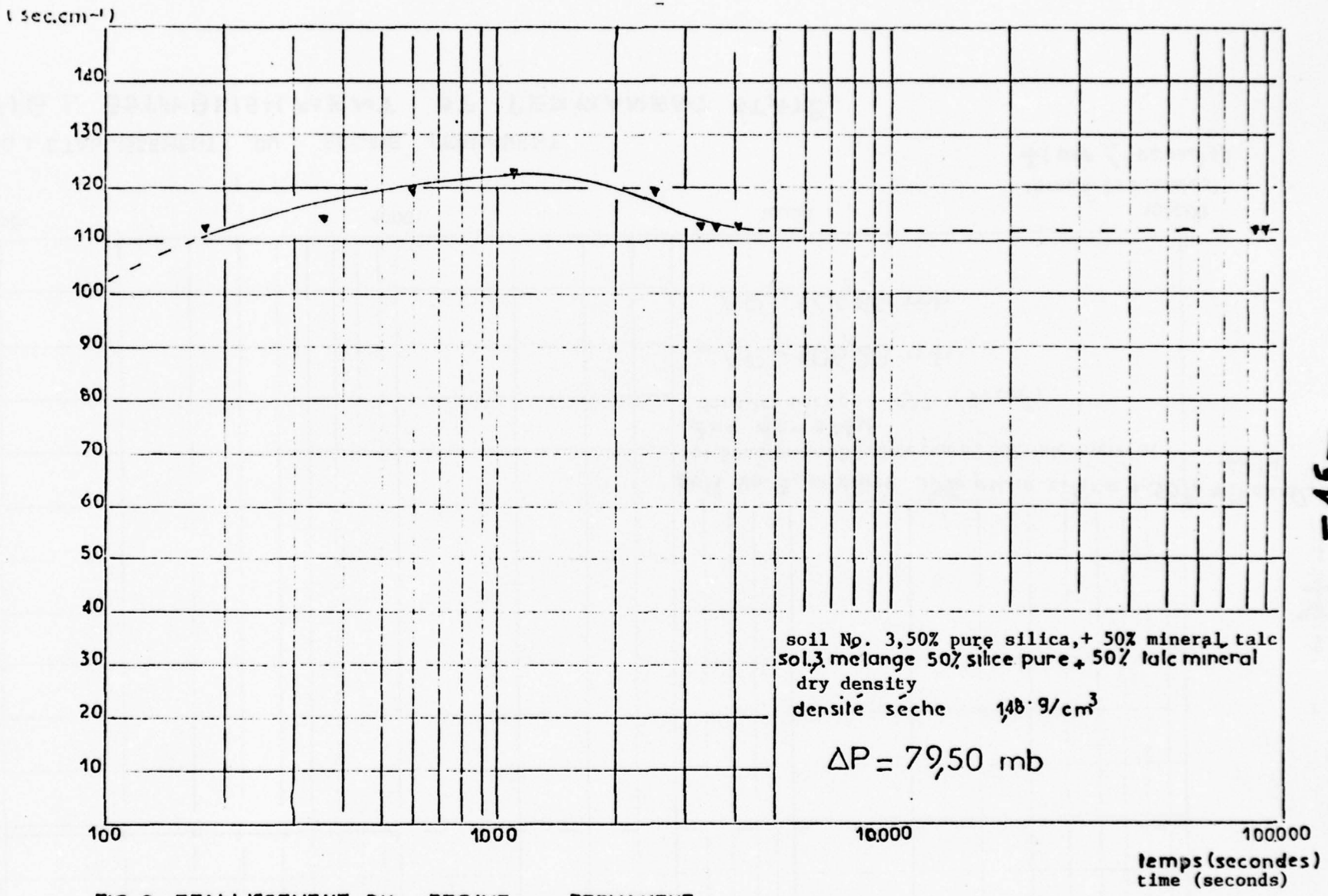

FIG. 2. ETABLISSEMENT DU REGIME PERMANENT

FIG. 2. ESTABLISHMENT OF PERMANENT STATE

LABORATOIRE CENTRAL
DES PONTS ET CHAUSSÉES

Central Lab. Dept. of Bridges & Hwys, Soil & Stone Sec.
Section des Sols
et des Pierres

S.6 ET S.7 - ANALYSE GRANULOMÉTRIQUE
and GRAIN SIZE ANALYSIS

DOSSIER :
FILE:

Paris le : [Date]

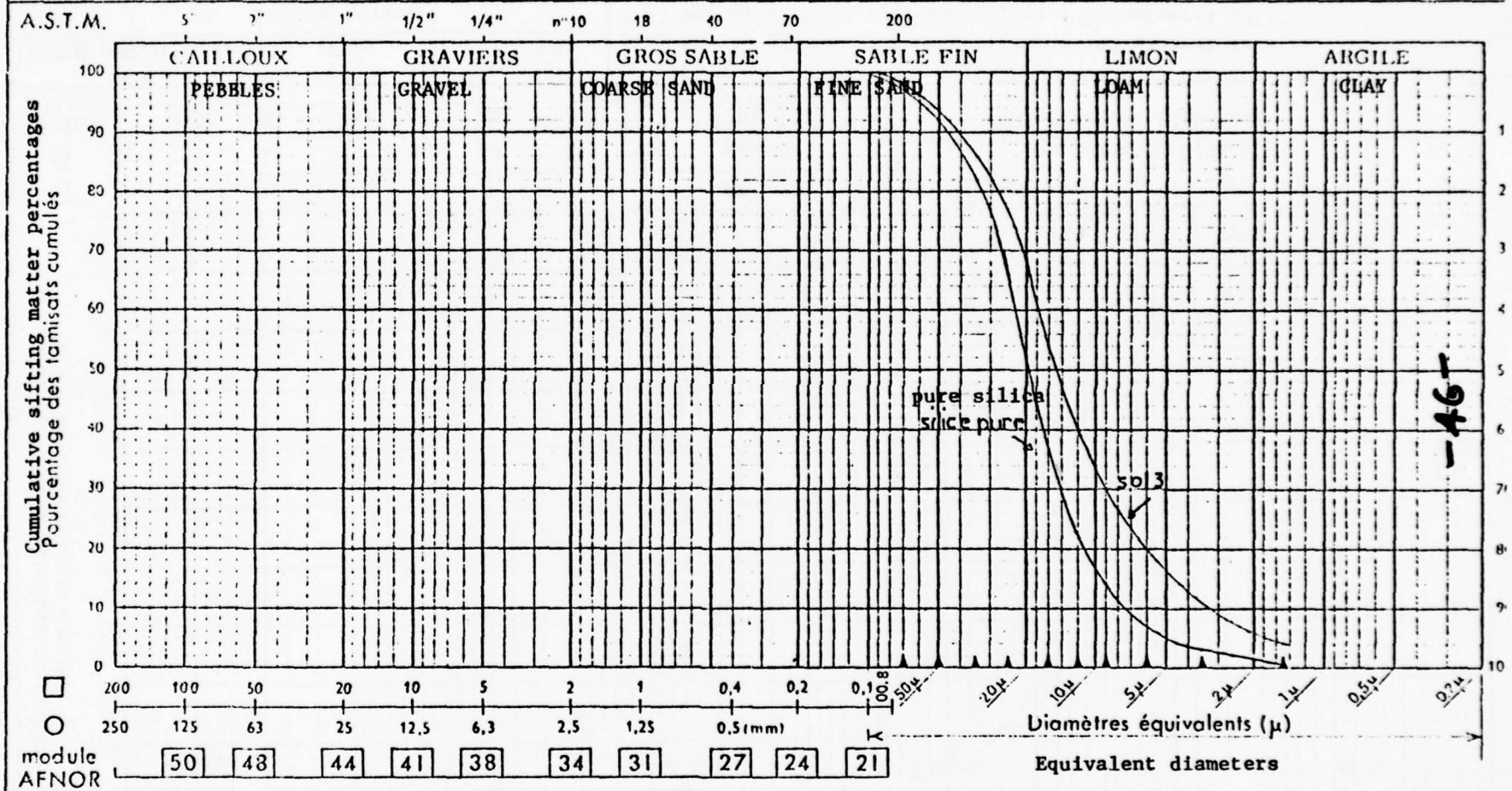

LIMITS OF ATTERBERG S.8		S.20 E.S.		Co3 Ca
L. L.	I. P.	Piston	Visual	

Soil No.3, mixture 50% pure silica + 50% mineral talc
sol.3 melange 50% silice pure + 50% talc mineral

FIG. 3. GRAIN SIZE CURVES
FIG. 3. COURBES GRANULOMETRIQUES

LABORATOIRE CENTRAL
DES PONTS ET CHAUSSÉES

Central Lab. Dept. of Bridges & Hwys, Soil and Stone Sec.
Section des Sols
et des Pierres

S.6 ET S.7 - ANALYSE GRANULOMÉTRIQUE
AND GRAIN SIZE ANALYSIS

DOSSIER :
FILE

Paris le : [date]

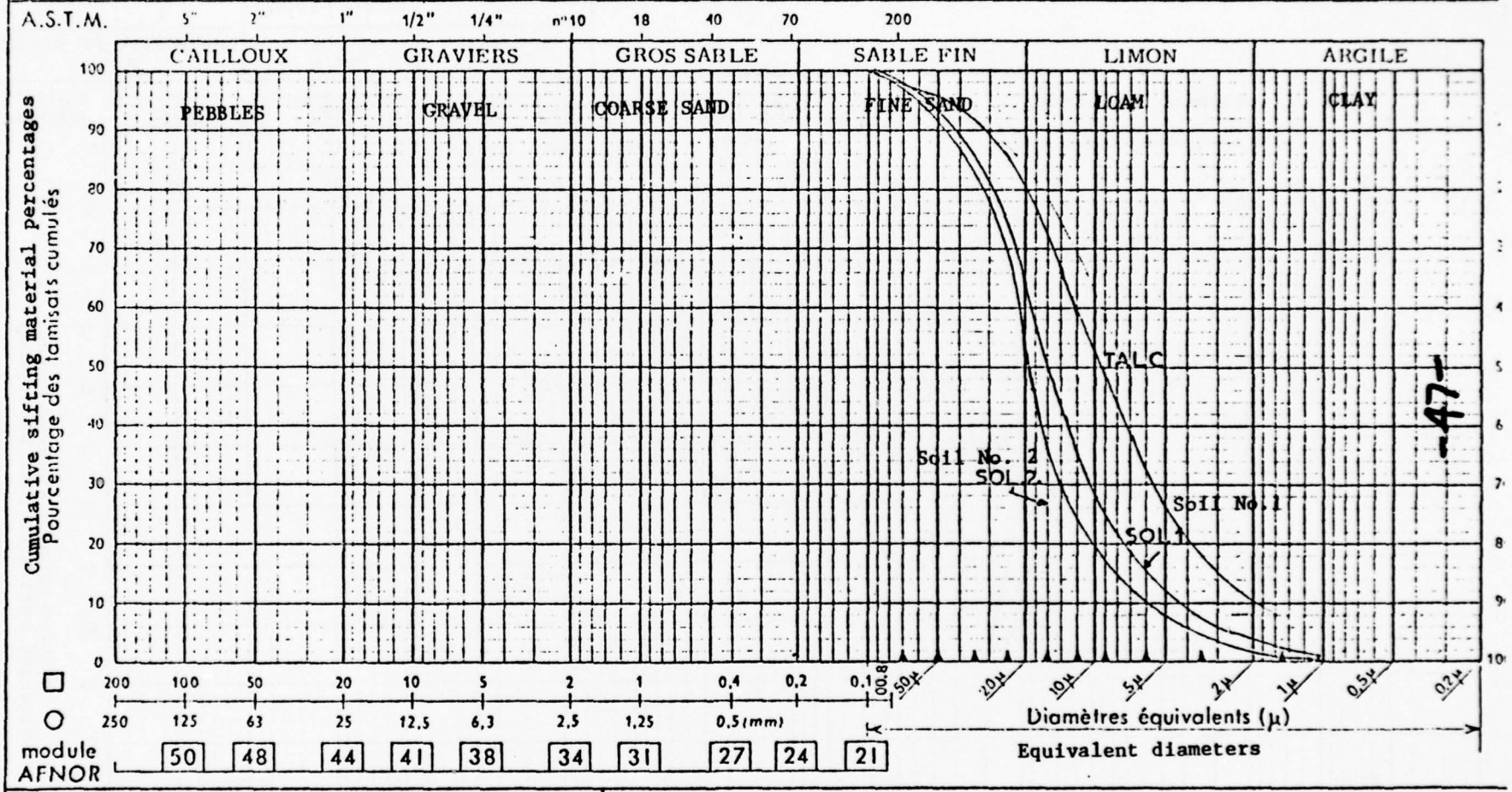

-47-

S.8 LIMITS OF ATTERBERG		S.20 E.S.		CO_3 Ca
L. L.	I. P.	Piston	Visual	

Soil No. 1, mixture 90% pure silica + 10% mineral talc
Soil No. 2, mixture 70% pure silica + 30% mineral talc

sol. 1. mélange 90% silice pure + 10% talc minéral
sol. 2. mélange 70% silice pure + 30% talc minéral

FIG 4 GRAIN SIZE CURVES
FIG. 4. COURBES GRANULOMETRIQUES

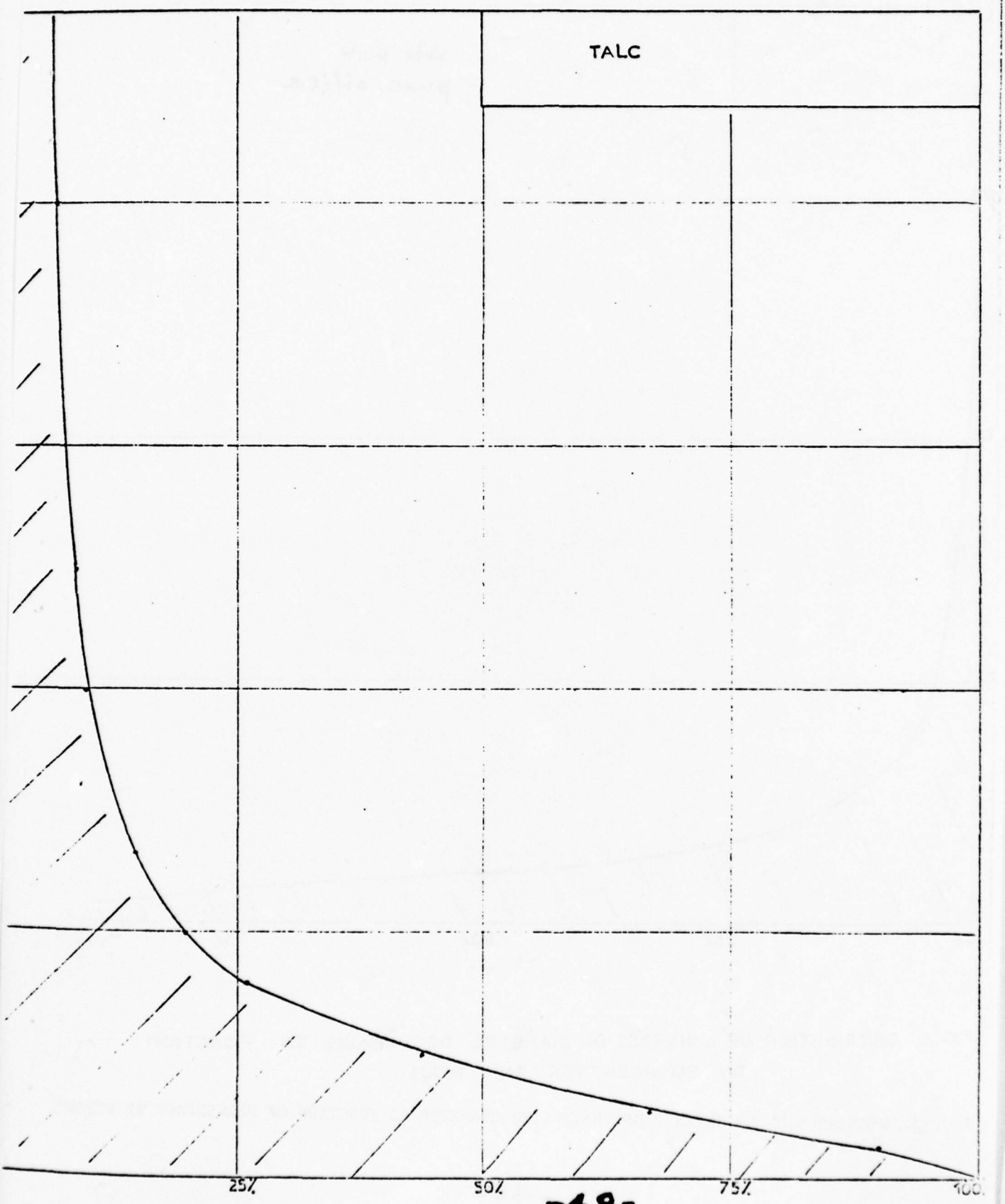
TALC
25%
50%
75%

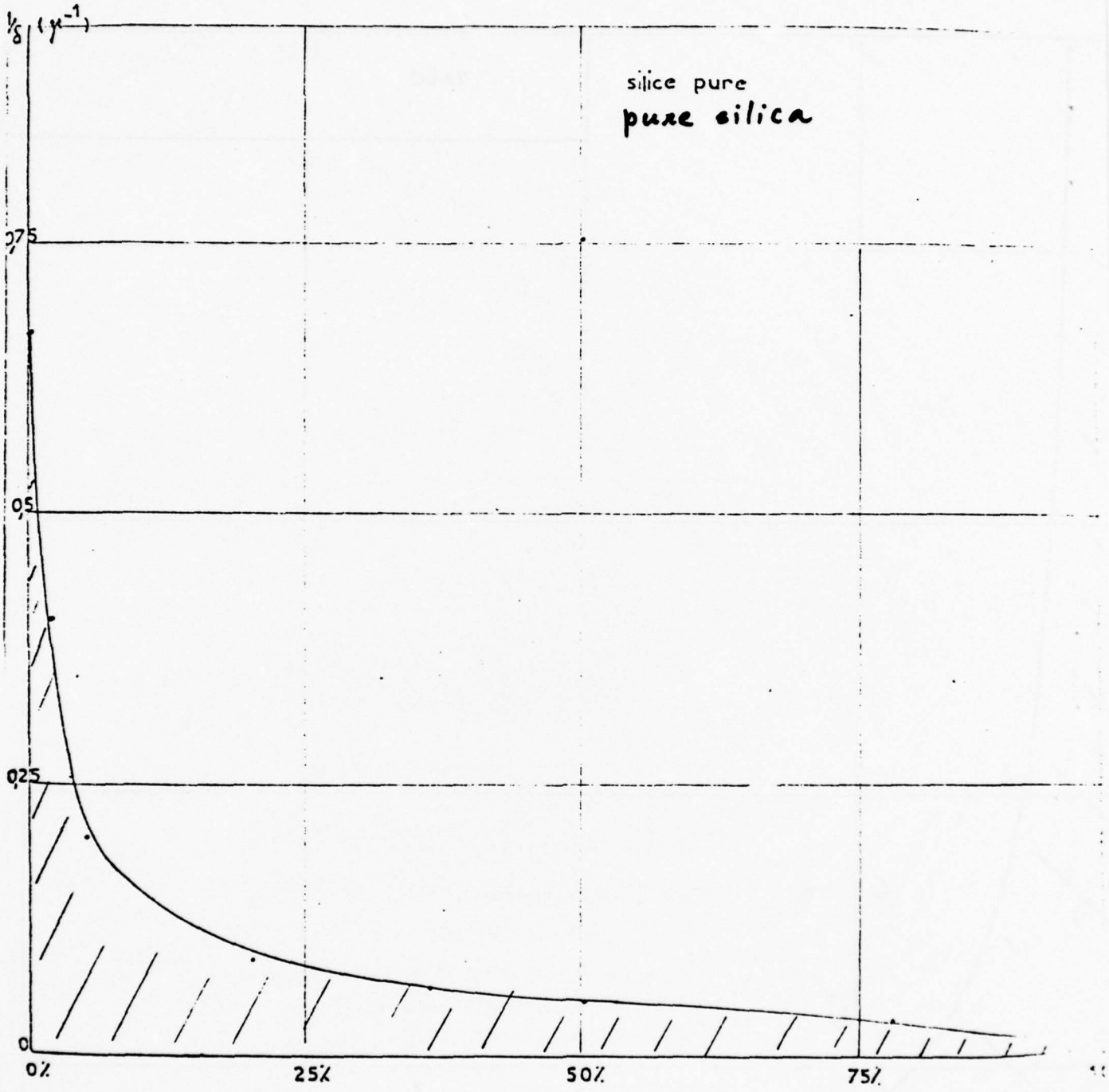

FIG.5. DISTRIBUTION DE L INVERSE DU DIAMETRE DES GRAINS EN FONCTION DU POURCENTAGE EN POIDS

FIG. 5. DISTRIBUTION OF INVERSE OF GRAIN SIZE DIAMETER AS FUNCTION OF PERCENTAGE BY WEIGHT

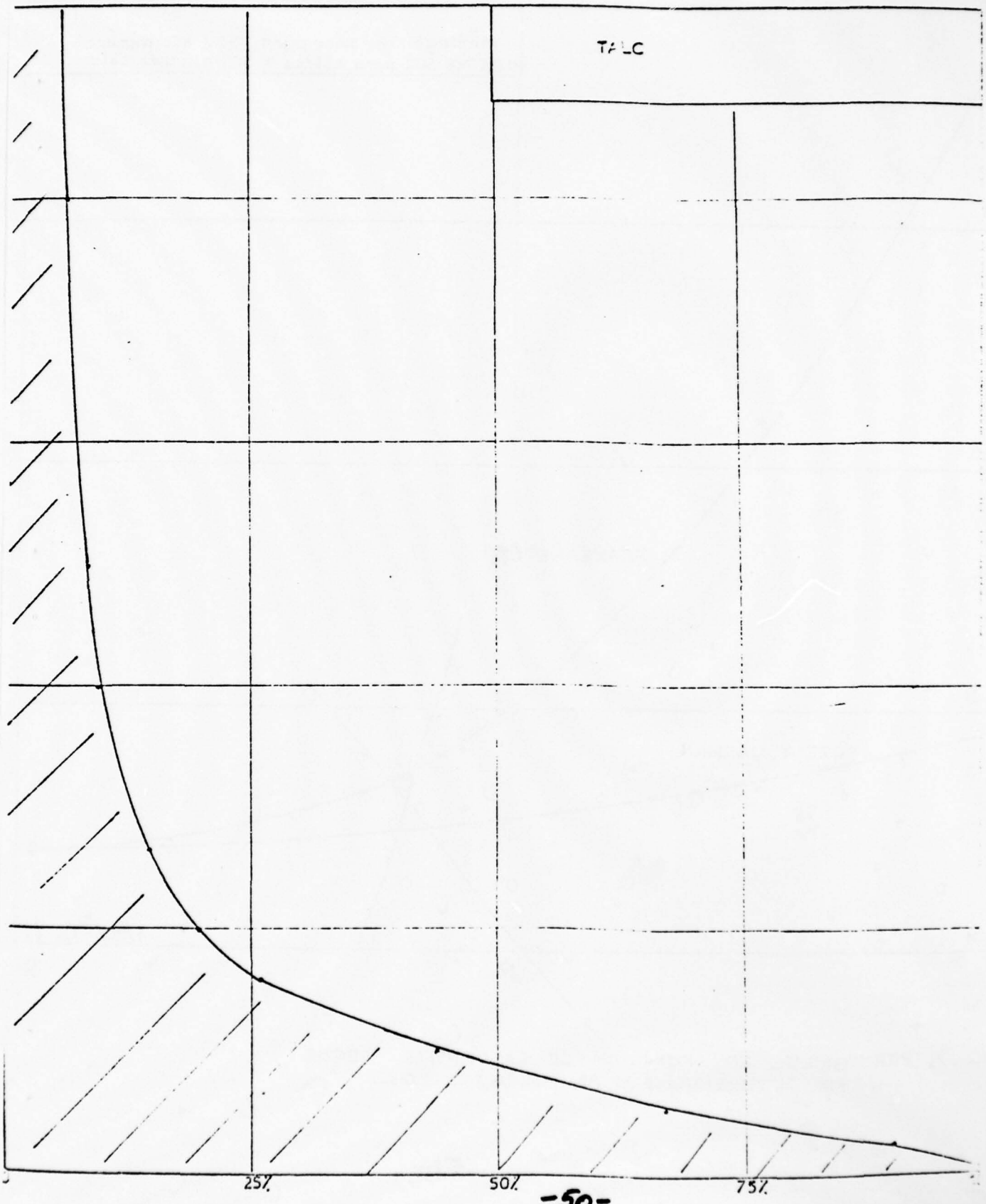
TALC
25%
50%
75%

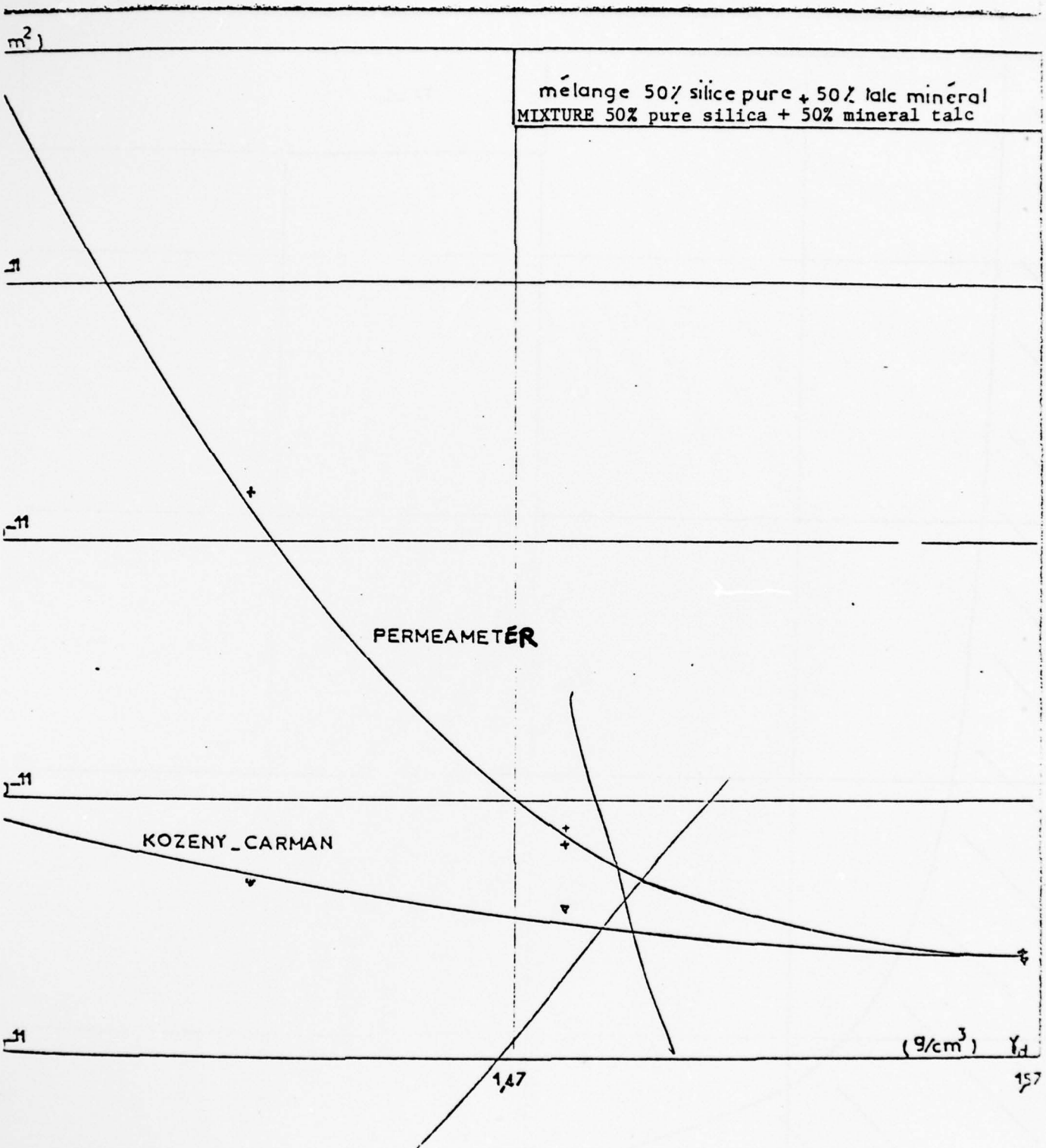

IG . 7. PERMEABILITE EN FONCTION DE LA DENSITE SECHE
FIG. 7. PERMEABILITY AS FUNCTION OF DRY DENSITY

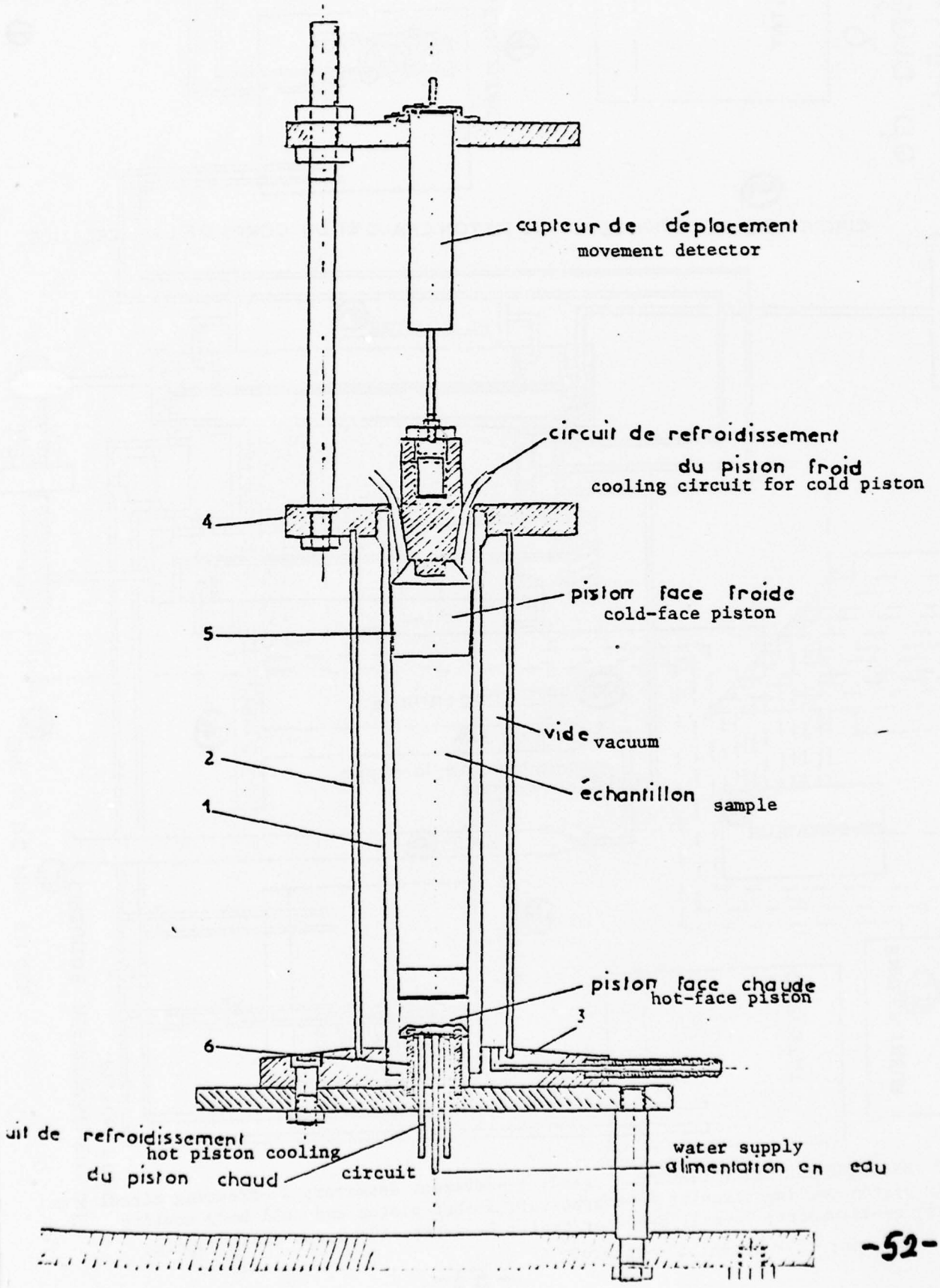
capteur de déplacement
movement detector
circuit de refroidissement
du piston froid
cooling circuit for cold piston
4
piston face froide
cold-face piston
5
vide vacuum
2
échantillon sample
1
piston face chaude
hot-face piston
3
6
uit de refroidissement
hot piston cooling
du piston chaud
circuit
water supply
alimentation en eau

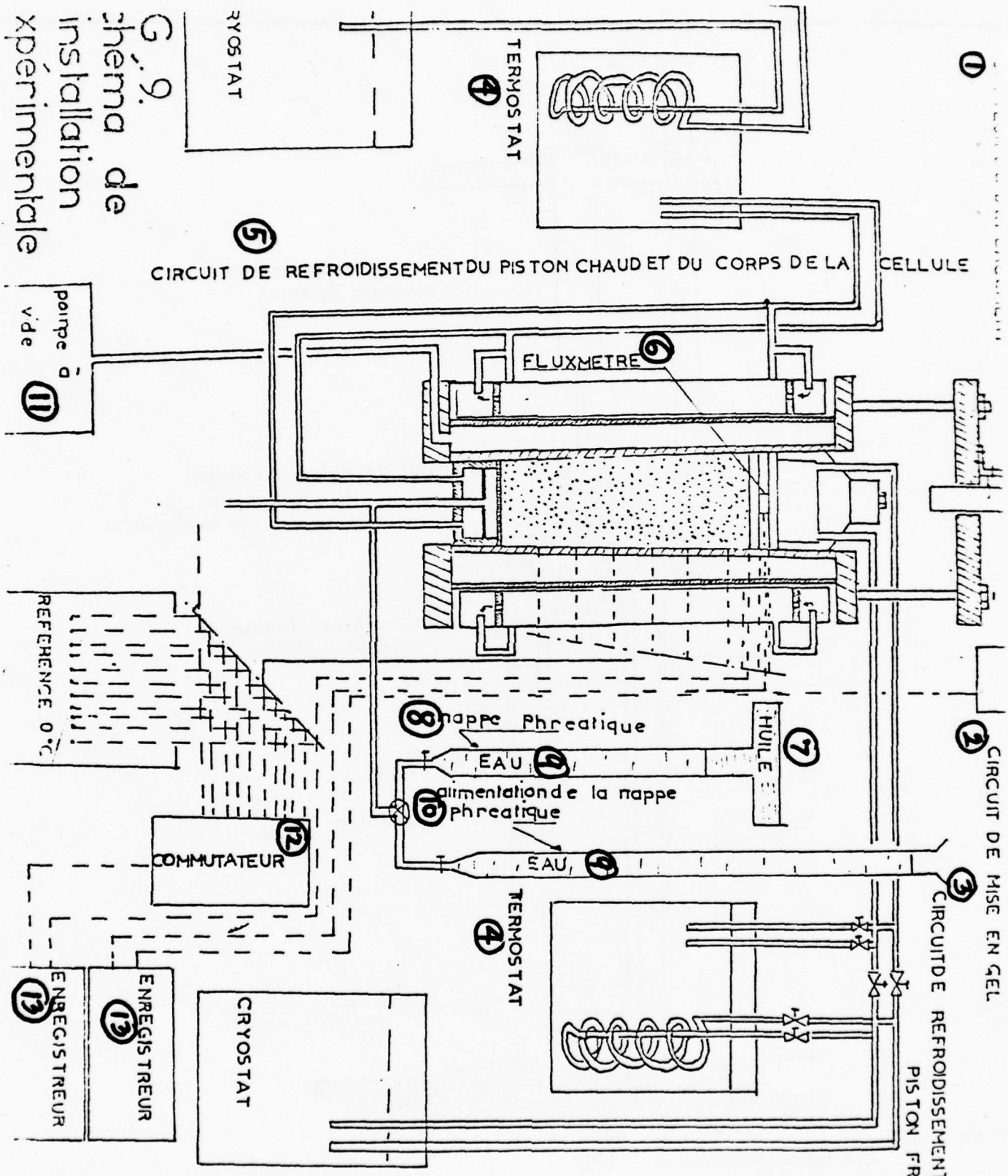

FIG. 9. EXPERIMENTAL SETUP DIAGRAM. Legend: 1--movement detector; 2--freezing circuit; 3--cold piston cooling circuit; 4--thermostat; 5--hot piston and cell body cooling circuit; 6--flowmeter; 7--oil; 8--water table; 9--water; 10--water table supply; 11--vacuum pump; 12--switch; 13--recorder.

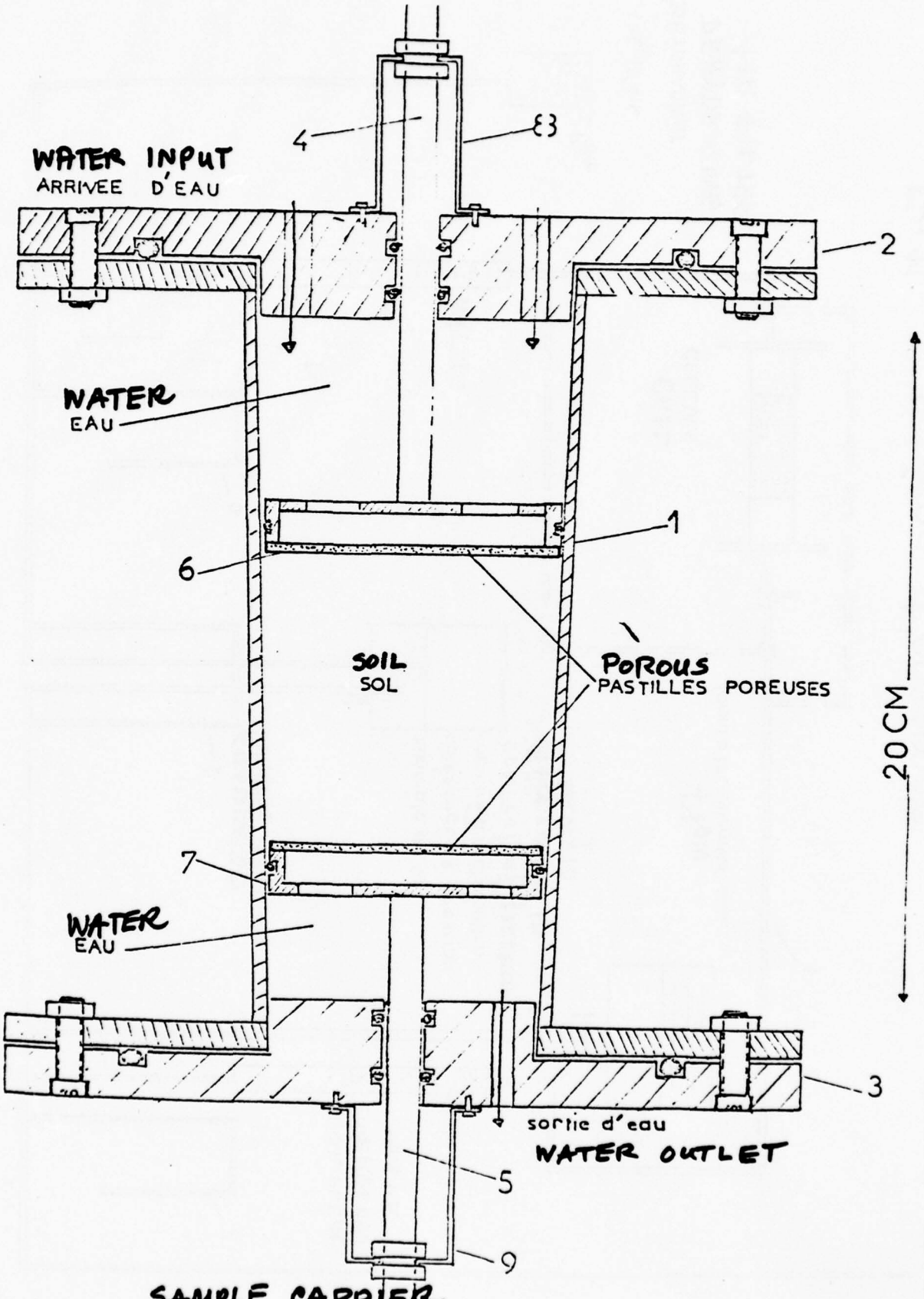

fig.10. porte_échantillon

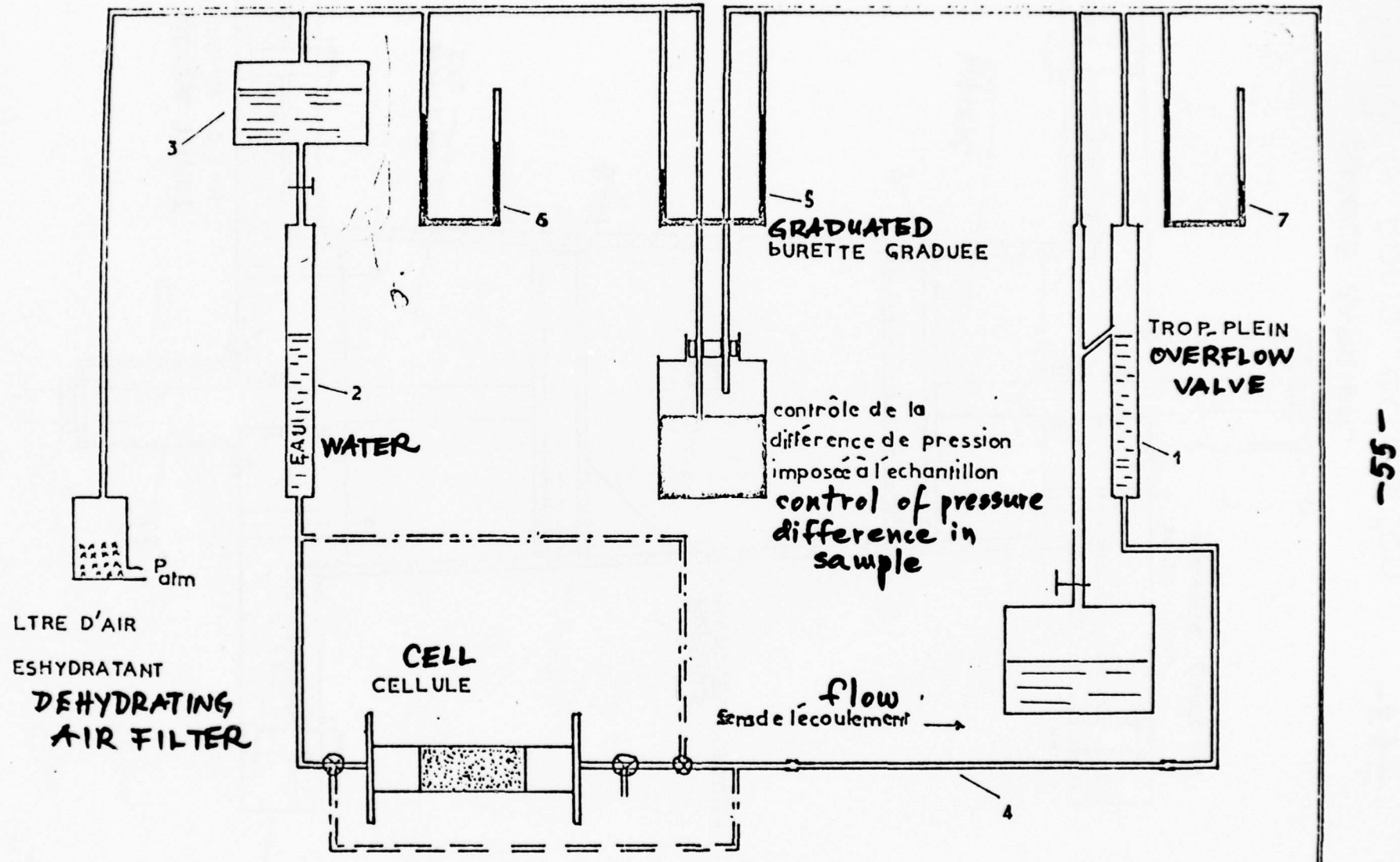

fig.11. schéma d'ensemble
General Diagram

Study Cell - Interstitial Pressure Measurements

fig.12. cellule d'etude _ mesure des pressions insterstitielles

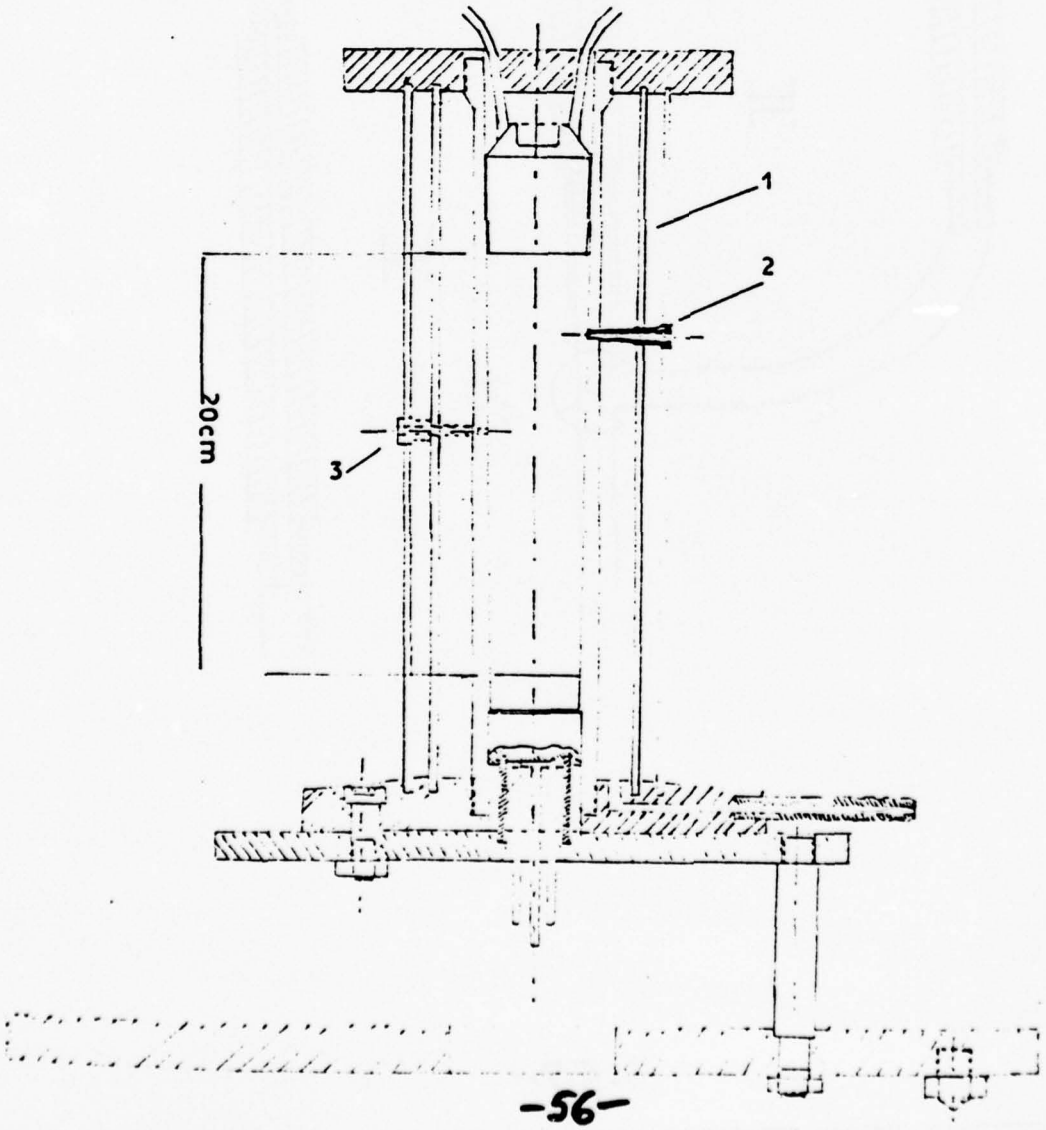

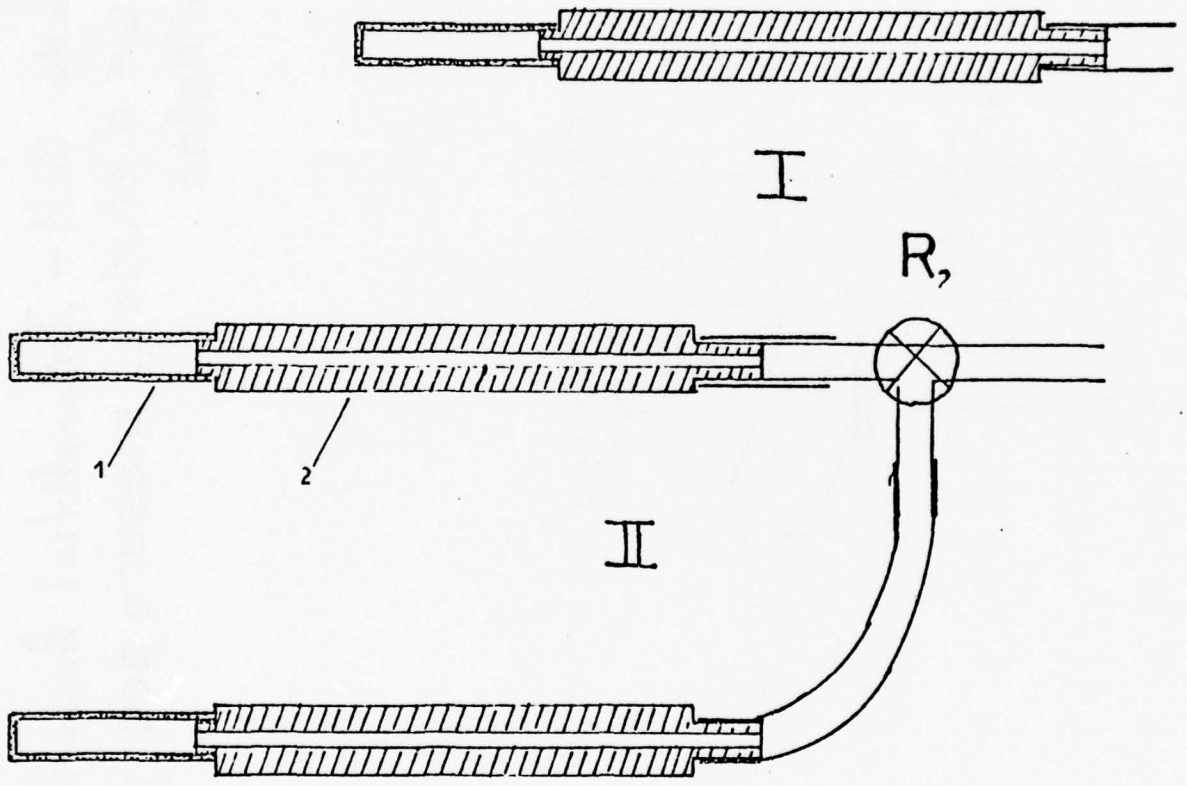

Connecting Circuits

fig 13 circuits de liaison

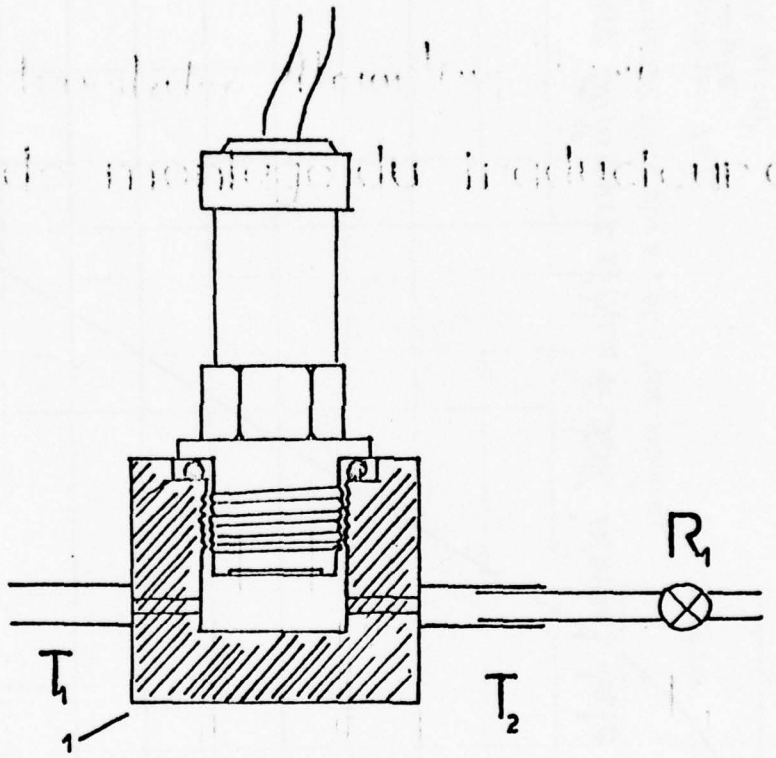

Pressure Translator Mounting Device

fig 14 dispositif de montage du traducteur de pression

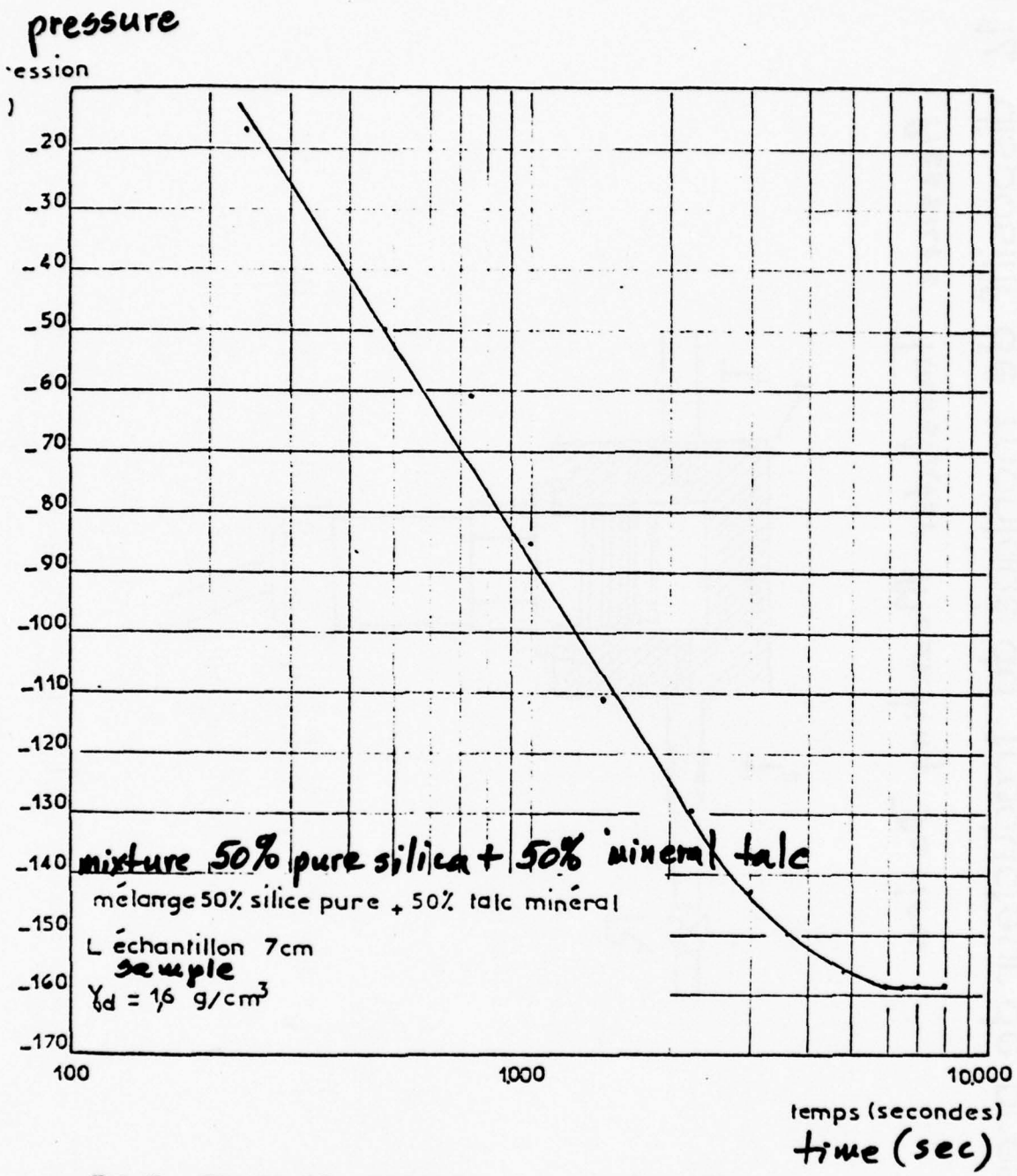

FIG. 15 TEMPS DE REPONSE DU TENSIOMETRE

TENSIOMETER RESPONSE TIME

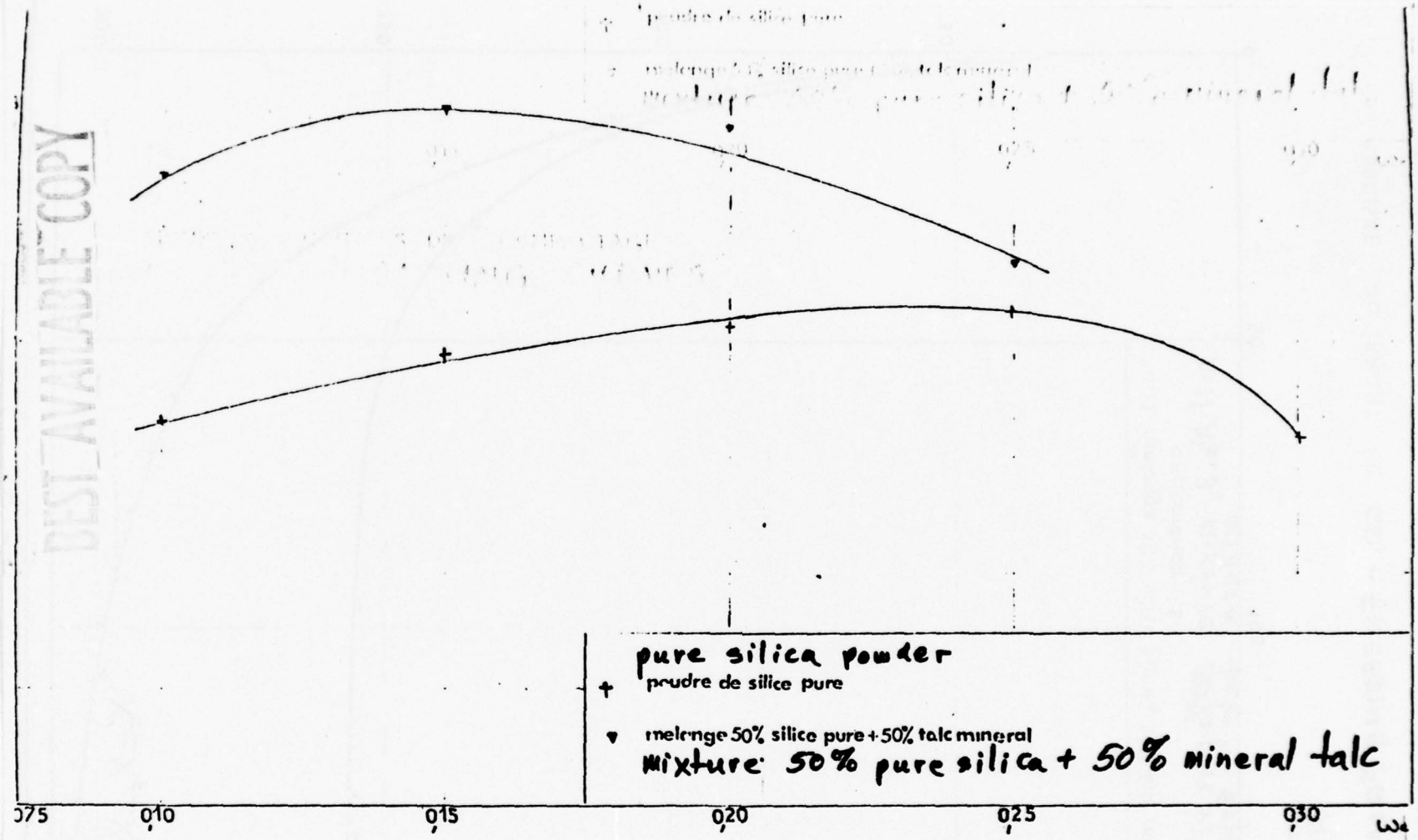

FIGURE .16. COURbES DE COMPACTAGE
COMPACTING CURVES

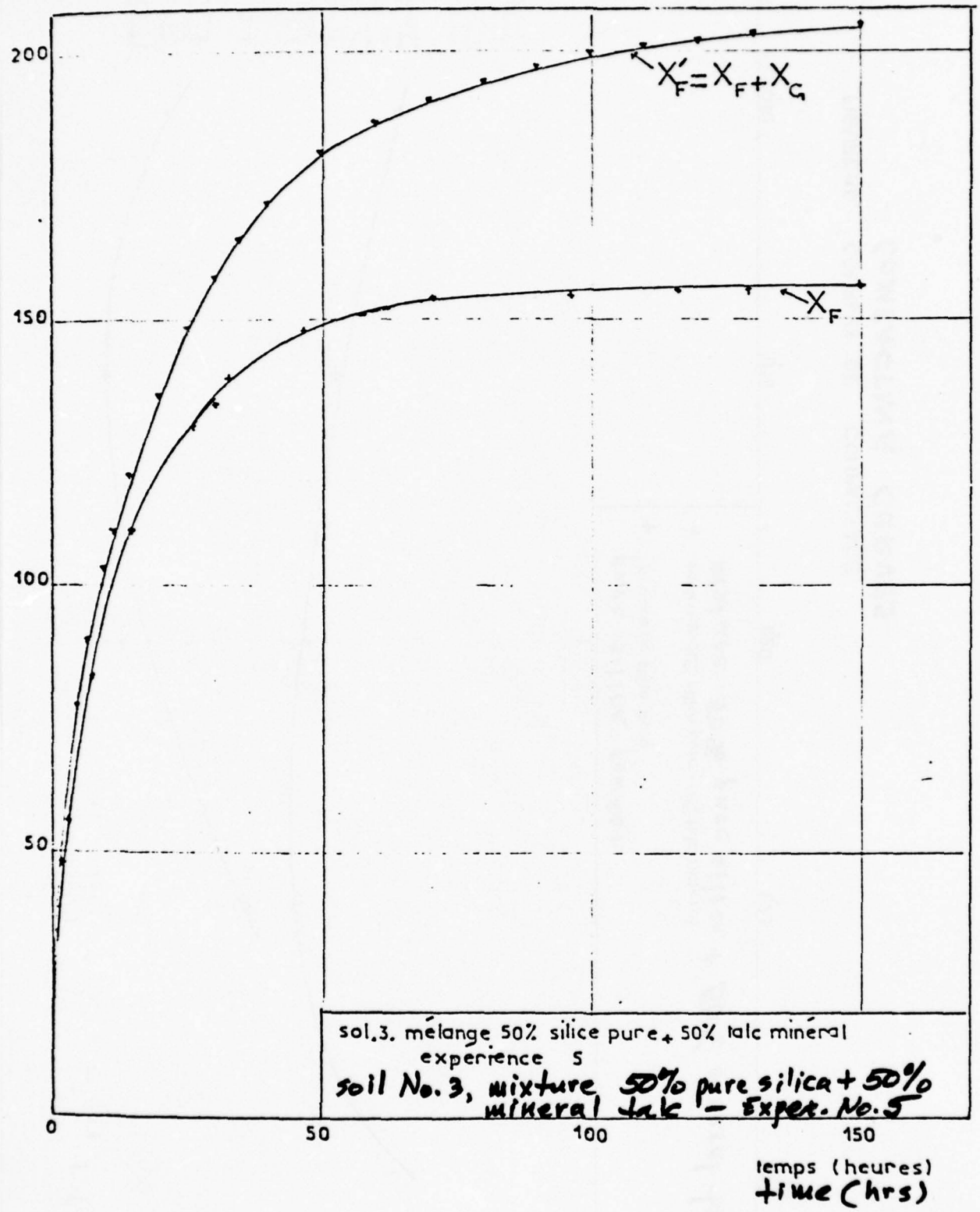

IG.17. ▾ ABSCISSE DU FRONT DE GEL – FREEZING FRONT ABSCISSA

\+ POSITION DU FRONT PAR RAPPORT A LA COTE INITIALE DE LA FACE FROIDE – POSITION OF FRONT WITH RESPECT TO INITIAL COLD-FACE LEVEL

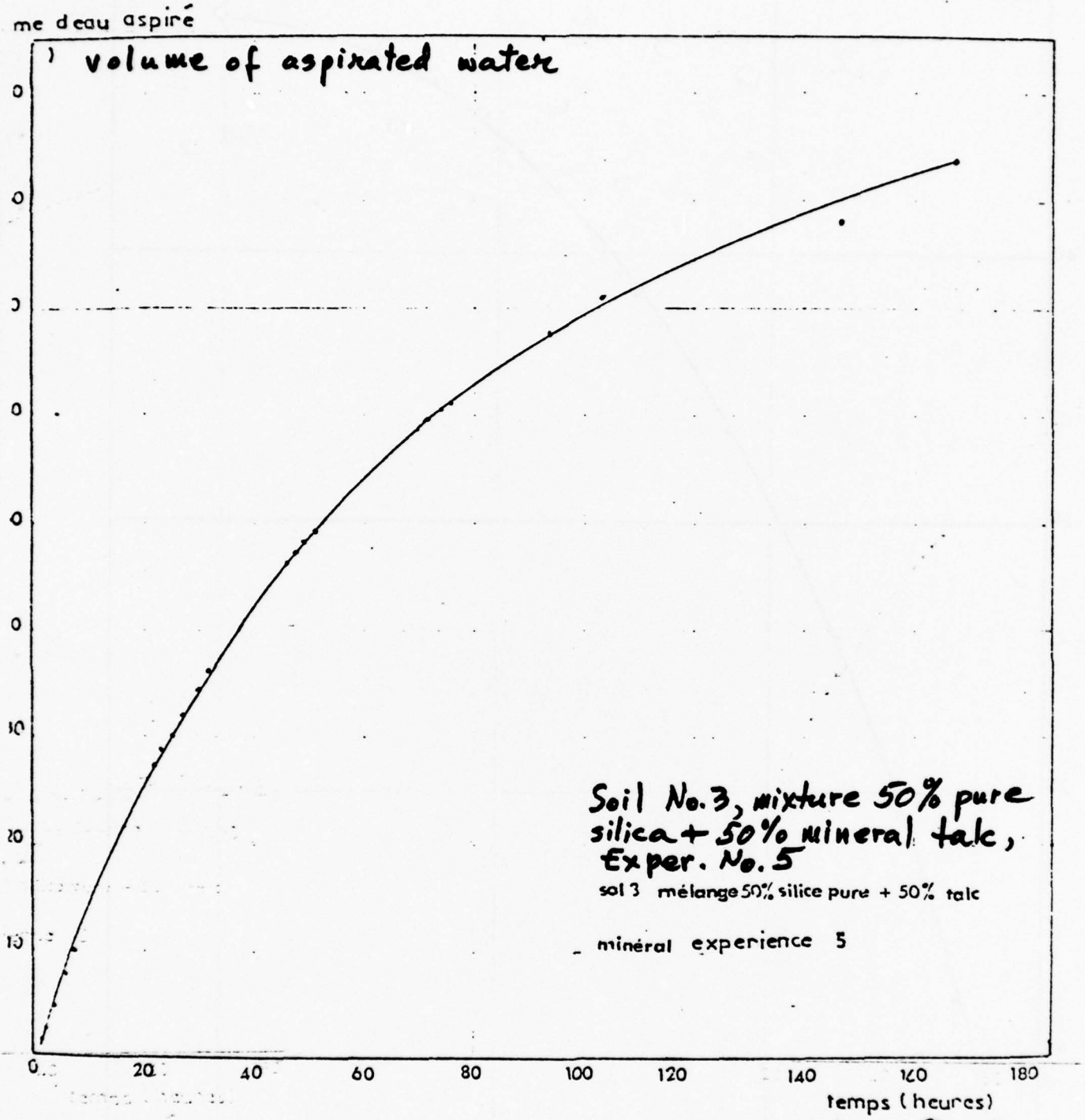

FIGURE 18 ASPIRATION D'EAU EN FONCTION DU TEMPS

WATER ASPIRATION AS FUNCTION OF TIME

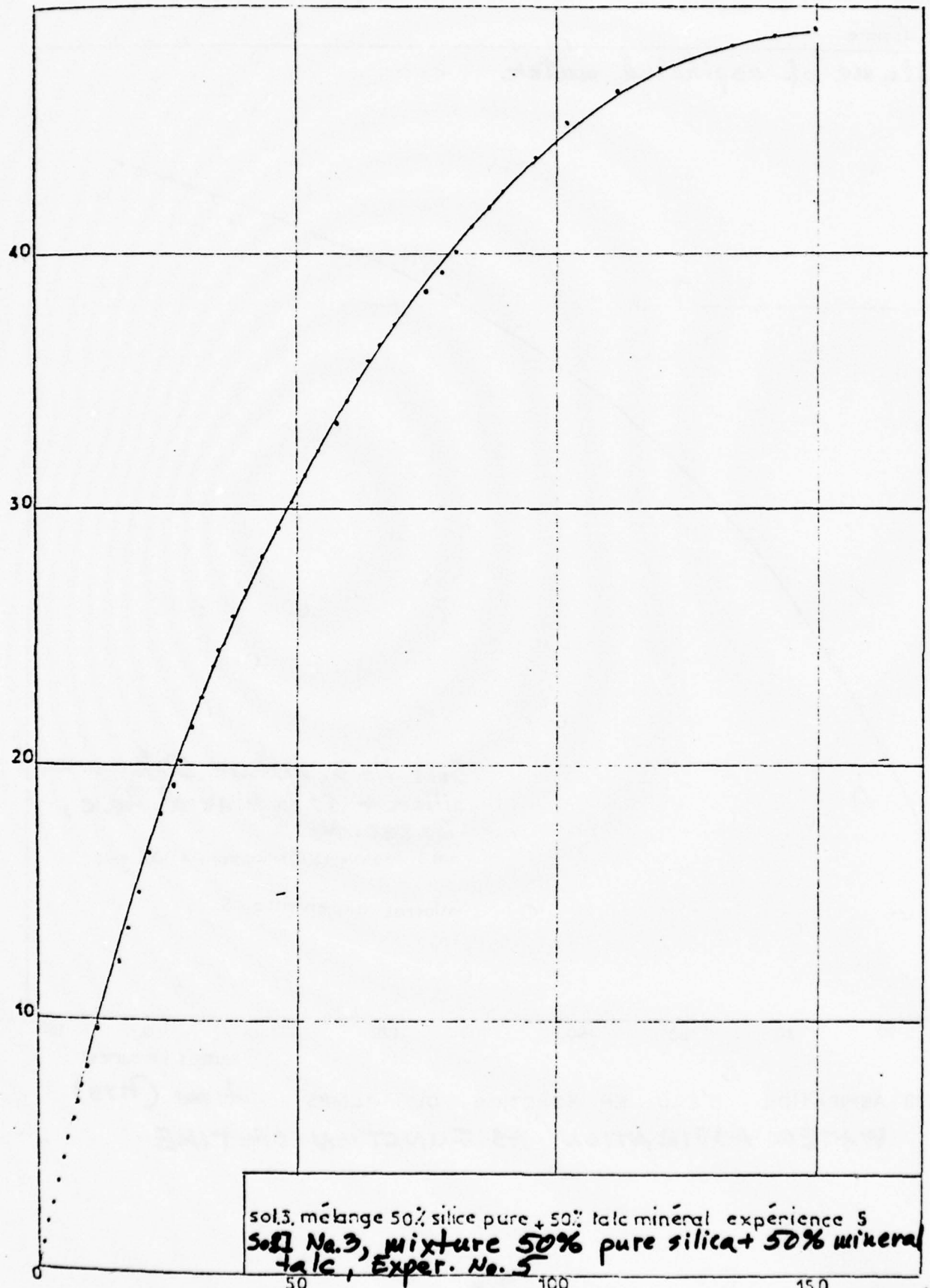

F.G. 19. GONFLEMENT EN FONCTION DU TEMPS
SWELLING AS FUNCTION OF TIME

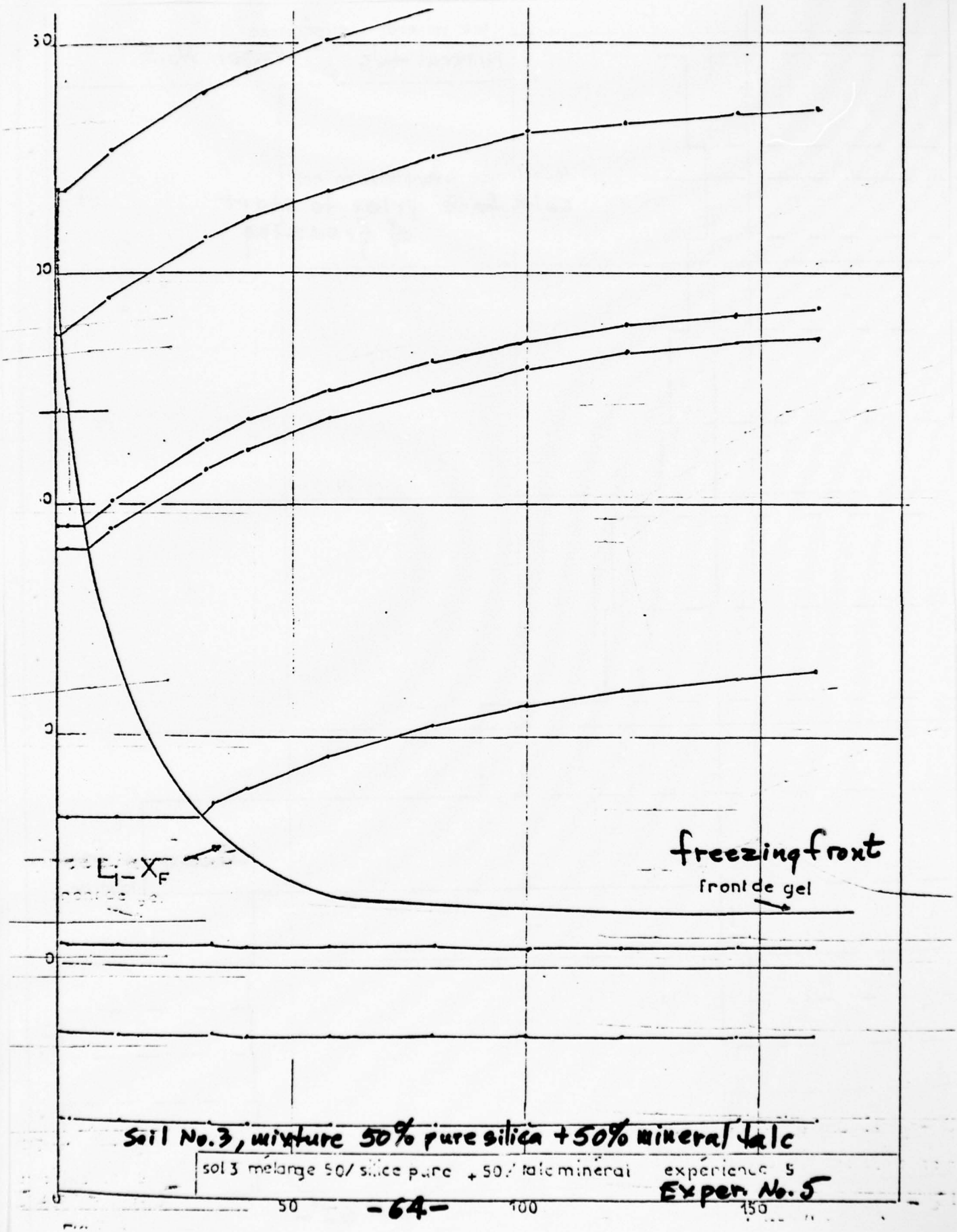
freezing front
front de gel
Soil No.3, mixture 50% pure silica + 50% mineral talc
sol 3 mélange 50/ silice pure + 50/ talc mineral
experience 5
Exper. No. 5

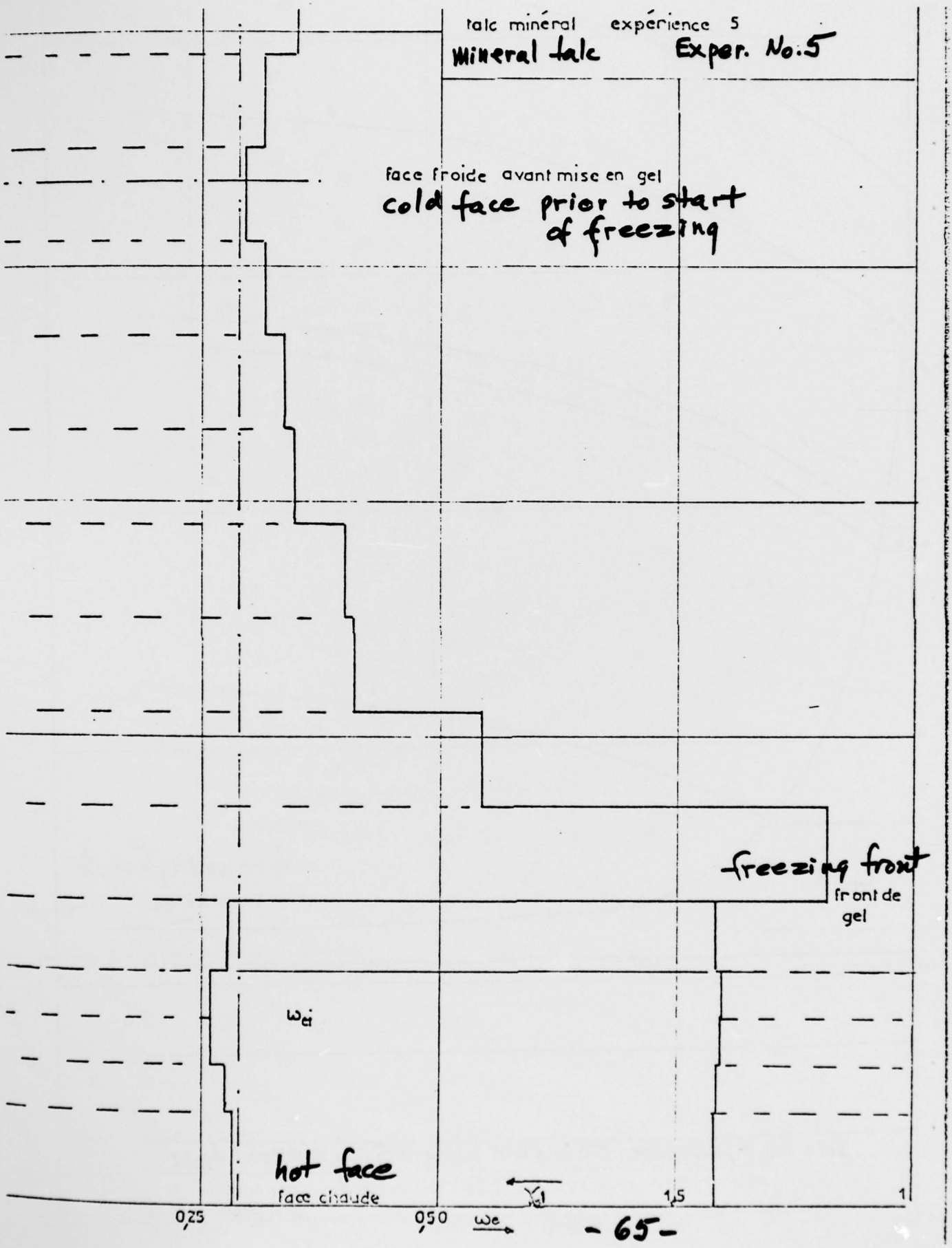
talc minéral expérience 5
Mineral talc Exper. No.5
face froide avant mise en gel
cold face prior to start of freezing
freezing front
front de gel
ω_{ei}
hot face
face chaude
χ_{el}
1,5
1
0,25
0,50
ω_e

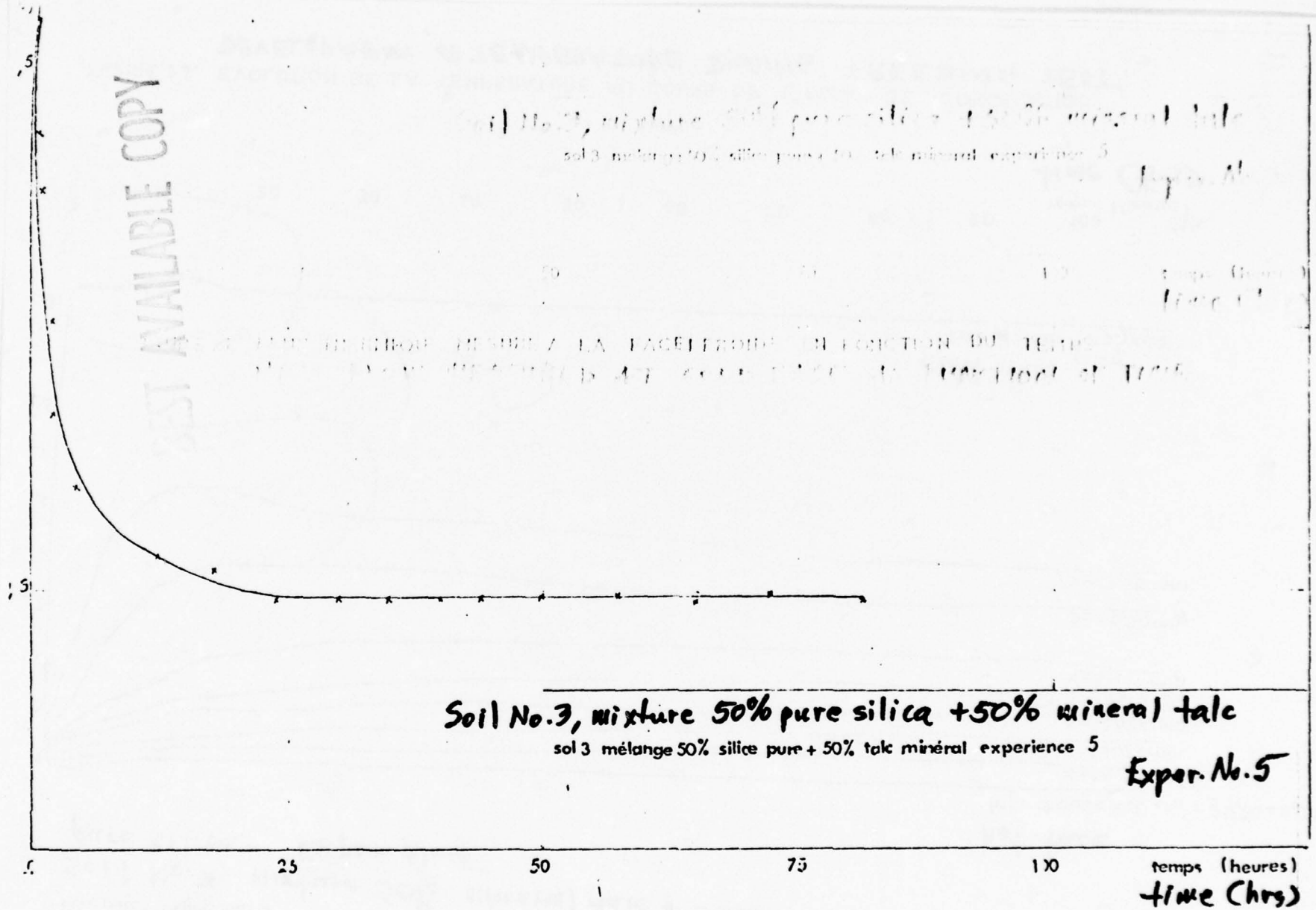

FIGURE 22 FLUX THERMIQUE MESURE A LA FACE FROIDE EN FONCTION DU TEMPS
HEAT FLOW MEASURED AT COLD FACE AS FUNCTION OF TIME

sol . 3 . mélange 50% talc minéral + 50% poudre

silice pure expérience 5

Soil No. 3, mixture 50% mineral talc + 50% pure silica - Exper. No. 5

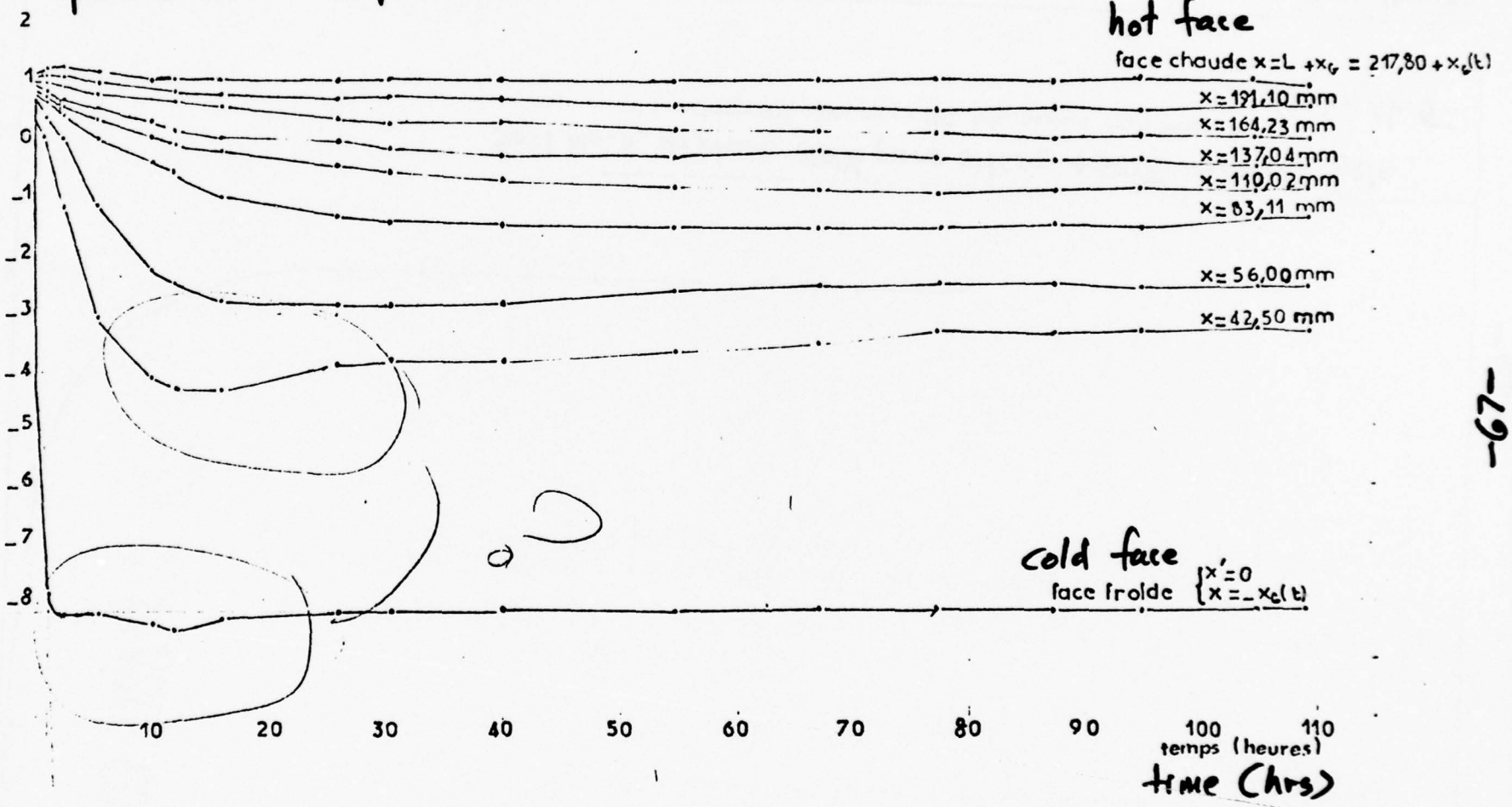

FIGURE. 23. EVOLUTION DE LA TEMPERATURE AU COURS DE L'ESSAI DE CONGELATION

DEVELOPMENT OF TEMPERATURE DURING FREEZING TEST

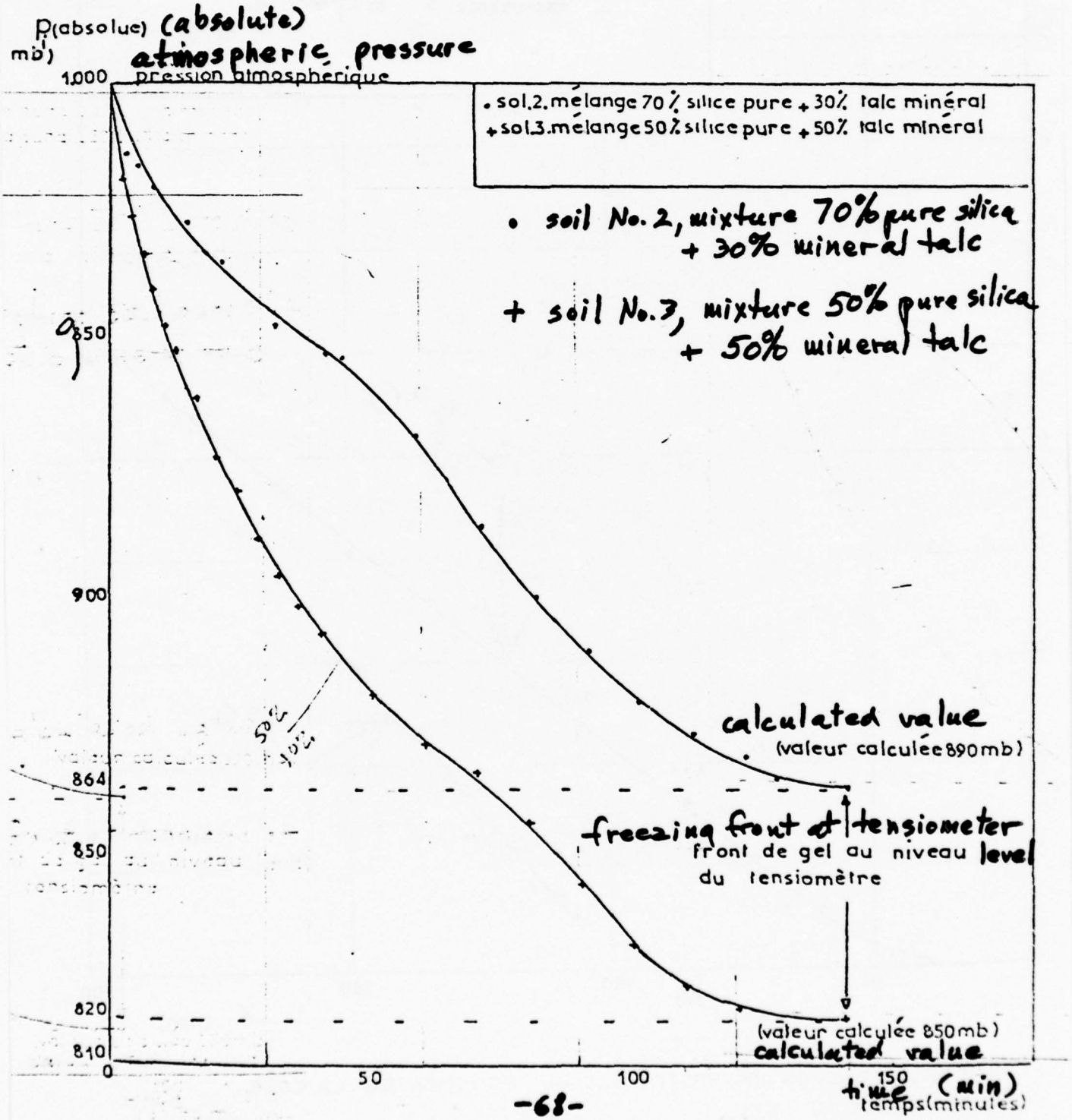

FIG. 24 EVOLUTION DE LA PRESSION INSTERSTITIELLE AU NIVEAU DU TENSIOMETRE
INTERSTITIAL PRESSURE DEVELOPMENT AT TENSIOMETER LEVEL

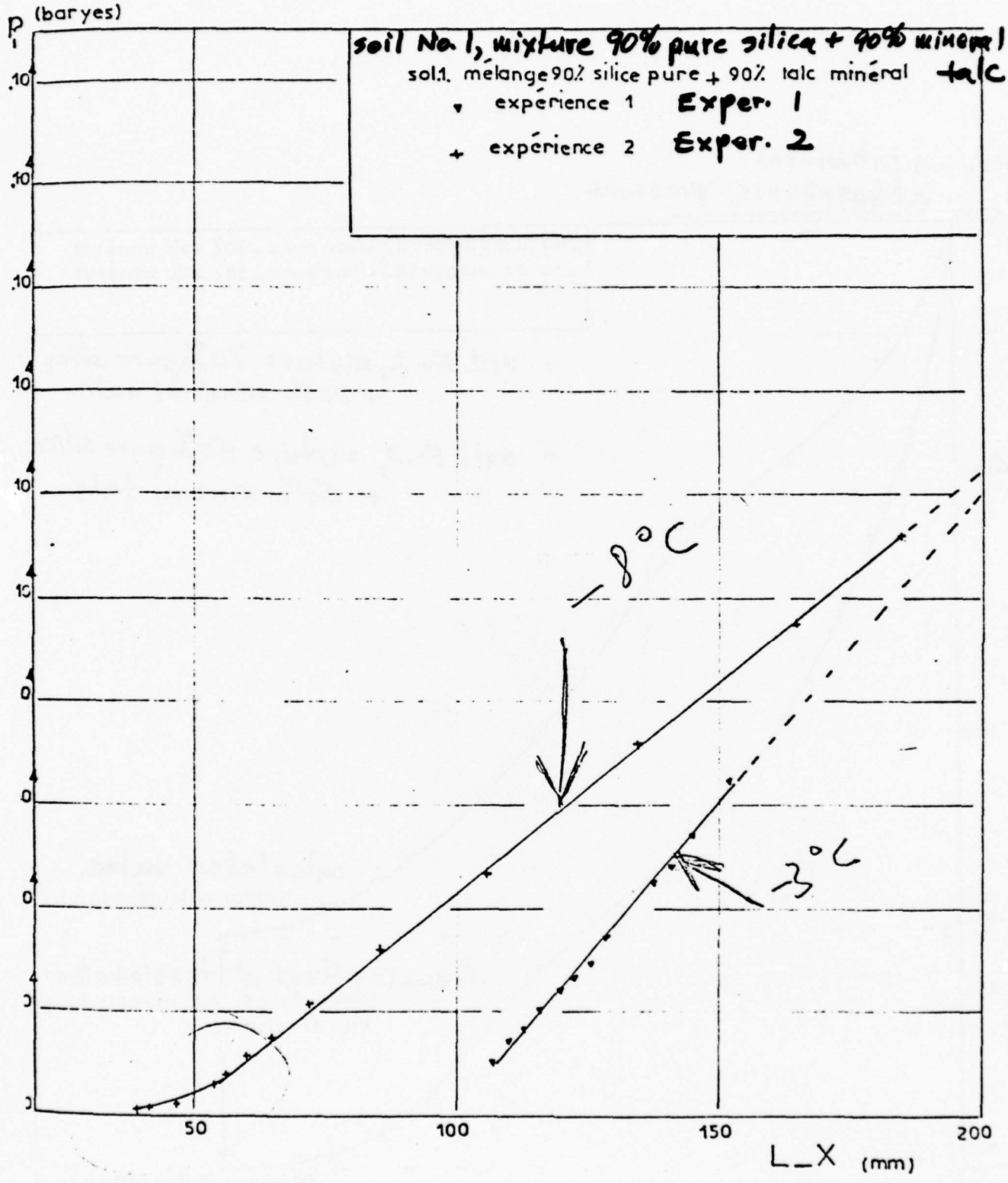

5. CHUTE DE LA PRESSION INSTERSTITIELLE EN FONCTION DE LA COTE DU FRONT DE GEL

INTERSTITIAL PRESSURE DROP AS FUNCTION OF FREEZING FRONT LEVEL

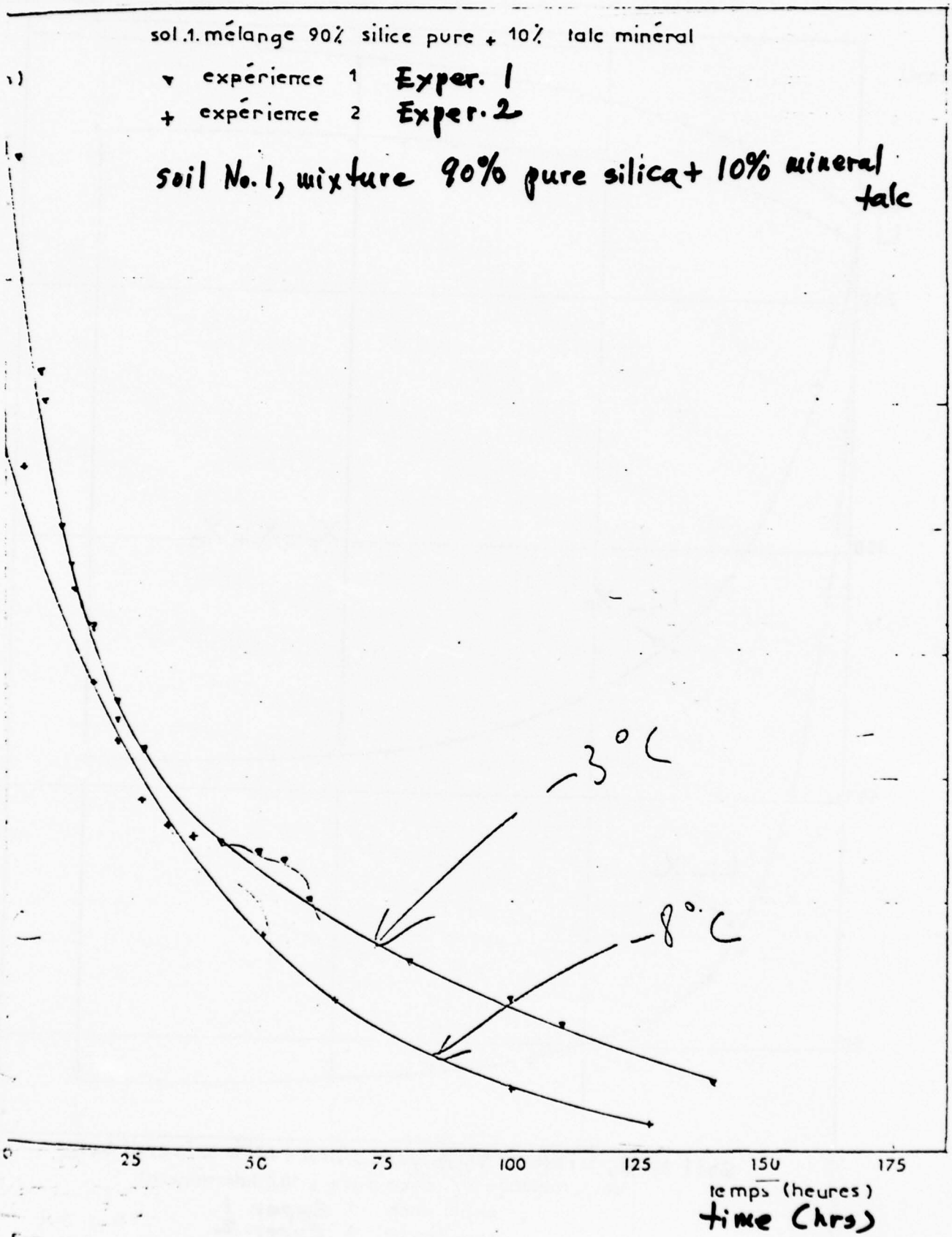

FIG. 26. VITESSE DE GONFLEMENT EN FONCTION DU TEMPS
SWELLING SPEED AS FUNCTION OF TIME

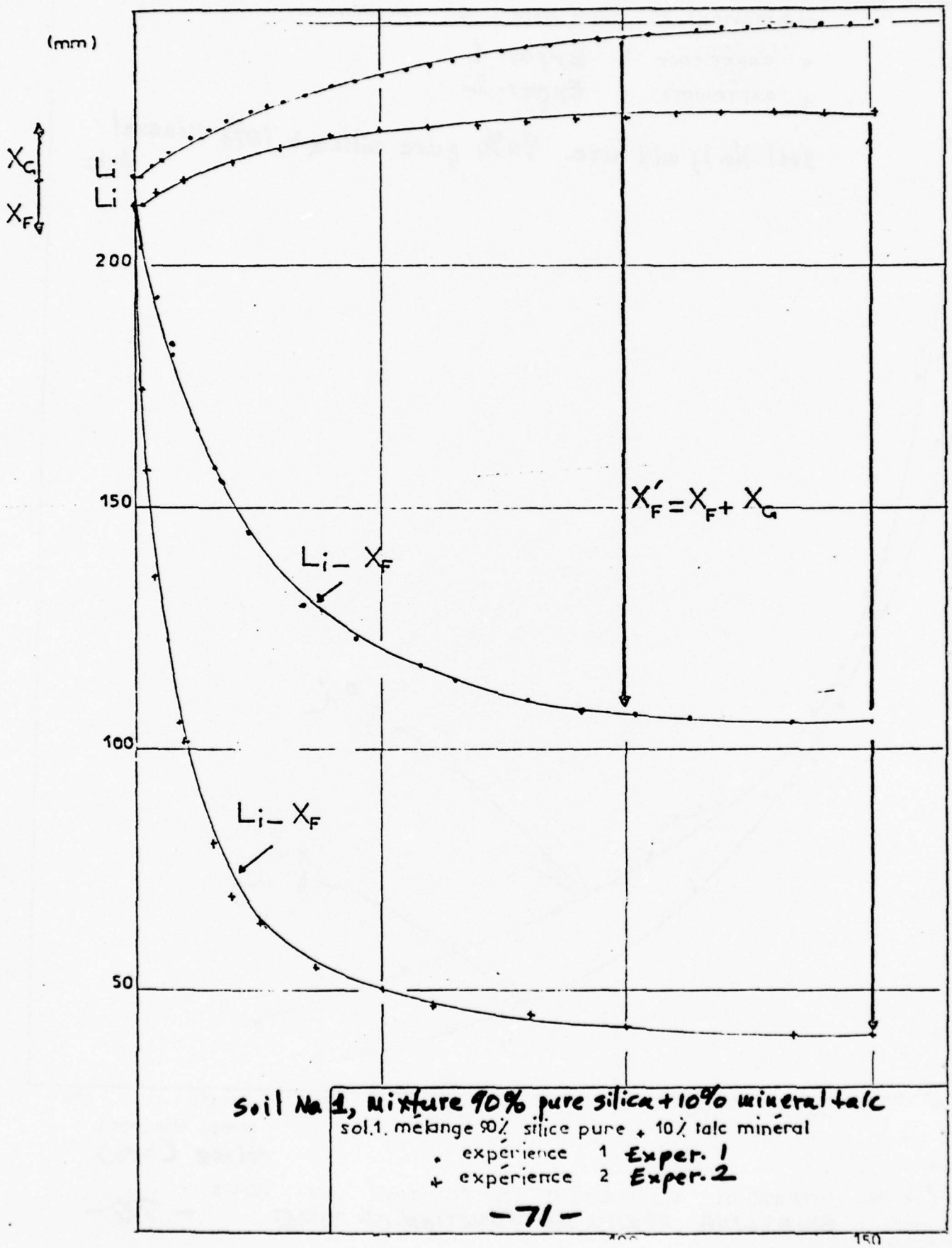

Soil No 1, Mixture 90% pure silica + 10% mineral talc

sol.1. mélange 90% silice pure + 10% talc minéral

• expérience 1 Exper. 1

+ expérience 2 Exper. 2

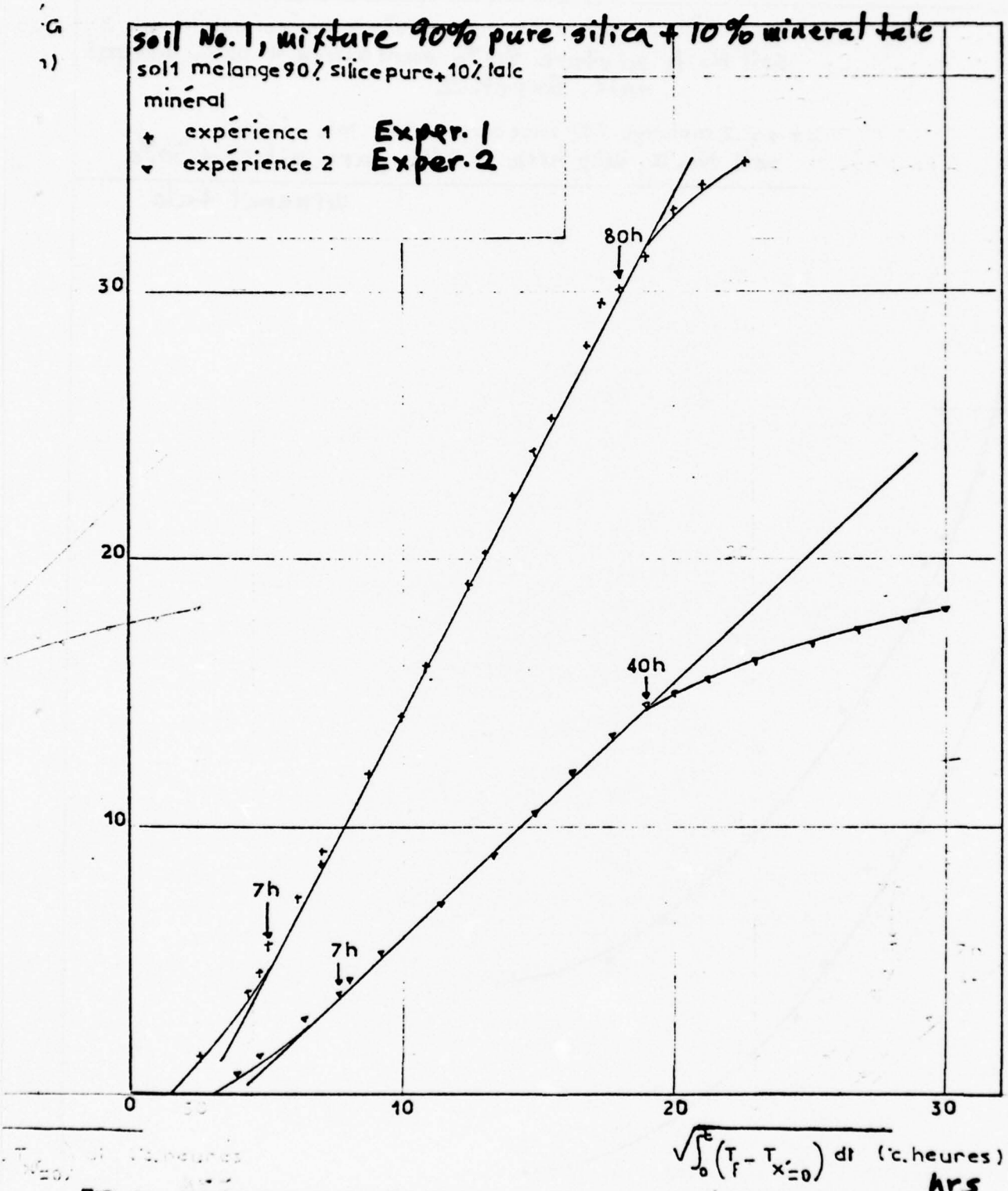

FIG. 28. GONFLEMENT EN FONCTION DE LA RACINE CARREE DE L'INDICE DE GEL

SWELLING AS FUNCTION OF SQUARE ROOT OF FREEZING INDEX

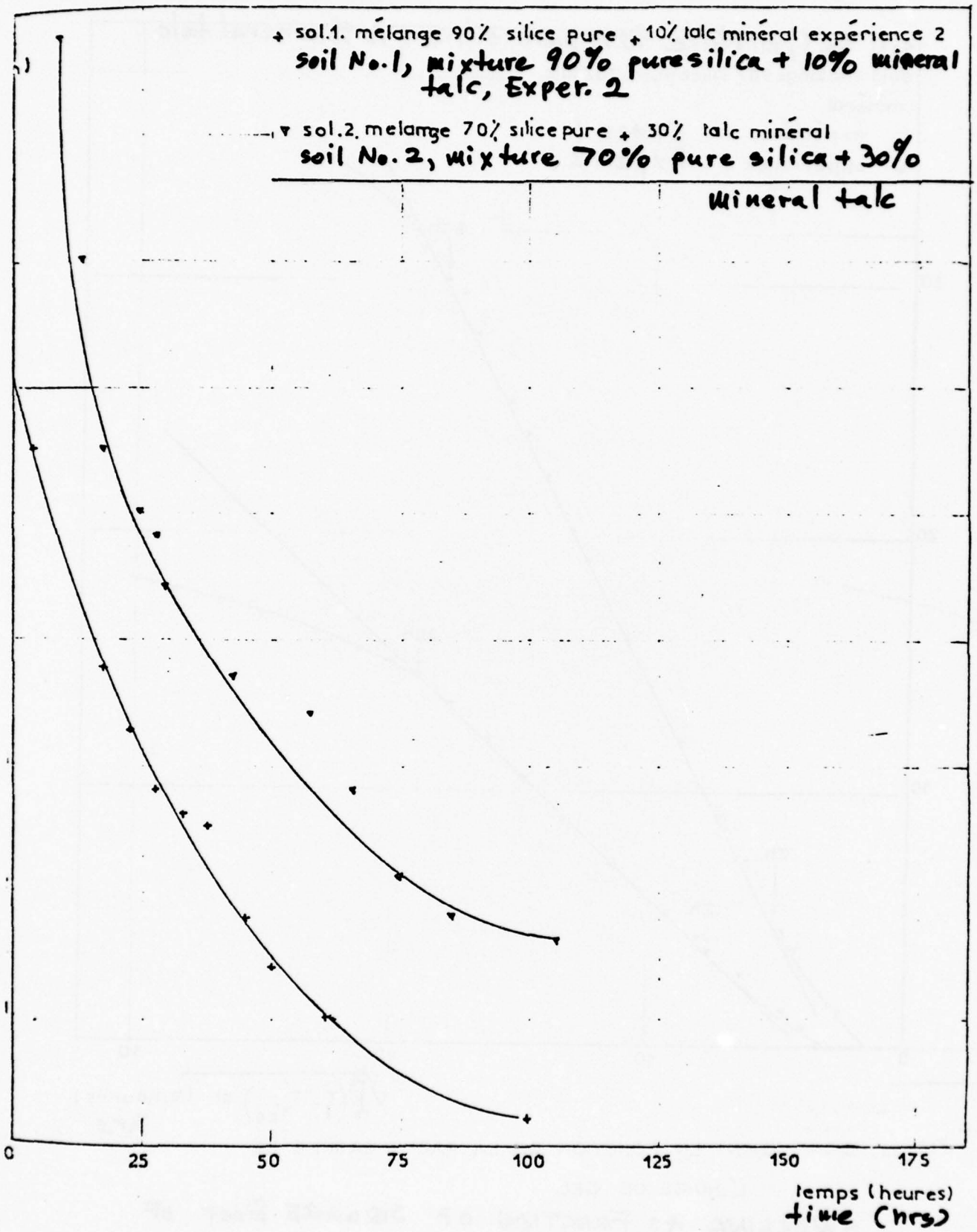

FIG. 29. VITESSE DE GONFLEMENT EN FONCTION DU TEMPS
SWELLING SPEED AS FUNCTION OF TIME

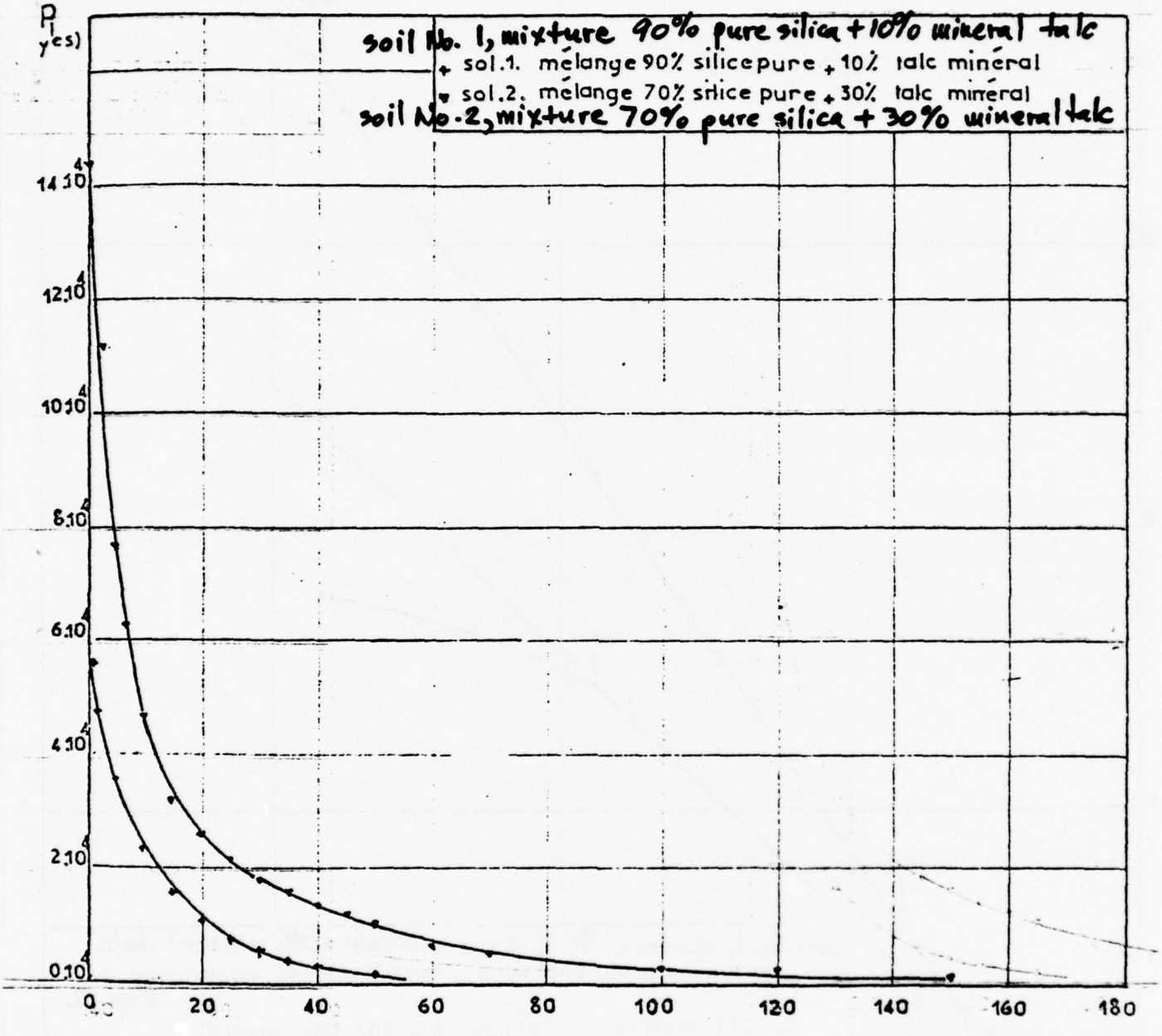

FIG 30 CHUTE DE LA PRESSION INTERSTITIELLE EN FONCTION DU TEMPS

INTERSTITIAL PRESSURE DROP AS FUNCTION OF TIME

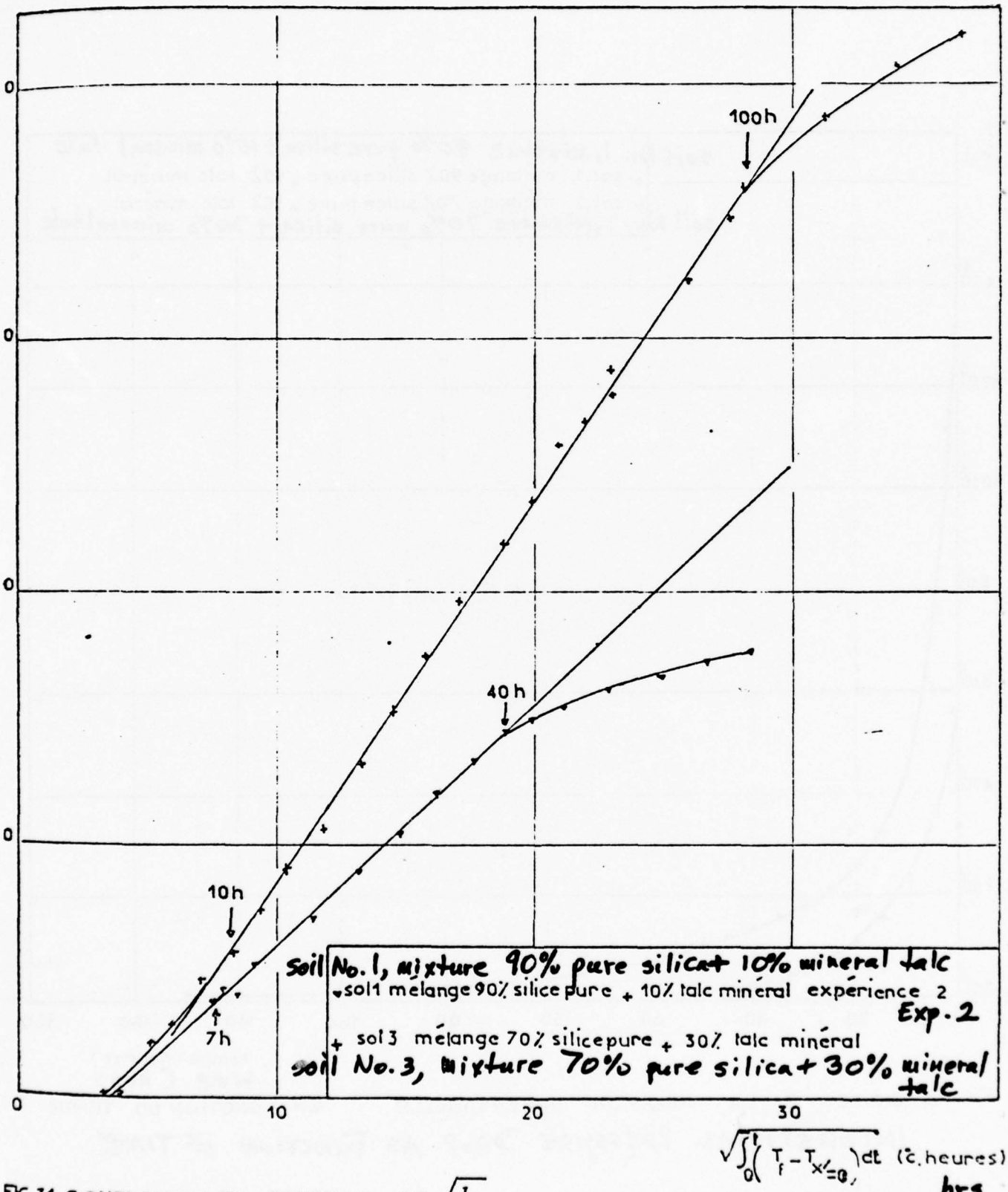

FIG.31. GONFLEMENT EN FONCTION DE $\sqrt{I}$

SWELLING AS FUNCTION OF

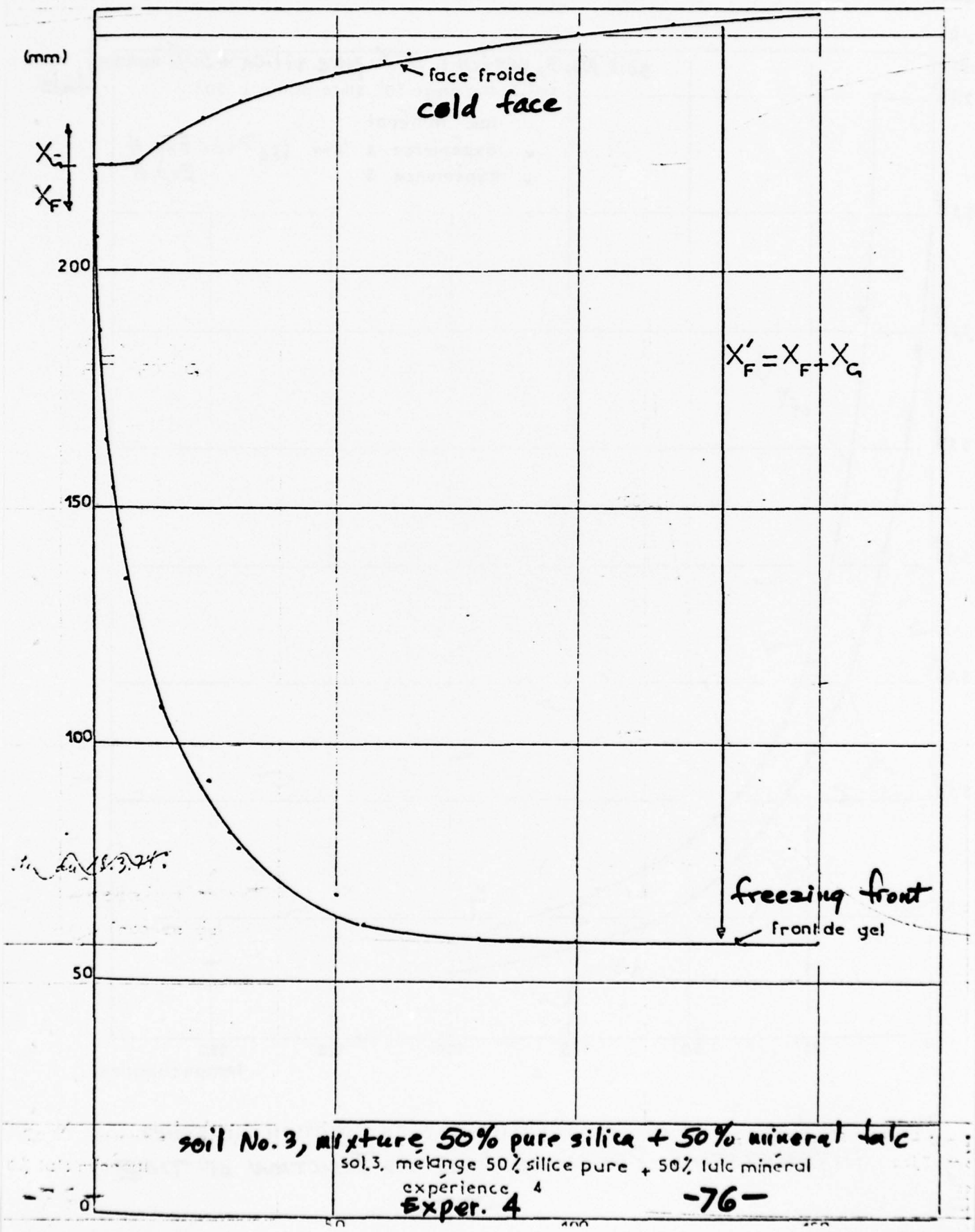

soil No. 3, mixture 50% pure silica + 50% mineral talc

sol 3. mélange 50% silice pure + 50% talc minéral

expérience 4

Exper. 4

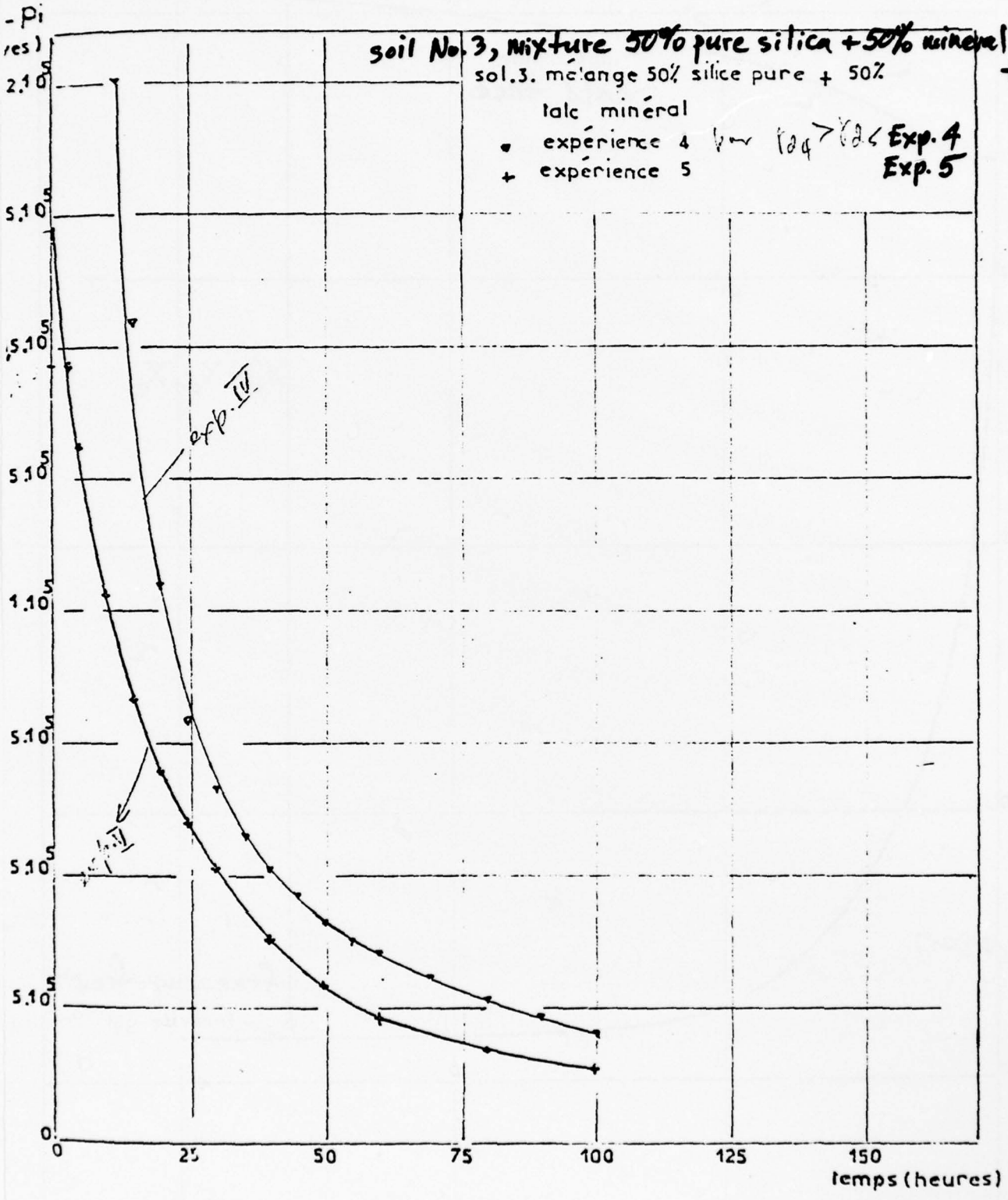

FIG. 33. CHUTE DE LA PRESSION INSTERSTITIELLE EN FONCTION DU TEMPS

INTERSTITIAL PRESSURE DROP AS FUNCTION OF TIME

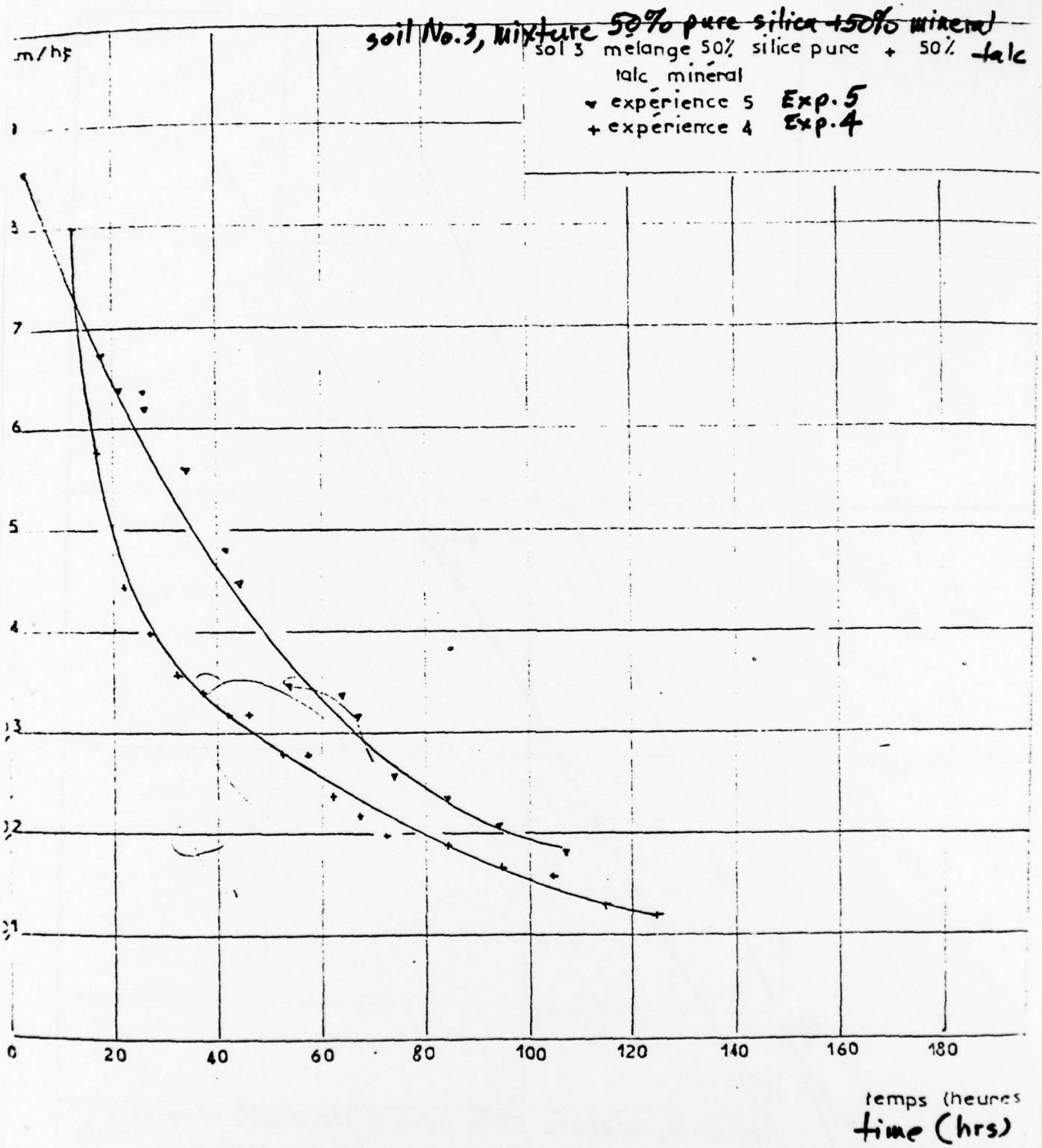

FIG. 34. VITESSE DE GONFLEMENT EN FONCTION DU TEMPS

SWELLING SPEED AS FUNCTION OF TIME

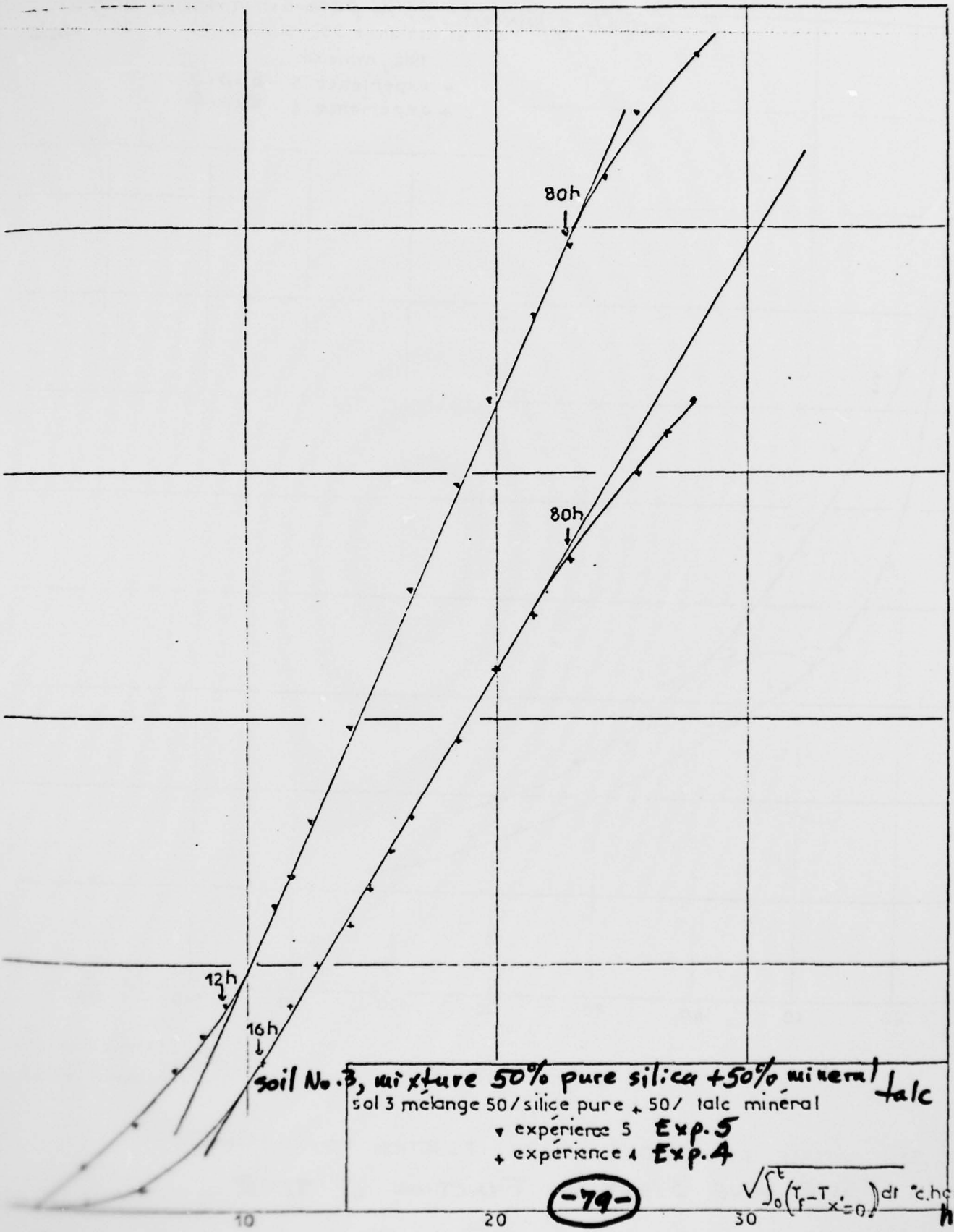

soil No. 3, mixture 50% pure silica + 50% mineral talc

sol 3 mélange 50/ silice pure + 50/ talc minéral

▼ expérience 5 Exp. 5

+ expérience 4 Exp. 4

$\sqrt{\int_0^t (T_f - T_{x=0}) dt}$ °c.hours

hrs

FIG. 35 GONFLEMENT EN FONCTION DE LA RACINE CARREE DE L'INDICE DE GEL

SWELLING AS FUNCTION OF SQUARE ROOT OF FREEZING INDEX

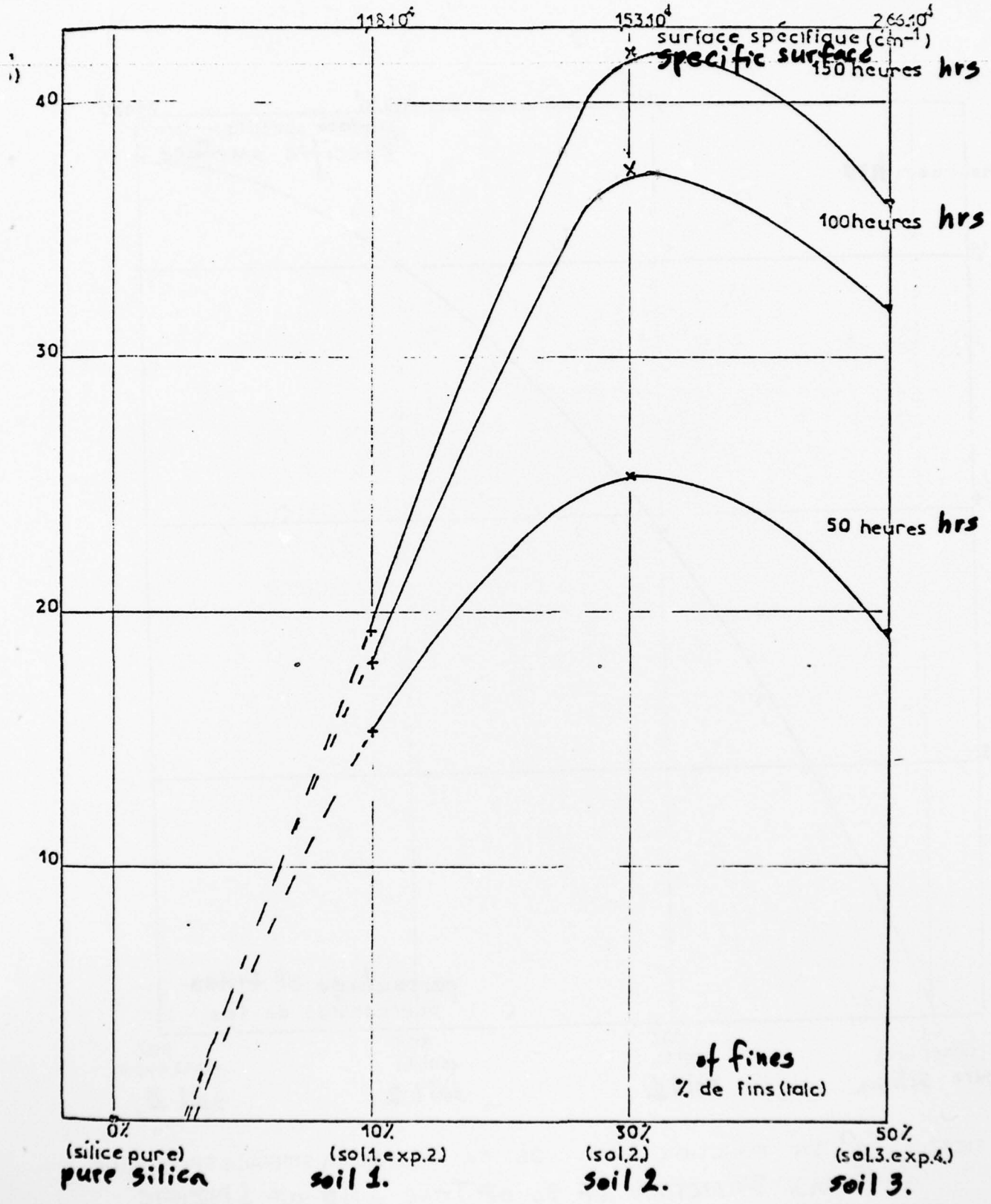

FIG.36. GONFLEMENT EN FONCTION DU % DE TALC
ET DE LA SURFACE SPECIFIQUE

SWELLING AS FUNCTION OF % OF TALC
AND OF SPECIFIC SURFACE

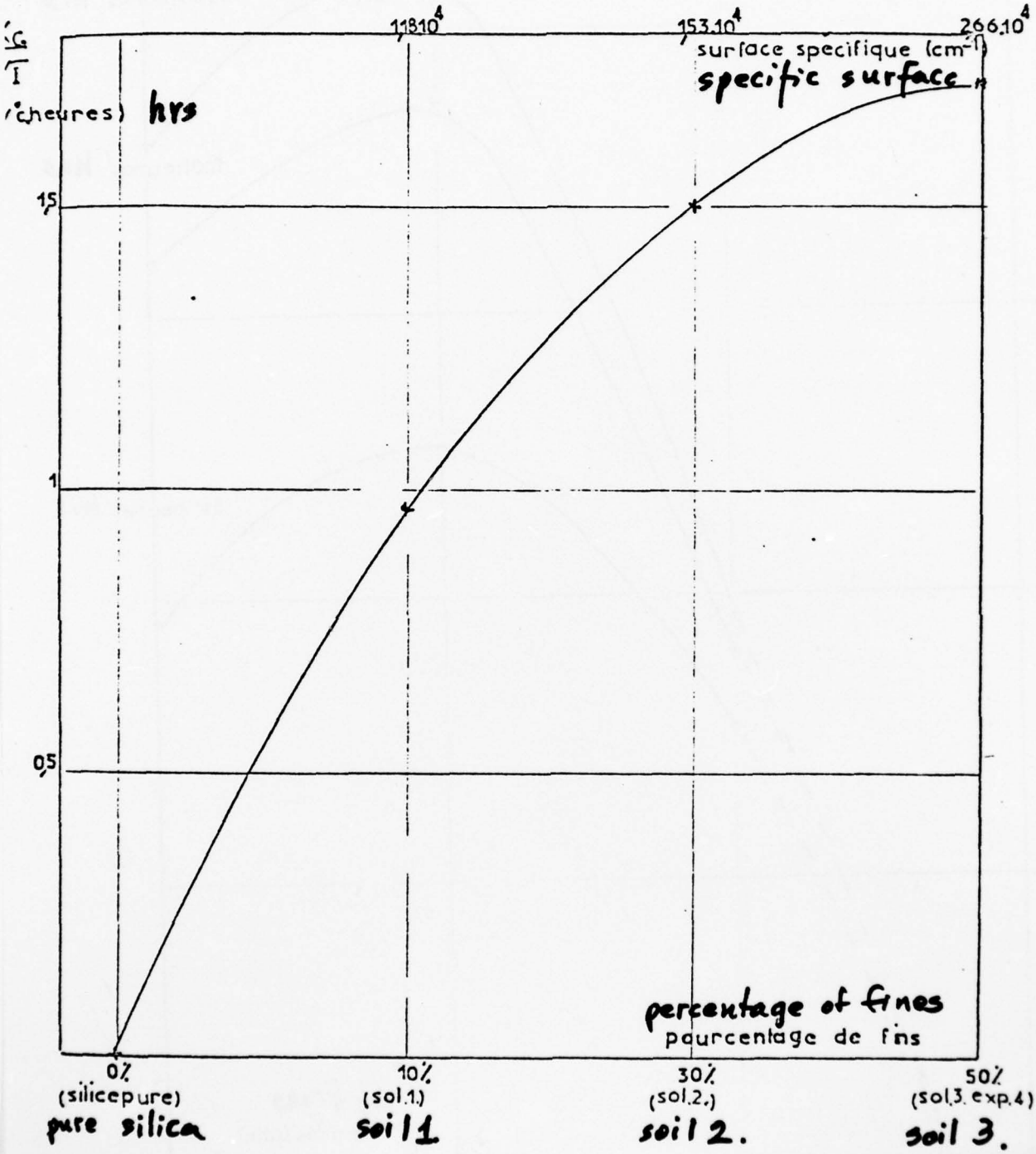

FIG.37. $\frac{\Delta X_G}{\Delta \sqrt{I}}$ EN FONCTION DU °/. DE TALC ET DE LA SURFACE SPECIFIQUE
AS FUNCTION OF % OF TALC AND OF SPECIFIC SURFACE

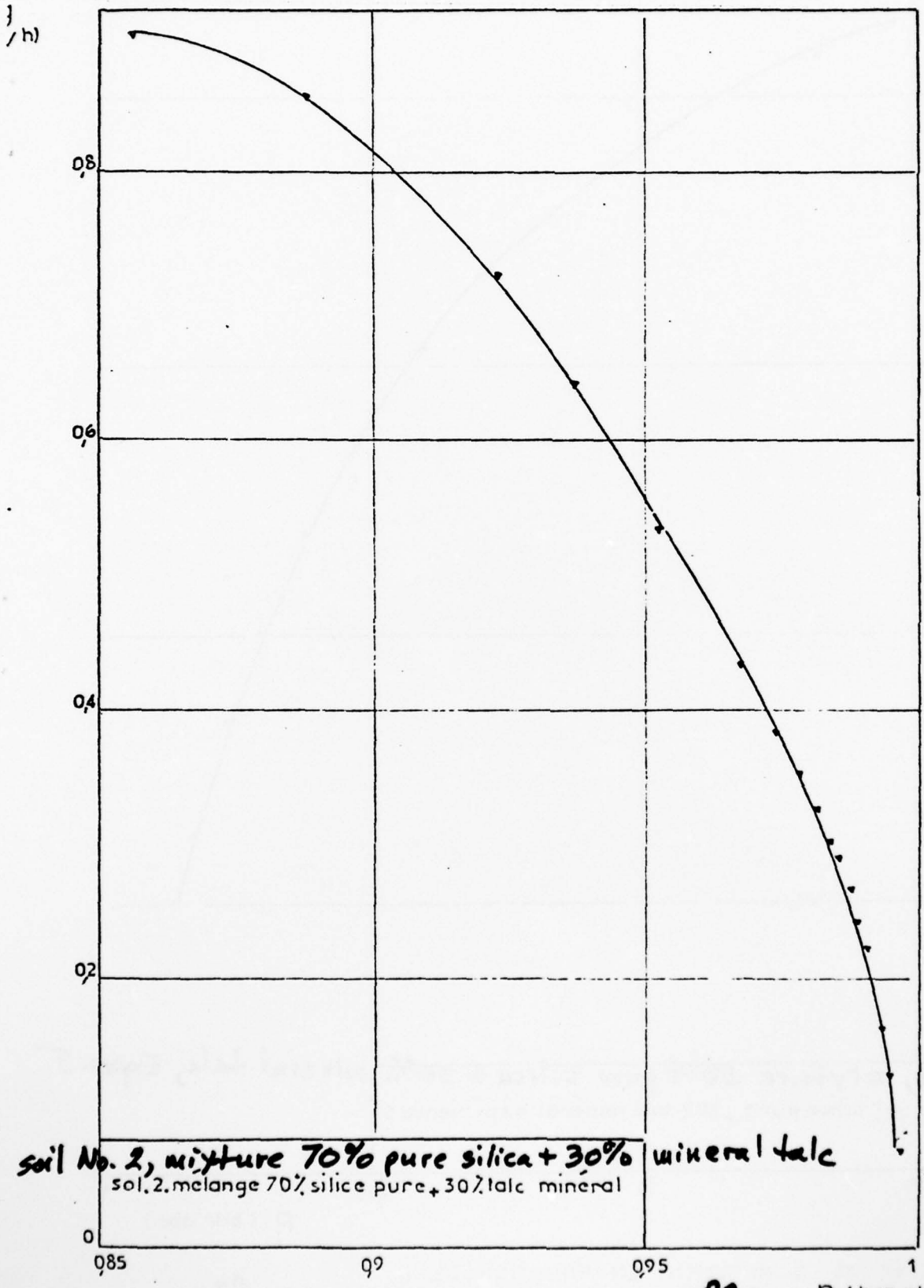

SWELLING SPEED AS FUNCTION OF

FIG. 38 VITESSE DE GONFLEMENT EN FONCTION DE P

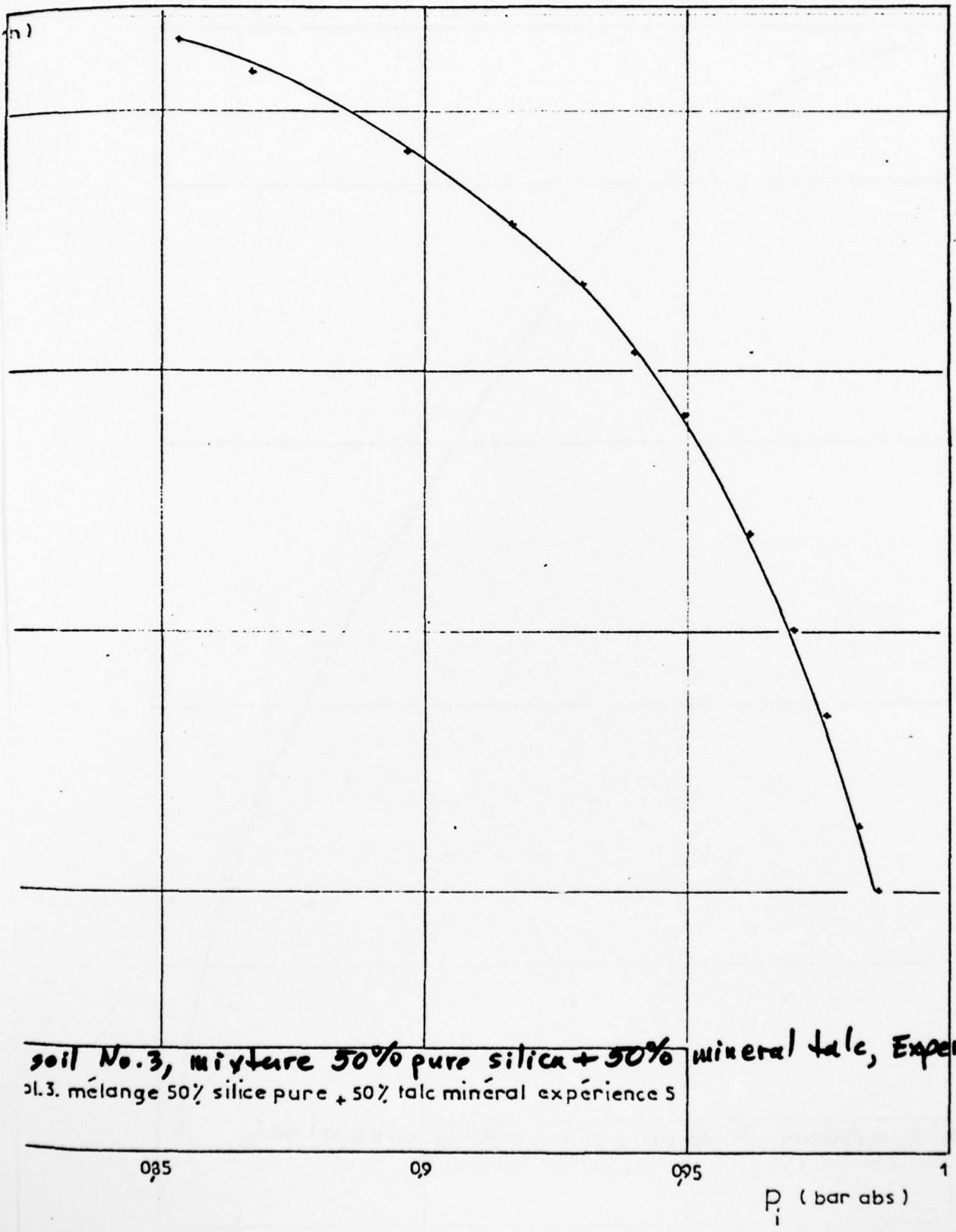

soil No.3, mixture 50% pure silica + 50% mineral talc, Exper.5

ol.3. mélange 50% silice pure + 50% talc minéral expérience 5

IG 39 VITESSE DE GONFLEMENT EN FONCTION DE P_i

SWELLING SPEED AS FUNCTION OF

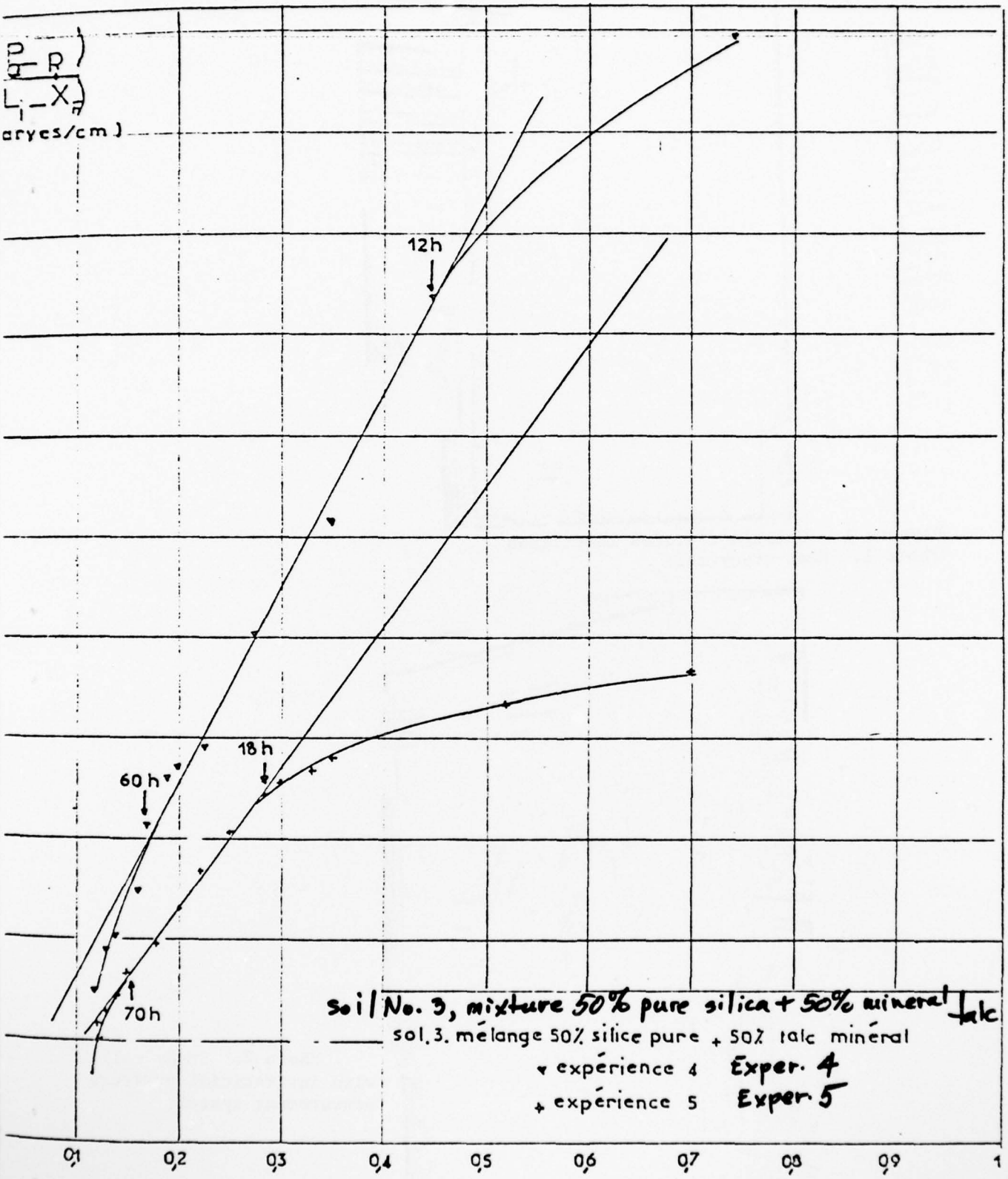

Soil No. 3, mixture 50% pure silica + 50% mineral talc

sol. 3. mélange 50% silice pure + 50% talc minéral

▾ expérience 4 Exper. 4

+ expérience 5 Exper. 5

$\frac{\Delta(P_a - P_i)}{\Delta(L_i - X_F)}$ AS FUNCTION OF $\frac{\Delta\sqrt{I}}{\Delta t}$

EN FONCTION DE $\frac{\Delta\sqrt{I}}{\Delta t}$ $\sqrt{\frac{\text{°C}}{\text{heure}}}$

hrs

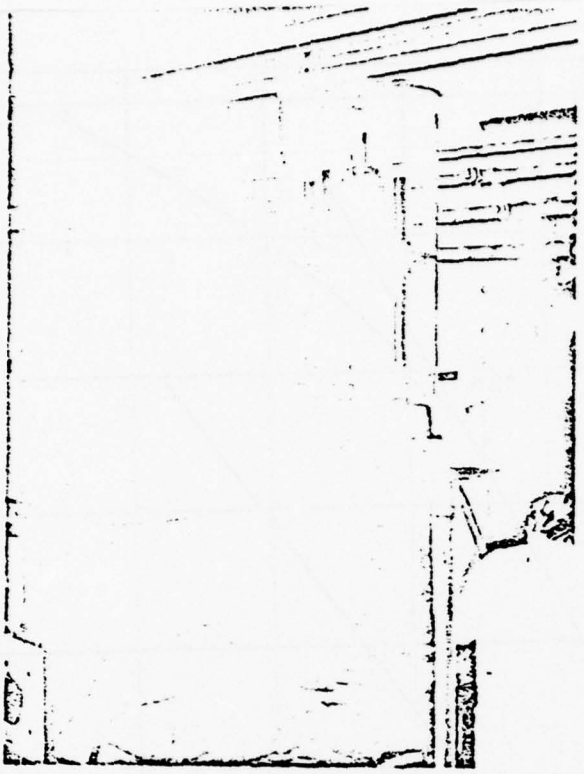

Planche 1 - Cellule d'études thermiques
Photo 1. Heat study cell

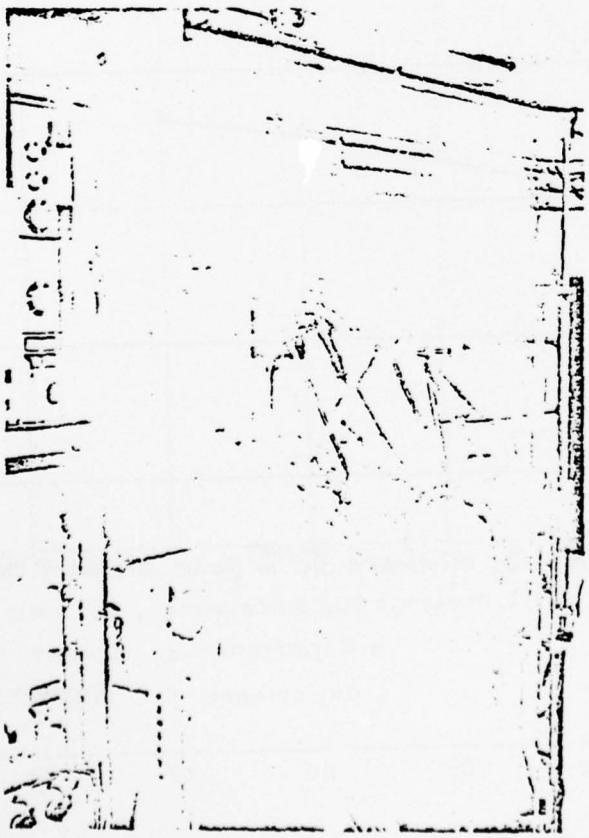

Photo 2. Study cell with interstitial pressure measurement system.

Planche 2 - Cellule d'étude avec système de mesure de la pression interstitielle

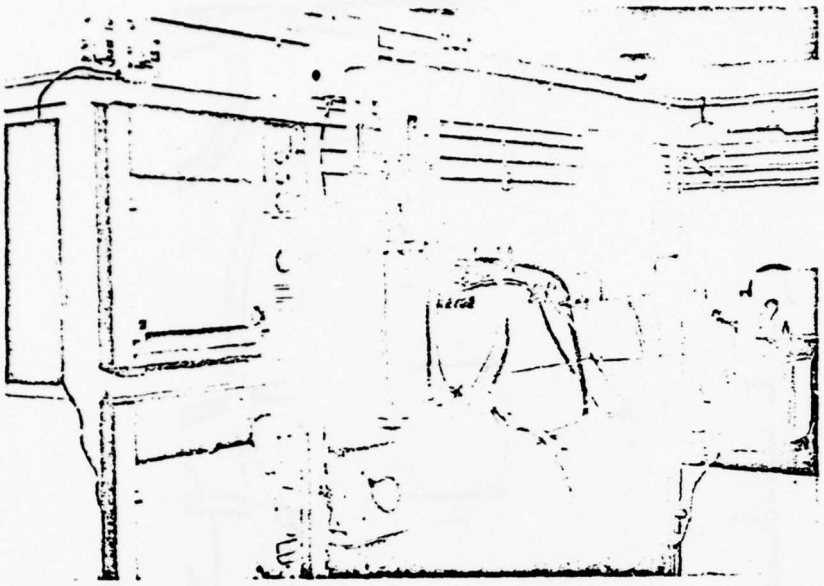

Planche 3 - Ensemble expérimental
Photo 3. Experimental setup

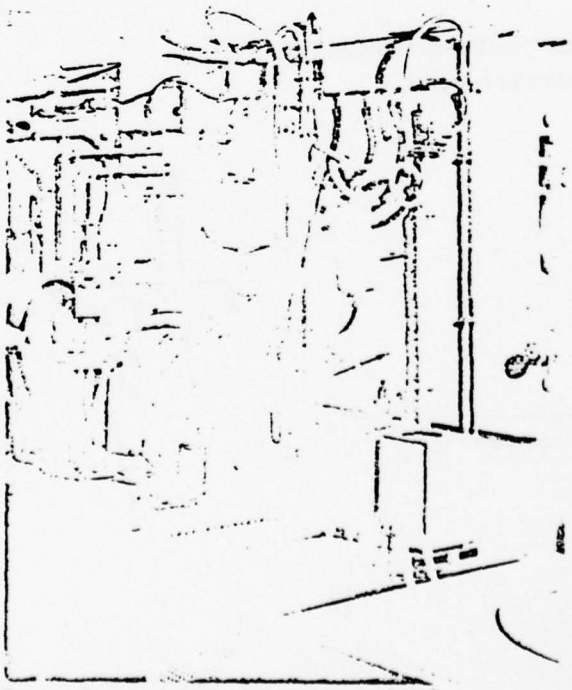

Planche 4 - Perméamètre (processus de saturation)
Photo 4. Permeameter (saturation process).

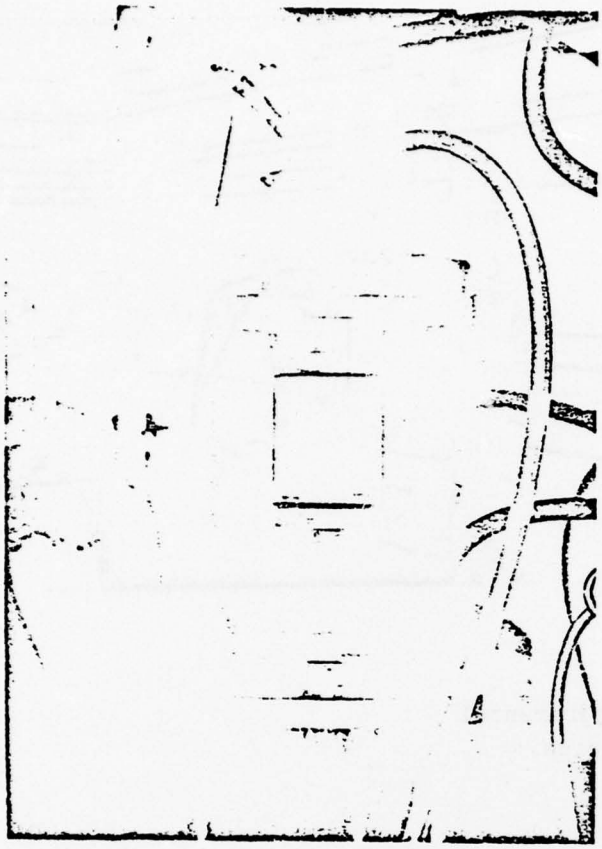

Planche 5 - Cellule porte-échantillon
Photo 5. Sample-carrier cell

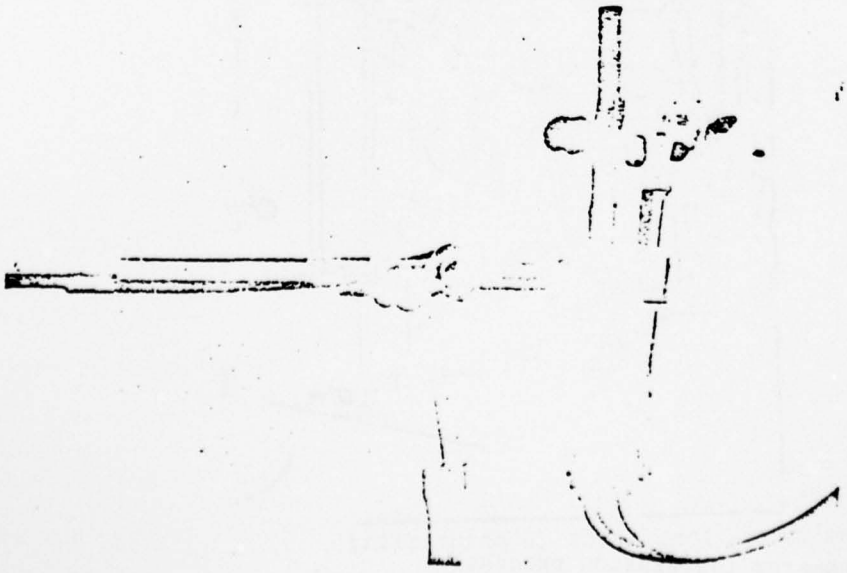

planche 6 - Tensiomètre de mesure

Photo 6. Measurement tensiometer

LIST OF FIGURES

LIST OF PHOTOS

TABLE OF CONTENTS